A NUMERICAL INVESTIGATION INTO THE PERFORMANCE OF THE SOIL NAIL WALL AND PILE FOUNDATION AT THE SWIFT DELTA I-5 INTERCHANGE

by

Trevor D. Smith
Department of Civil Engineering
Portland State University
Portland, Oregon

December 1993

1. Report No. FHWA-OR-RD-95-15	2. Government Accession No.	3. Recipient's Catalog No.
4. Title and Subtitle A NUMERICAL INVESTIGATION INTO THE PERFORMANCE OF THE SOIL NAIL WALL AND PILE FOUNDATION AT THE SWIFT DELTA I-5 INTERCHANGE Final Report		5. Report Date December 1993
		6. Performing Organization Code
7. Author(s) Trevor D. Smith		8. Performing Organization Report No.
9. Performing Organization Name and Address Department of Civil Engineering Portland State University Portland, Oregon 97207		10. Work Unit No. (TRAIS)
		11. Contract or Grant No. SPR #5292
12. Sponsoring Agency Name and Address Oregon Department of Transportation Research Unit 2950 State Street Salem, OR 97310 Federal Highway Administration 400 Seventh Street SW Washington D.C. 20590		13. Type of Report and Period Covered Final Report (1992-1993)
		14. Sponsoring Agency Code

15. Supplementary Notes

16. Abstract

Finite Difference Methods (FDM) and Finite Element Methods (FEM) studies are reported studying the soil nail wall construction at the Swift Delta I-5 Interchange bridge reconstruction in North Portland, Oregon. Five (5) layers of soil nails were installed between existing bridge supporting pipe piles, and a shortcrete finished face applied to stabilize the fill sand. Instrumentation on the project at two sections, S1 and S2, included strain gages on the nails, and on a single pile at S1, load cells on the nail heads, inclometers in the wall and in the fill at S2 outside of the bridge, and tiltmeters with an extensometer on the pile cap at S1.

Some interpretive comments are made on the measured wall and nail readings, which are used to back calculate possible earth pressures by FDM techniques. The lateral load program COM624P is used to explore the limitations of FDM techniques for direct pile analysis in Swift Delta's soil/nail/pile system. Two dimensional FEM analysis are conducted by a new code, Finite Element analysis of NAILS (FENAIL), written specifically for this study. Modeling in both linear elasticity, and nonlinear plasticity, is reported at the bridge instrumented section S1 and the wall section S2 outside the bridge footprint. The model features included: full geostatic conditions, excavation modeling sequences and nail activation with beam elements. An innovative *interference* element is introduced to link the "out of mesh" pile to the soil and nail model, and generate pseudo 3 dimensional (3D) effects.

A full 3D FEM analysis is reported of the top soil nail, adjacent pile and soil, by the code ABAQUS running on a CRAY MPX supercomputer. Linear elastic, anisotropic elastic and a single elastic plastic model were completed to study interaction and global stiffness contributions from the pile and nail.

Based on FENAIL work overall replication of the Swift Delta soil nail wall is good. In general, only limited pile influence can be seen and deflections and stresses do not appear highly sensitive to the piles presence. The reinforced soil mass behaves similar to a reinforce wall structure without piles. The lack of any significant pile influence is also found in the 3D ABAQUS study under nail tension conditions. However, the pile's lateral load stiffness response is improved by nailing of the soil mass.

| 17. Key Words Soil Nail Walls	18. Distribution Statement Available through the Oregon Department of Transportation Research Unit		
19. Security Classif. (of this report) Unclassified	20. Security Classif. (of this page) Unclassified	21. No. of Pages	22. Price

Form DOT F 1700.7 (8-72)   Reproduction of completed page authorized

d:\forms\technical.rpt

SI* (MODERN METRIC) CONVERSION FACTORS

APPROXIMATE CONVERSIONS TO SI UNITS

Symbol	When You Know	Multiply By	To Find	Symbol
		LENGTH		
in	inches	25.4	millimeters	mm
ft	feet	0.305	meters	m
yd	yards	0.914	meters	m
mi	miles	1.61	kilometers	km
		AREA		
in²	square inches	645.2	millimeters squared	mm²
ft²	square feet	0.093	meters squared	m²
yd²	square yards	0.836	meters squared	m²
ac	acres	0.405	hectares	ha
mi²	square miles	2.59	kilometers squared	km²
		VOLUME		
fl oz	fluid ounces	29.57	milliliters	mL
gal	gallons	3.785	liters	L
ft³	cubic feet	0.028	meters cubed	m³
yd³	cubic yards	0.765	meters cubed	m³

NOTE: Volumes greater than 1000 L shall be shown in m³.

Symbol	When You Know	Multiply By	To Find	Symbol
		MASS		
oz	ounces	28.35	grams	g
lb	pounds	0.454	kilograms	kg
T	short tons (2000 lb)	0.907	megagrams	Mg
		TEMPERATURE (exact)		
°F	Fahrenheit temperature	5(F-32)/9	Celsius temperature	°C

APPROXIMATE CONVERSIONS FROM SI UNITS

Symbol	When You Know	Multiply By	To Find	Symbol
		LENGTH		
mm	millimeters	0.039	inches	in
m	meters	3.28	feet	ft
m	meters	1.09	yards	yd
km	kilometers	0.621	miles	mi
		AREA		
mm²	millimeters squared	0.0016	square inches	in²
m²	meters squared	10.764	square feet	ft²
ha	hectares	2.47	acres	ac
km²	kilometers squared	0.386	square miles	mi²
		VOLUME		
mL	milliliters	0.034	fluid ounces	fl oz
L	liters	0.264	gallons	gal
m³	meters cubed	35.315	cubic feet	ft³
m³	meters cubed	1.308	cubic yards	yd³
		MASS		
g	grams	0.035	ounces	oz
kg	kilograms	2.205	pounds	lb
Mg	megagrams	1.102	short tons (2000 lb)	T
		TEMPERATURE (exact)		
°C	Celsius temperature	1.8 + 32	Fahrenheit	°F

```
°F -40    0   32  40  80  98.6 120 160 200 212 °F
   |___|___|___|___|___|___|___|___|___|___|
°C -40  -20   0   20  37  40   60  80  100 °C
```

ACKNOWLEDGEMENTS

DISCLAIMER

accuracy of the code FENAIL. All use and interpretation of the FENAIL code should be assumed by the user.

The post processing of much of the output data from the computer programs was completed in English units, as was all colar output. For clarity of presentation this output is left in its original form and the units made clear in the text. Conversion can be made by the reader with the assistance of page vi.

This report does not constitute a standard, specification, or regulation.

ASSOCIATED REPORTS

This report represents the summary report for the contract scope of work on the Swift Delta Soil Nail wall numerical studies conducted for the Oregon Department of Transportation (ODOT), Research Office. The work was performed between January and September of 1993 to assist ODOT interpret the measured data and assess the performance of the foundation/wall system. Additional work, beyond the contract scope, can be found for all aspects of the research study from the following associated Portland State University, Department of Civil Engineering, reports.

Report Number	Contents
GE-ODOT-02-93	FENAIL User Manual
GE-ODOT-03-93	ABAQUS Work in Two Dimensions for Swift Delta Project
GE-ODOT-04-93	FENAIL Exploration of Swift Delta Sections S1 and S2

THIS PAGE INTENTIONALLY LEFT BLANK.

A NUMERICAL INVESTIGATION INTO THE PERFORMANCE OF THE SOIL NAIL WALL AND PILE FOUNDATION AT THE SWIFT DELTA I-5 INTERCHANGE

TABLE OF CONTENTS

APPENDICES

APPENDIX A: A SET OF USER FEEDBACK COMMENTS FOR COM624P
APPENDIX B: BOREHOLE LOG TB124 AND TB125

THIS PAGE INTENTIONALLY LEFT BLANK.

A NUMERICAL INVESTIGATION INTO THE PERFORMANCE OF THE SOIL NAIL WALL AND PILE FOUNDATION AT THE SWIFT DELTA I-5 INTERCHANGE

LIST OF FIGURES

**A NUMERICAL INVESTIGATION INTO THE PERFORMANCE
OF THE SOIL NAIL WALL AND PILE FOUNDATION AT THE
SWIFT DELTA I-5 INTERCHANGE**

LIST OF TABLES

THIS PAGE INTENTIONALLY LEFT BLANK.

1.0 INTRODUCTION

1.1 PURPOSE AND SCOPE

The Oregon Slough Bridge is located seven miles north of Portland at MP307.46 on Interstate 5 as it crosses the Swift Highway and North Marine Drive. A reconstruction of this interchange in the early 1990's was funded by the Oregon Department of Transportation (ODOT) and the Federal Highway Administration. To improve and add lane access beneath the south end of the existing bridge a soil nail wall was selected to remove the existing end slope and permanently stabilize the face. Throughout the 1970's in Europe, and into the 1980's in the U.S., the soil nailing concept has received growing recognition for its cost savings, rapid construction time and lack of any external support which might otherwise restrict workspace.

The technique consists of placing rows of grouted unstressed bars (nails) in the soil to improve shear strength and produce a reinforced stiff mass of soil in the axis of the nails direction. Mobilization of transfer shear stress on the grout/soil interface for an initially unstressed nail produces slightly more outward wall deflection than a more traditional tie back wall. Nail spacing is usually governed by the arching distance between nails and to ensure a close to uniform stiffened soil mass. Finally, a welded wire fabric reinforced shotcrete face is applied before the next excavation cut (often termed 'lift') sequence is commenced.

The excavation for the Swift Delta wall brought the cut face close to the existing 356 mm (14 in.) diameter pipe piles supporting the south end abutment of the bridge deck, and the soil nails were placed on 1.37 m (4½ ft.) horizontal centers, midway between the pipe piles. Total wall length for the project was 78 m (256 ft.), with 50.3 m (165 ft.) beneath the bridge deck, at a maximum height just over 5.8 m (19 ft.) (Sakr 1991), Figure 1.1. Since the project represented one of the earliest permanent soil nail walls used in a bridge application in the U.S., funding was available under the FHWA Experimental Features program for a detailed instrumentation program.

Two principal cross sections, Section 1 (S1) and Section 2 (S2) (hereafter referred to as S1 and S2), were chosen to monitor nail and pile behavior and assist in assessing the interaction with, and influence of, the bridge supporting piles. S1 is under the bridge deck at the west end close to the maximum wall height, with 3.3 m (10 ft.) of surcharge, and S2 is outside the bridge influence with a 2:1 slope above the wall. Instrumentation at each section S1 and S2 is illustrated in the following Section (Figures 2.2 and 2.3) and comprised at each section:

- Strain gauges along each of the nails

- A nail load cell is placed at the wall face for rows 1, 3, and 5.

- Two earth pressure cells

- Two inclinometers to monitor wall deflection, one installed behind the wall finished face prior to construction and one installed in the second layer of the shotcrete face.

and in addition at S1 only:

- Three tiltmeters and one extensometer to monitor pile cap rotation and horizontal deflection respectively.

Selected results from this instrumentation data and summary interpretation is given in the following section. Monitoring and recording of this data occurred frequently during construction and into the first 6 months after construction. Additional monitoring will be continued for the subsequent 3 years after this period to permit study of the long term performance.

This research report summarizes the numerical modeling by finite difference methods (FDM) and finite element methods (FEM) of the soil-nail-wall-pile interaction phenomena at Swift Delta. The modeling was directed towards a better understanding of the Swift Delta wall foundation system, and to aid in the interpretation of the instrumentation data. The 2H:1V slope removal ahead of the foundation piles and the installation of a permanent soil nail wall in front of these piles was a 'first' for this technique and does present questions that advanced numerical techniques can assist in answering. These questions can be summarized as follows:

- What role do foundation piles play in the structural interaction (stiffening) of the wall-nail-fill system?

- From a practical standpoint is it conservative to design the soil nailed wall assuming no pile influence?

- What additional lateral loads, if any, were the existing piles subjected to from the end slope removal?

- Does a critical distance, or wall height/distance ratio, exist from the piles to the wall that prevents significant interaction?

- What recommendations could be made, based on this Swift Delta Study, that can help future design of lane widening projects, soil nail wall design and construction and/or instrumentation projects?

2

1.2 SUBSURFACE CONDITIONS

A complete report of the subsurface investigations conducted by ODOT Region 1 is available (ODOT 1988). Of the 27 borings made in 1988 for the design of the interchange reconstruction two borings, TB 124 and TB 125 (shown in Appendix 3) are of direct use in establishing the soil profile of the wall. Two further borings TB 127 and TB 128 were made in May 1989. These were drilled behind the wall control line to install vertical slope inclinometers. Figure 1.2 presents the location of these borings and Figure 1.3 a summary profile used in this study for both instrumentation sections. The wall was built entirely in the medium dense clean sand fill, SP, confirmed by construction observation, with ground water table below the wall base. The sand was damp to moist, which provided some apparent cohesion and allowed construction to be successful. The properties of this SP material was of prime concern for the numerous modeling attempts that were undertaken. The sole shear test conducted on the sand was the Direct Shear test of sample U-2 from TB 127 taken from a depth of 5.5 m (18'-0"). The three test results are given on Figure 1.4 and show c = 0, phi = 32.4°. It is clear the sand is close to its critical void ratio with neither strong dilatant or contracting tendencies.

To add to the understanding of the behavior of the sand unit, and form a basis to develop constitutive parameters, five prebored pressuremeter tests (PMT) were performed in December of 1990 and May of 1991. These were made with a PUP pressuremeter (Smith and Denham 1991), of which four were tested with a BX size probe (62 mm dia.) and one with an EX size probe (32 mm dia.). Table 1.1 presents a summary of these test results, arranged in order by depth, with full test results given in Figure 1.5 and 1.6.

Table 1.1 Summary of Pressuremeter Tests

Test No.	Probe Type	Depth m	(ft)	Net Limit Pressure kPa	(ksf)	PMT Modulus MPa	(ksf)
1	BX	1.1	(3.6)	204	(3.8)	2.42	(45.0)
2	EX	1.3	(4.25)	260	(4.8)	1.55	(29.0)
5	BX	1.33	(4.38)	338	(6.3)	2.52	(47.0)
3	BX	1.92	(6.29)	413	(7.7)	3.05	(57.0)
4	BX	2.73	(8.96)	482	(9.0)	3.00	(56.0)

All boreholes were drilled unsupported by hand augers and each test conducted in accordance with ASTM D4719. The results given in Figure 1.5 and 1.6 show high quality data generally consistent with testing uniform sand at increasing depth, Figure 1.7.
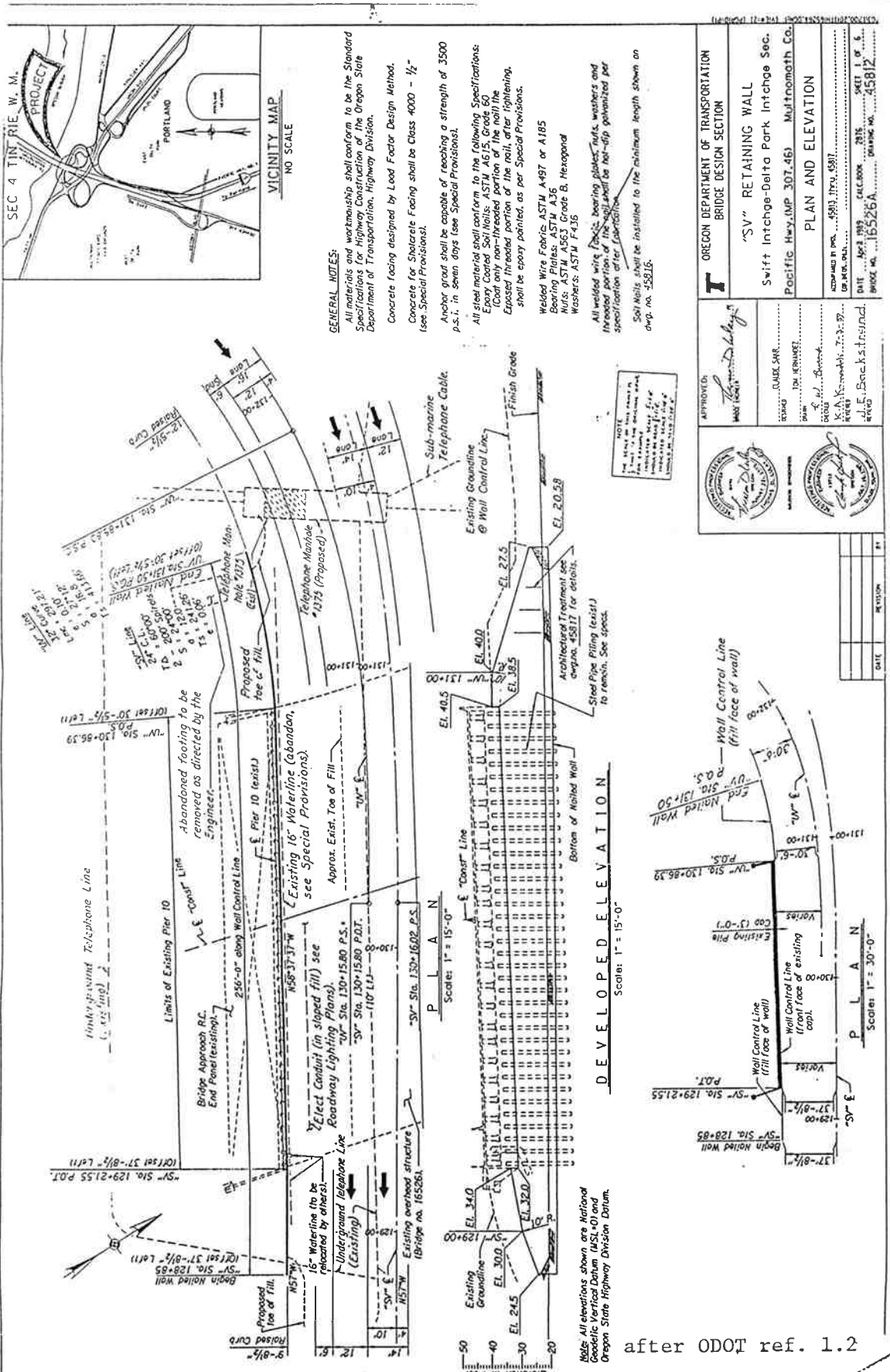
Figure 1.1 Project Location on Interstate 5 in Portland, OR

SEC 4 T1N R1E W. M.

PROJECT

PORTLAND

VICINITY MAP
NO SCALE

Area of PMT Tests   TP-1

End Nailed Wall
"UV" Sta. 132+00
30'-6" Lt.

132+00

D

TB-127

D'

B

B'

TB-124

TB-125

Section
S2

TB-128
131+00

A

A'

"S" ₵

"Const." ₵

Section
S1

114+00

"U" ₵

113+00

114+00

130+00

113+00

Existing Bridge Abutment

"U" Sta. 130+15.80 P.S.
"SV" Sta. 130+15.80 P.O.T.
(10' Lt.)

129+00

Begin Nailed Wall
"SV" Sta. 128+85
37'-8½" Lt.

C   TP-2

129+00

Proposed Wall

"SV"

C'
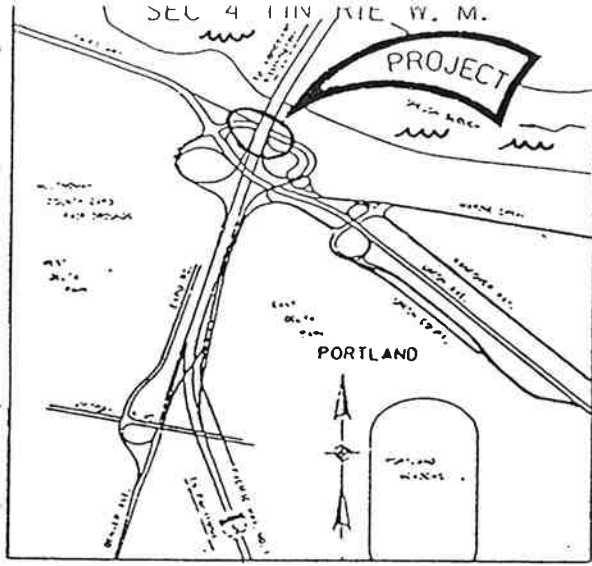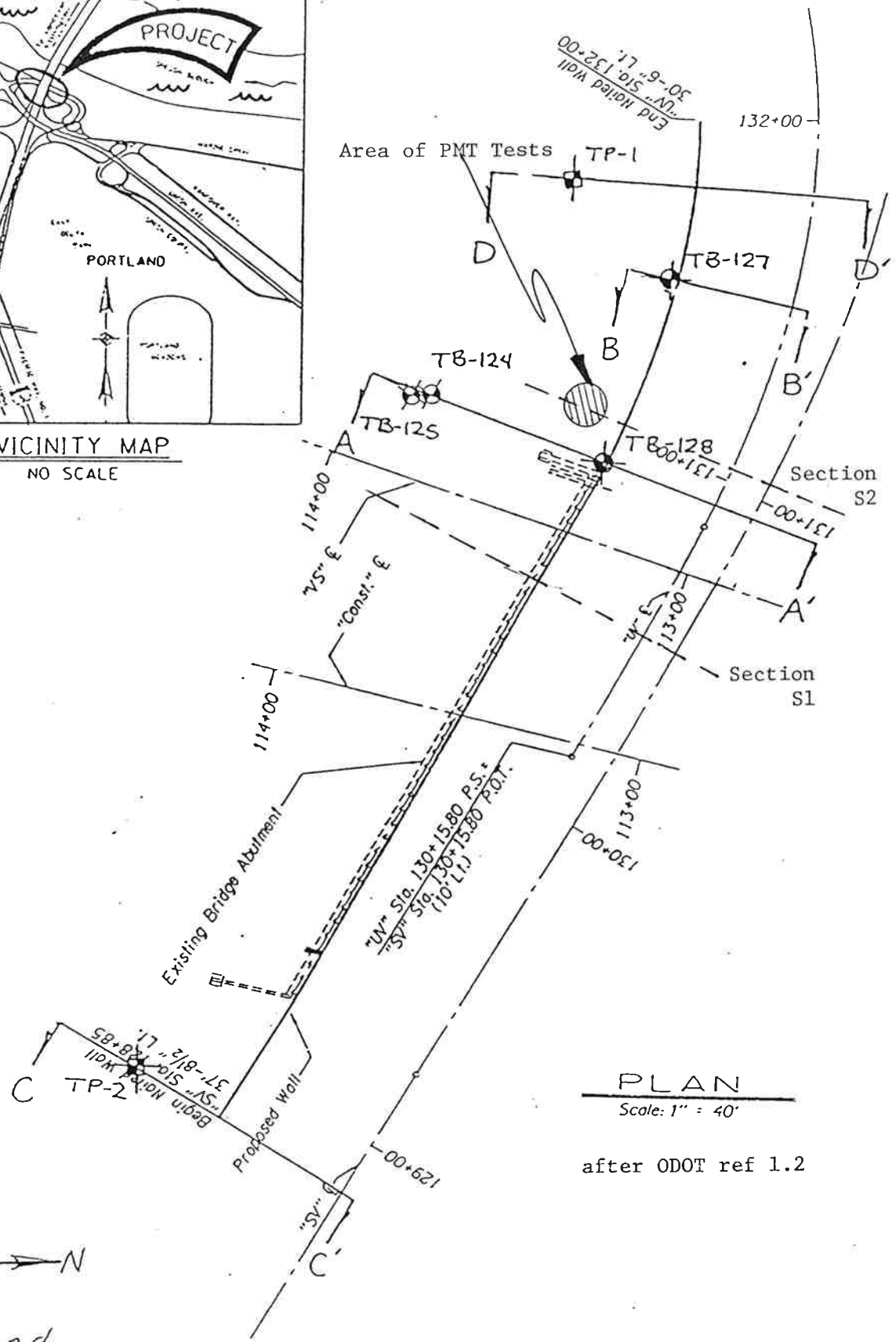
PLAN
Scale: 1" = 40'

after ODOT ref 1.2

N

Legend

Test Pit (TP)

Boring (TB)
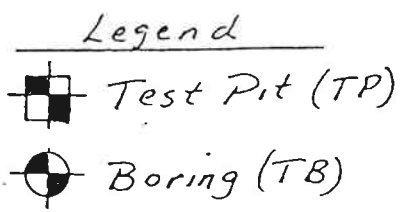
Figure 1.2 Locations of pertinent Test Pits and Boreholes for
the wall

5

TOP OF WALL

El.

40

30

SAND
$\phi = 32.4°$

BOTTOM OF WALL

20

▽ GWL

10

$\phi = 23.5°$
$c = 130 \text{ pcf}$
$\gamma_d = 90 \text{ pcf}$

0

New fill, Silt with gravels, fine sand
SM - GM - ML

Clayey Silt lens, ML
SPT 4 to 6 Bpf; torvane 0.5 - 0.75 tsf.

Clean Sand, SP. Medium dense, poorly graded
to uniform, damp to moist. $\phi = 32.4°$

Silt (Alluvium), ML - CL, trace to some clay,
trace fine sand. SPT 6-29 Bpf (increase w/depth.)
$\phi = 23.5°$, $c = 130 \text{ pcf}$, $\gamma_d = 90 \text{ pcf}$

GEOLOGIC PROFILE AT INSTRUMENTATION SECTIONS
(STA. 130 + 58.95 AND STA. 131 + 04.81)
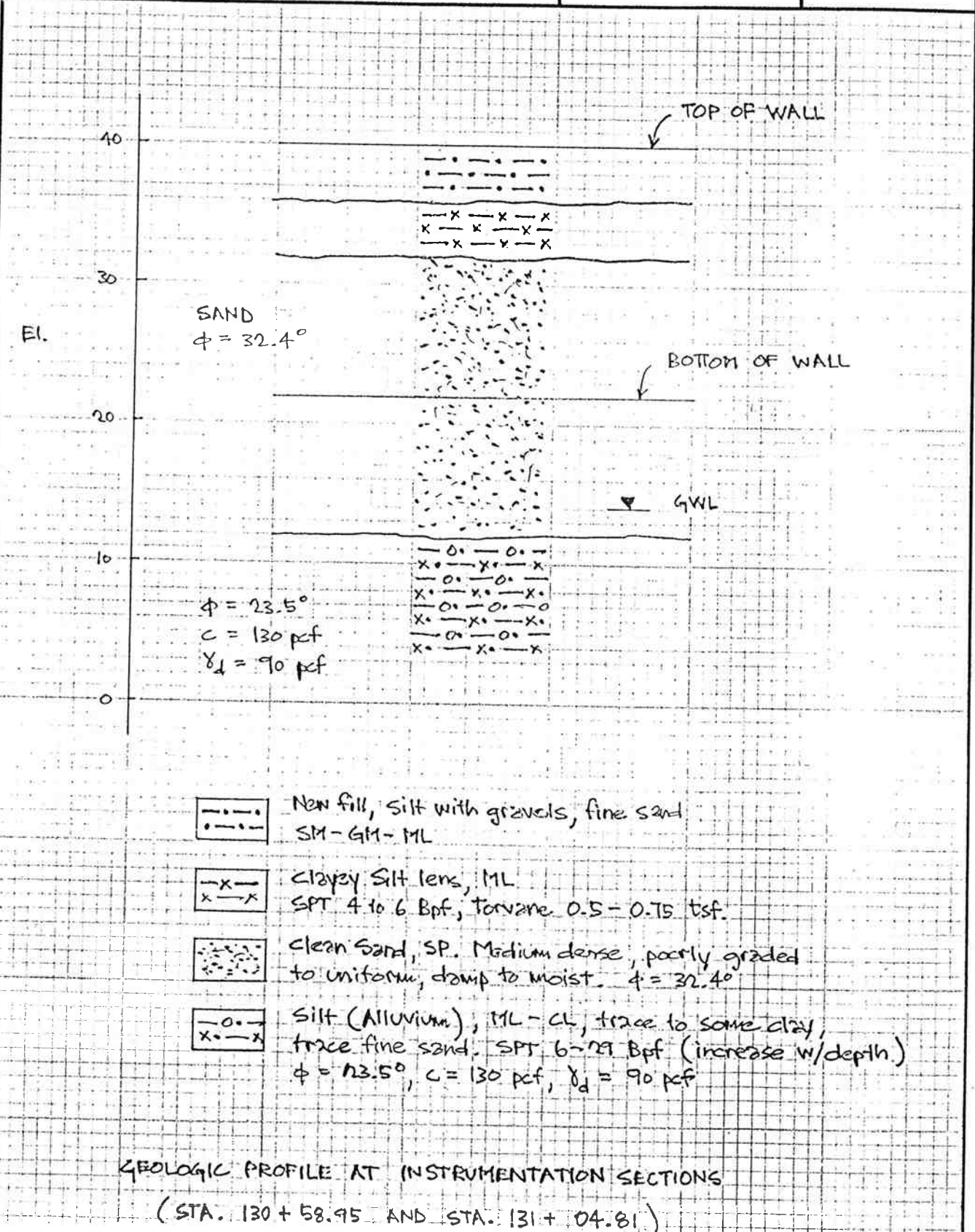
Figure 1.3 Simplified Soil Profile at S1 and S2 Instrumentation
Sections

6
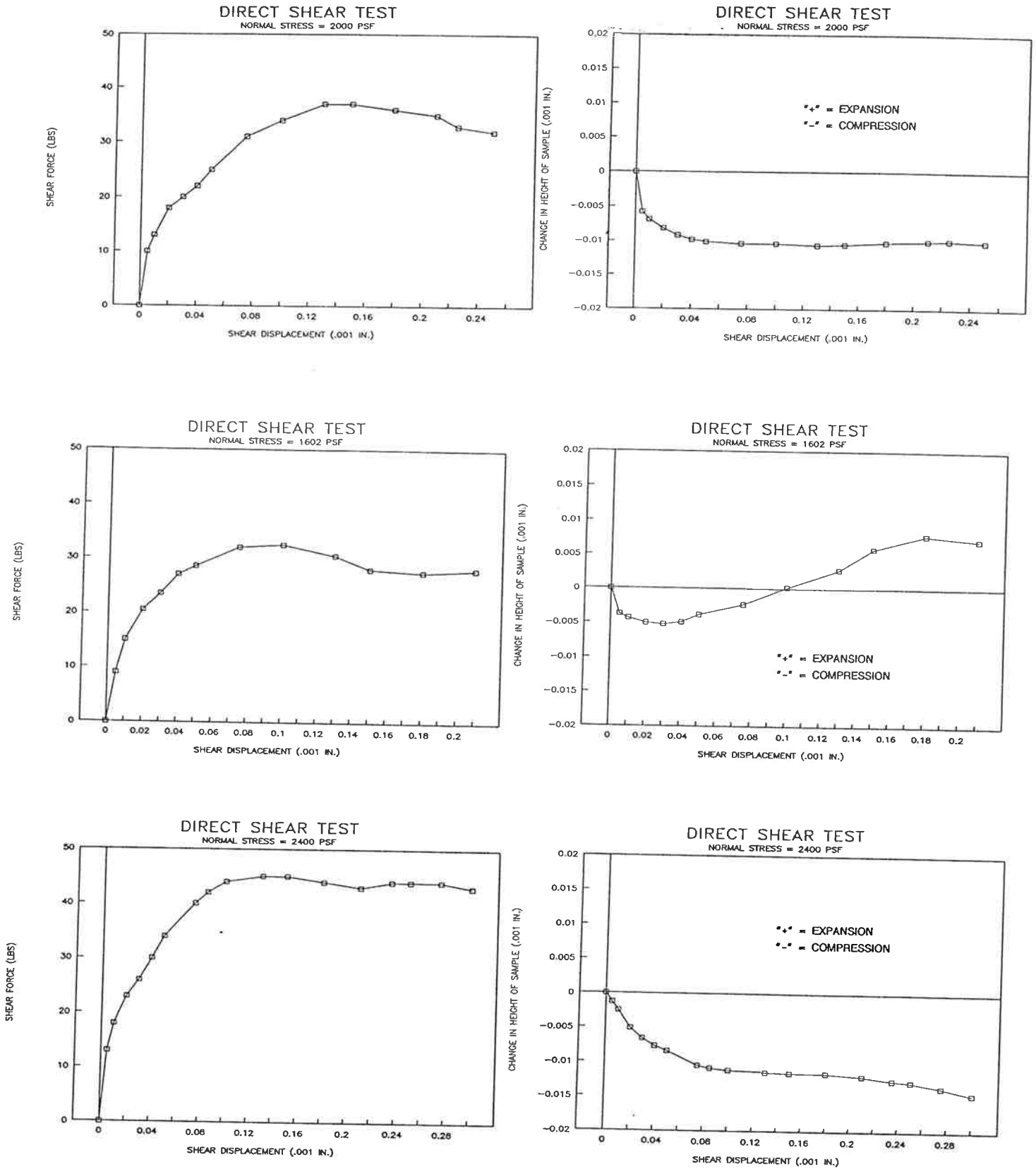
Figure 1.4 Direct Shear Test results on SP clean sand

7
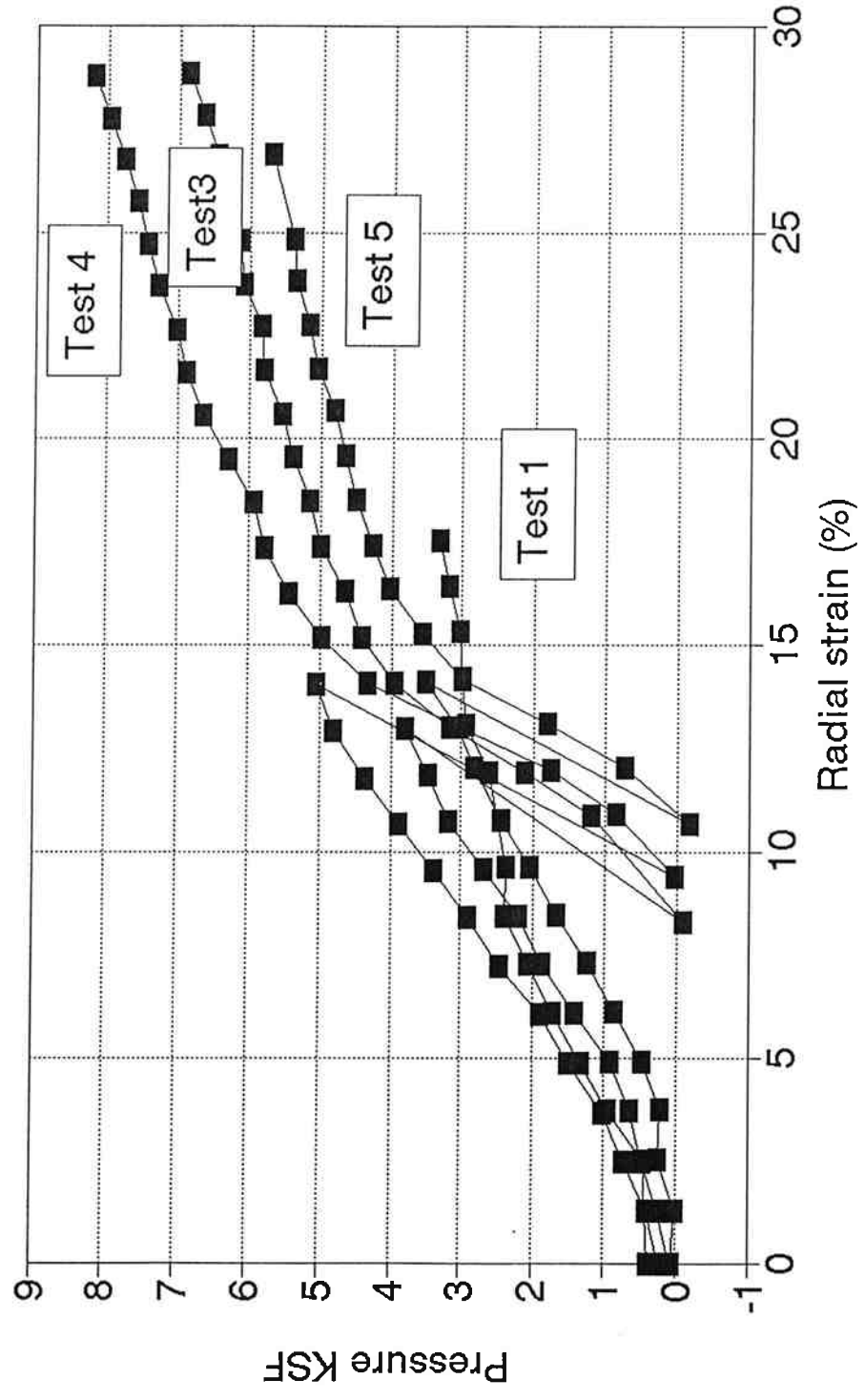
Figure 1.5 PMT Test Results with BX Probe
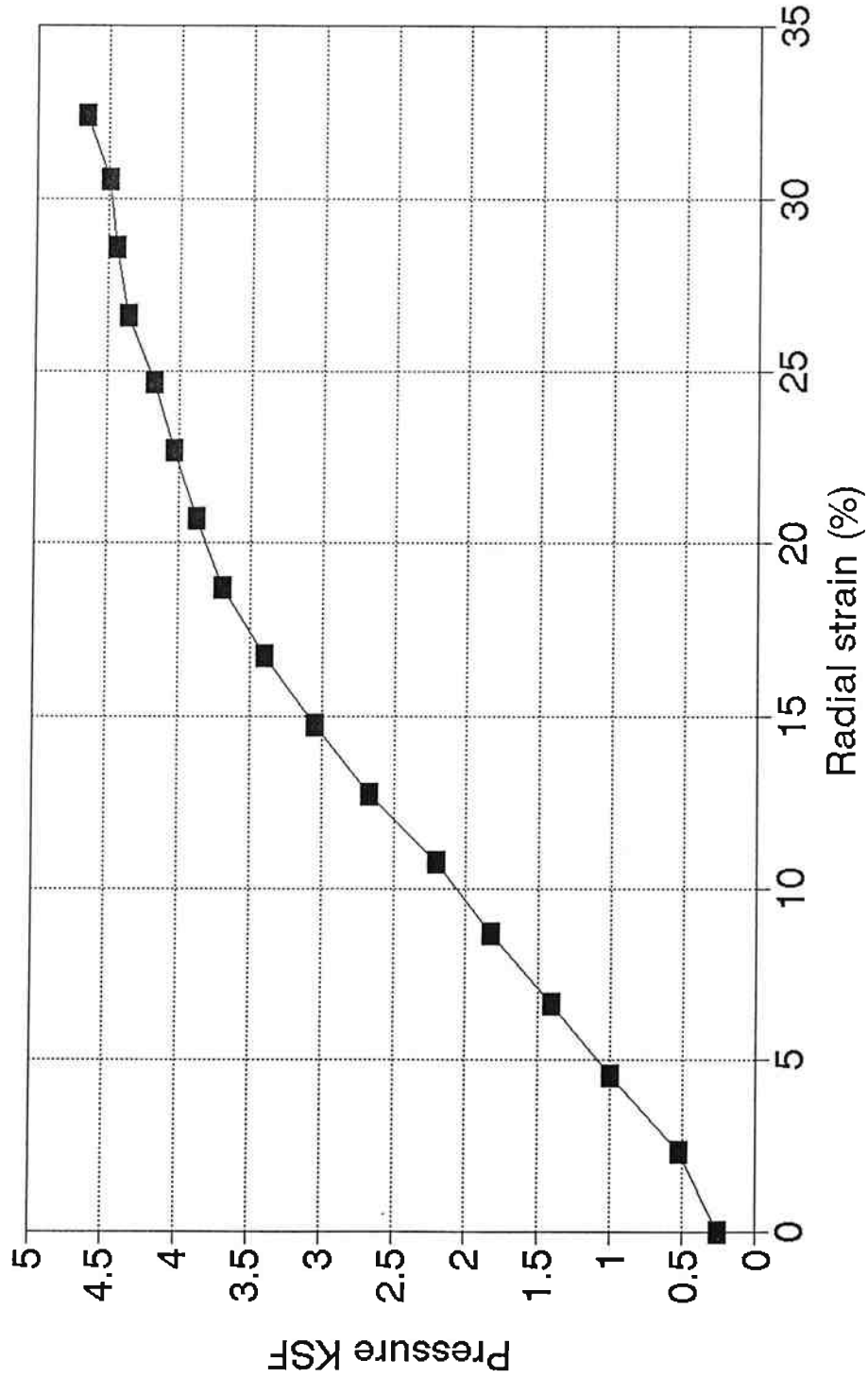
Figure 1.6 PMT Test Results with EX Probe
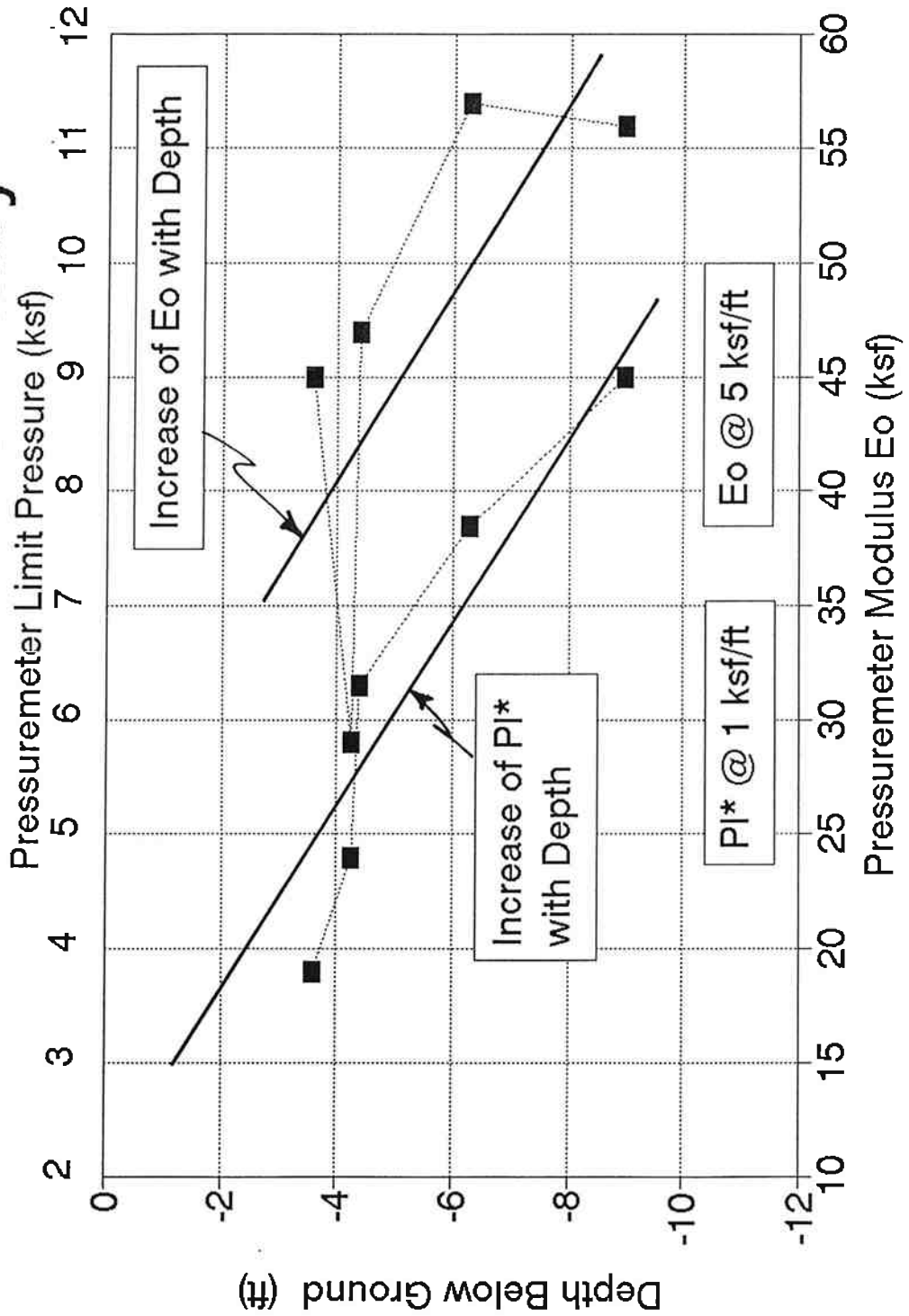
Figure 1.7 PMT Limit Pressure and Modulus Summary with Depth

2.0 INTERPRETATION OF MONITORED WALL PERFORMANCE

2.1 PAST WALLS

Prior to giving summary results and interpretation of the instrumentation data at Swift Delta a review of past instrumented soil nail walls is helpful. A collection of monitored full scale and model scale wall performances was made by Elias and Juran (1991). With respect to deflection they noted very little deflection data is present in the literature but did generalize their observations as:

- Angular distortions decrease with higher nail length/ wall height (L/H) ratios

- The ratio of top of wall horizontal deflection to vertical settlement increases with decreasing L/H ratios, to a maximum of 1.0

- The ratio of wall top horizontal deflection to wall height (H) for most instrumented projects is typically in the range 0.001H to 0.003H

- Increasing nail inclination will increase movement and angular distortion at any point. This becomes worse for nail angles over 20 degrees.

- In general model scale data overpredicted deflections 2 to 4 times.

From four full scale working projects in Pennsylvania, Kentucky, California and France Elias and Juran (1991) conclude maximum nail forces are never fully developed at the end of construction but increase for months after, with no discernable increase in lateral deflections. These nail force increases ranged from 15 to 35% of the end of construction forces, as a minimum, in the first 6 months.

They also concluded that maximum working nail forces in non-plastic, cohesionless, uniform soil showed good comparison to measured when the classic Terzaghi and Peck empirical braced excavation wall pressures were used. For the more complex geometries and soil layers, particularly cohesive soils, very poor comparisons were found. No data was found with respect to any sites having vertical foundation piles, which might better match the Swift Delta features.

Denby, Argo and Campbell (1992) reported upon the movements given by inclinometers behind the 21 m (68 ft.) deep soil nail wall used as temporary support for a parking garage in Seattle. They observed maximum horizontal wall deplacements in good agreement with the relationship

$\Delta X = 0.002H$, where H is the height of excavation, and ΔX is the horizontal deflection. Vertical downward movements approached horizontal movements. They also commented that exposed outwash pockets of sand and gravel soil at 13.7 m (45 ft.) caved frequently. This was attributed to the increase in vertical shear stress due to the downward movement of the shotcrete wall, necessary to mobilize the soil resistance on the shotcrete to soil interface.

Pile movements approaching 75 mm (3 in.) were observed by Finno (1991) when a deep excavation was made close to a heavily loaded pile supported cap. The retaining wall system in this instance was comprised of tie backs rather than soil nails.

Of more direct relevance is the laboratory and full scale testing results presented by Juran, et. al., (1990). So called 'working stress' predictions were made based on their 'kinematical' solution, which assumes that soil shear resistance is fully mobilized along the potential sliding surface at all times during construction. Their predictions still remain to be independently verified using the kinematical method and the validity of some of their assumptions are in doubt.

2.2 SWIFT DELTA INTERCHANGE PROJECT

The quality and volume of the instrumentation data from Swift Delta provides a unique data base unmatched in other instrumented projects. Wall and soil horizontal movements continue to be detected by 4 inclinometer casings, two were set 1.07 m (3½ ft.) behind the wall in the vicinity of S2 and two within the shotcrete wall, with SD 132 near S1 and installed prior to the final finished shotcrete application. A horizontal pile cap extensometer was also installed and anchored 18.6 m (61 ft.) into the fill. Further, pile cap rotation was monitored by 3 tiltmeters installed at the west and east ends of the cap, plus the mid point. Nail behavior is monitored at both sections S1 and S2 by pairs of axial strain gages located along the full length of each nail, in addition to electronic load cells at nail layers 1, 3 and 5 on the wall face. Two earth pressure cells were positioned against the shotcrete face midway between nails adjacent to S1 and S2. Finally, an attempt was made to capture induced bending stress in the piles by attaching 2 vibrating wire strain gauges to each exposed front face of two adjacent piles, at depths of 1.5 m (5 ft.) and 3 m (10 ft.) below the cap.

A summary of the geometric position of all instrumentation is given in Figures 2.1, 2.2 and 2.3 taken from the instrumentation data review paper of Kimmerling and Chassie (1993). For an overview summary of both Kimmerling and Chassie (1993) and Sakr, C. (1993) the following discussions and figures are limited to that data most relevant to the FDM and FEM predictions reported in later sections of this report.

Figures 2.4 and 2.5 show the short term midrow strain gauge readouts (in micro strain) along layer 3 nails only at S1 and S2. Both short term and long term (up to end of 1992) trends indicate increasing nail loads (using average strain) with time. Of some significance is the pronounced nail bending stress indicated at S1, from Figure 2.4, at gauges C1/C2. The pronounced bending may arise from the vertical shotcrete wall "slip" to mobilize shear behind

12

the wall, induced by the subsequent excavation lift. The same bending is indicated in row 2 and 1 but not row 4 or 5 at S1 from the full results shown by Sakr (1993). Bending stress is also indicated at S2 for row 1 and row 2 with an interesting anomaly of reverse bending at the gauges C5/C6 of row 4 in short and long term. At S2 the bending does appear to influence the top nail over a larger zone length from the wall face, up to 1.6+ m (5+ ft.), when compared to 1.0 m (3 ft.) at S1. The top nail at S1 shows no bending in the short term. Recall S1 has the piles immediately behind the wall and S2 has a 2:1 slope with no piles present. Overall peak nail strains (and thus nail loads) are lower at S2. Vertical wall settlement was not independently recorded.

The amount of strain gauge data, still being measured to the present day, is very extensive. It is unclear what firm generalities can be made regarding nail loads, particularly when the average strain gauge based tension force is compared with the load cell mounted at the wall faces. The wall face loads shown for rows 1, 3 and 5 at S1 and S2, on Figures 2.6 and 2.7 respectively, are taken from the load cell data.

Clearly the magnitude of the variations of inferred load at the nail head from strain gauge data along the nail length are 3 to 10 orders of magnitude (row 1 on S2 to row 3 on S1) higher than the variations from load cell readings alone. This leads to two possibilities. The load cell data from beneath the nut is not representative of the load immediately behind the shotcrete face, or, rapid variations in strain (and shear transfer through the grout) exist between the shotcrete and first gauge. It should be noted that it is within this distance the piles are located at S1. In any event, when compared to the large changes in tensile load given by the strain gauges the load cell changes seen to have little relationship.

A calibrated grouted test nail curve was used to transpose nail axial strains to nail tensile loads. Figures 2.6 and 2.7 show a full set of nail loads at S1 and S2, respectively, through 10/28/92. These distributions match well with other instrumented soil nail walls and show peak loads present at a distance back from the wall face, close to midlength. The nail loads at the wall face, given by the load cell, are more likely in the short term to represent an adjustment from the 135 Nm (100 lb.ft) "lock off" torque, and remains close to constant in the long term. Face loads ranged from 20% to 40% of peak nail tensile loads, consistent with other walls. Wall earth pressure cells were deemed unreliable and are therefore discounted.

Extensometer pile cap movements show rapid early movements during construction of up to around 9 mm (0.35 in.), Figure 2.8. It should be noted that consistent with nail load increases was an outward wall movement for 2 years following completion of wall construction, Figure 2.9. This movement has no stopped. Ground movements at SD 129 and SD 130 (at S2) show double the SD 131 and SD 132 outward movement, at 20 mm (0.78 in.).

Of the four strain gauges attached to the front face of two existing piles, only gauge 21 shows any response, indicating in excess of 200 micro strain in tension. However, this indicates a pile tensile stress change of 44 MPa (6.38 ksi) on the front face (relief of compression). This would translate in bending to an increase in compression on the back face. In the absence of a 180

degree pattern of gauges the speculation that gauge 21 is responding to true pile bending is difficult to defend.

Overall the instrumentation evidence at S1 under the bridge deck, seems to indicate close to horizontal translation of the cap, further, 2 of the 3 cap tiltmeters give a zero reading. Horizontal movement of the wall top is of the order 12 mm to 19 mm (0.5 to 0.75 in.). Nail loads are responding by higher tension, possibly due to grout fracture from tension, and creep in the grout/sand interface.
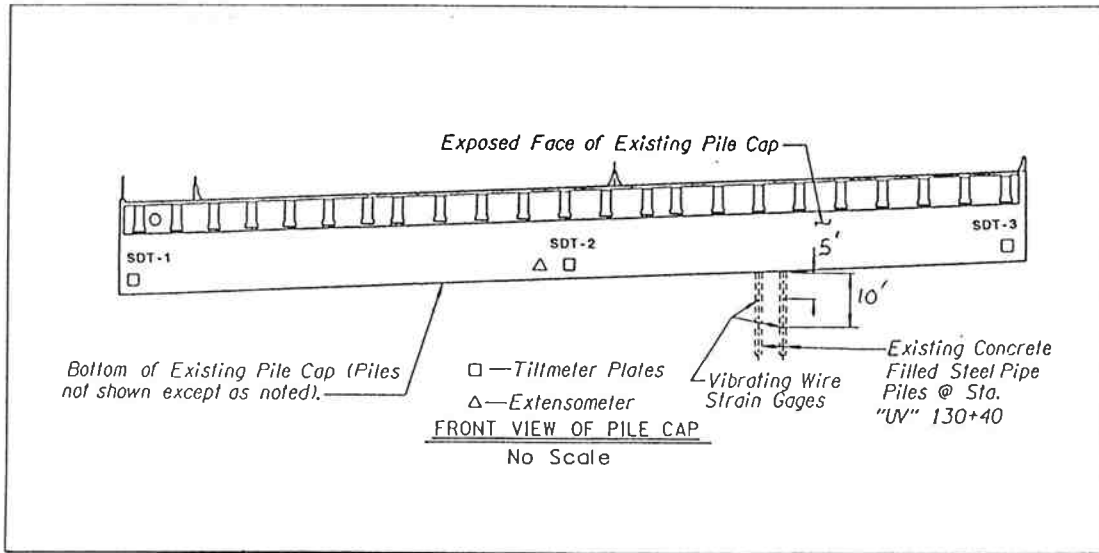
Elevation View of Instrumentation Locations
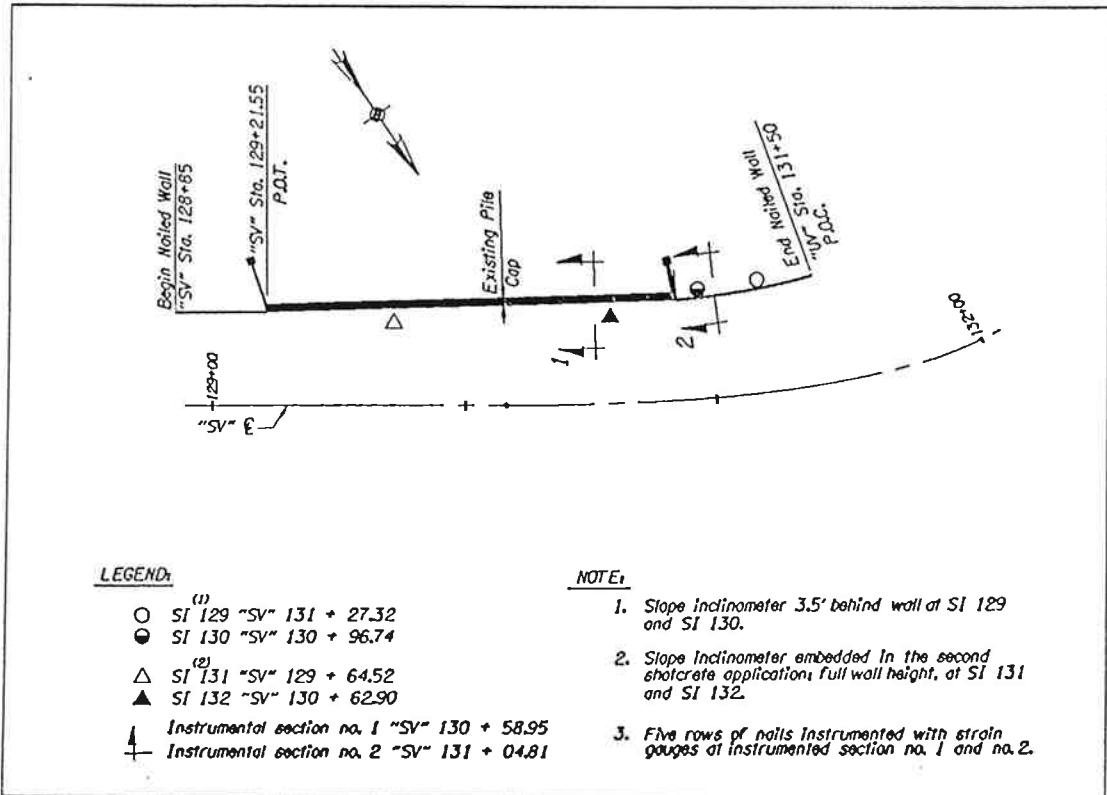
Plan View of Instrumentation Locations

Figure 2.1 Instrumentation Locations on Wall
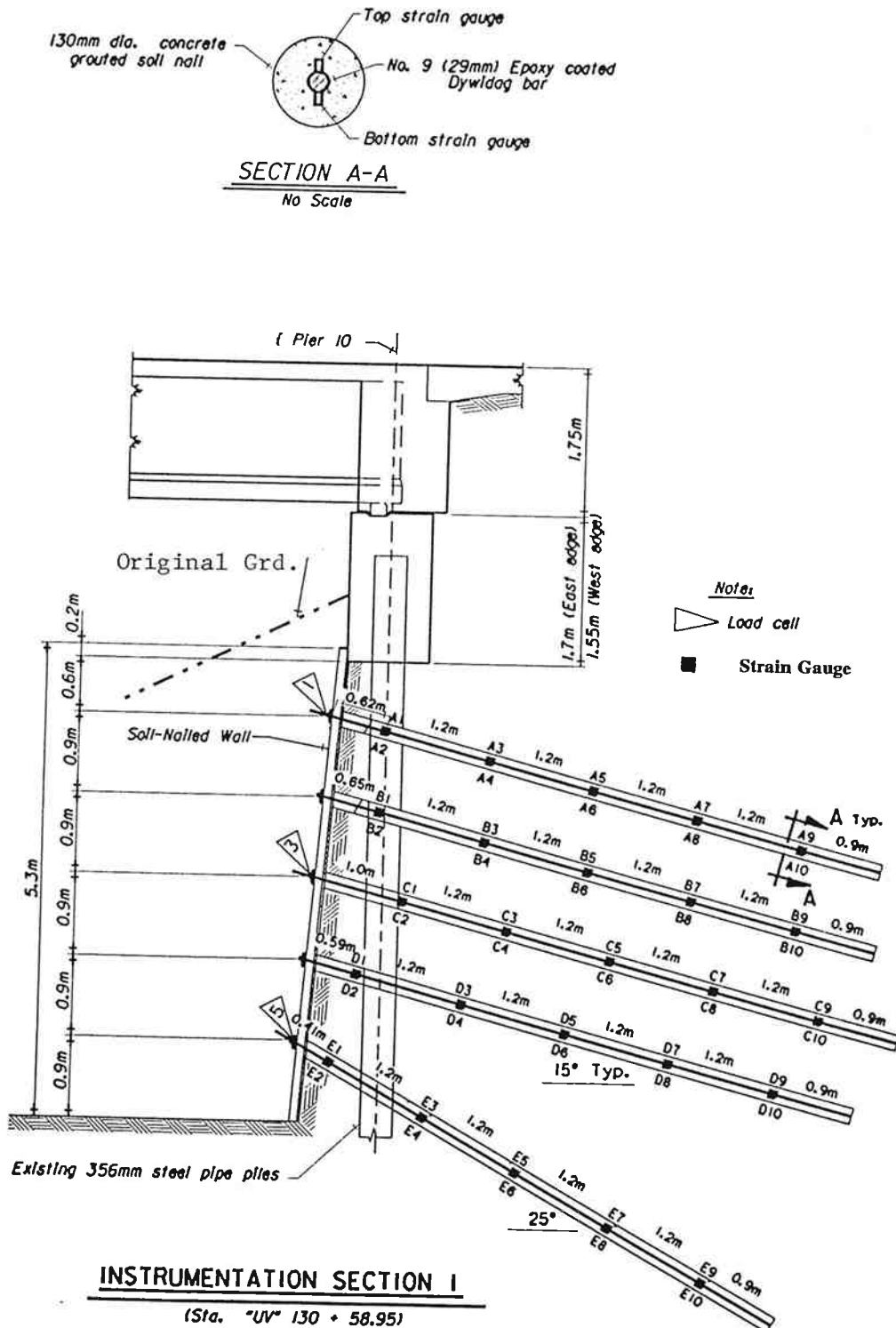
Figure 2.2 Instrumentation at Section S1
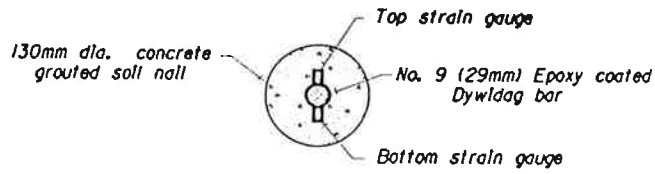
SECTION A-A
No Scale
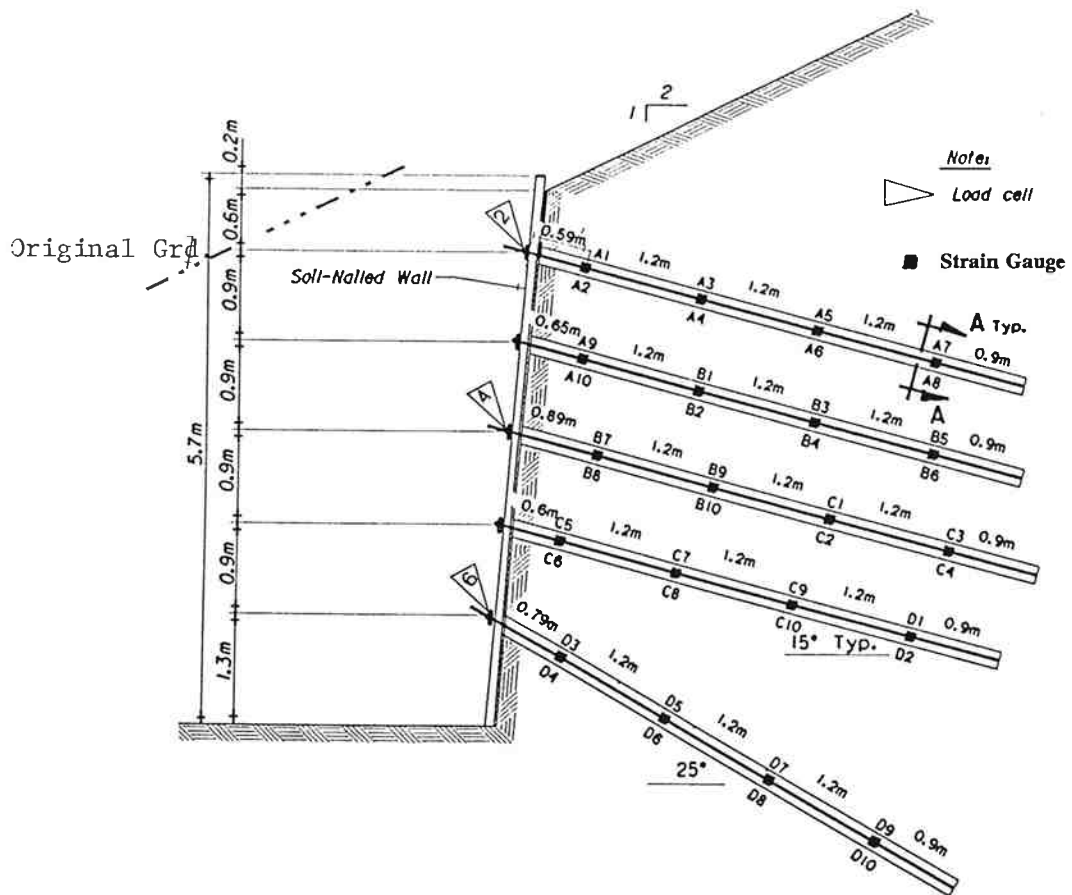
INSTRUMENTATION SECTION 2
(Sta. "UV" 131 + 04.81)

Figure 2.3 Instrumentation at Section S2
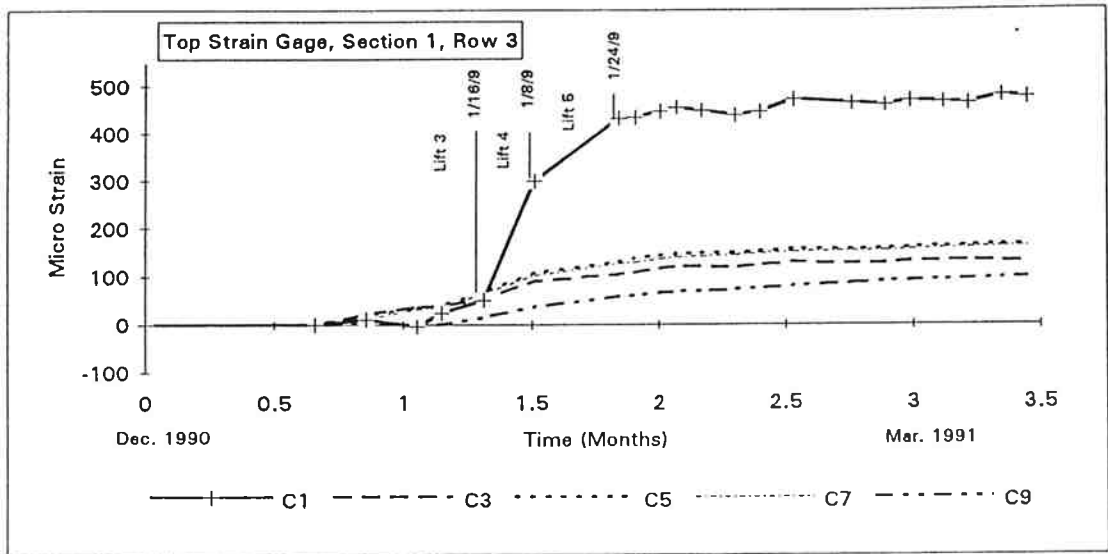
- Typical Short Term Readings of Top Strain Gage at Section 1
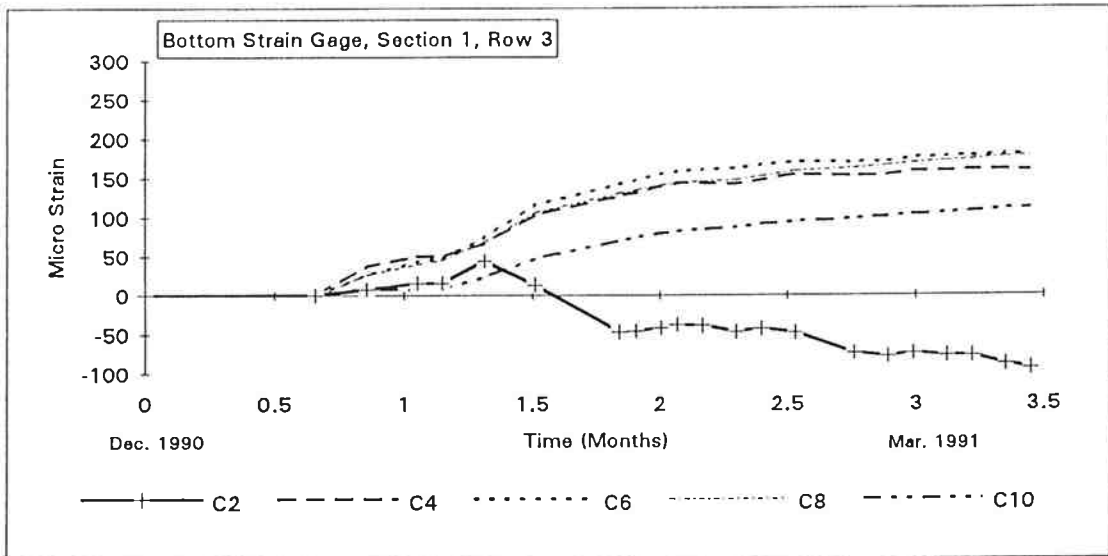
- Typical Short Term Readings of Bottom Strain Gage at Section 1
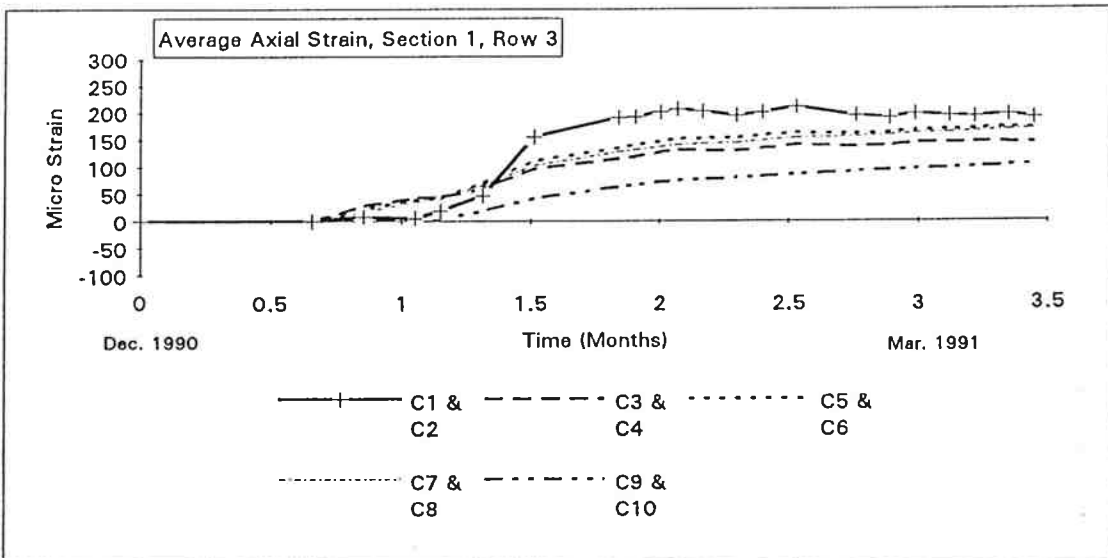
- Typical Short Term Average Axial Strain at Section 1

Figure 2.4 Short Term Nail Strain at S1
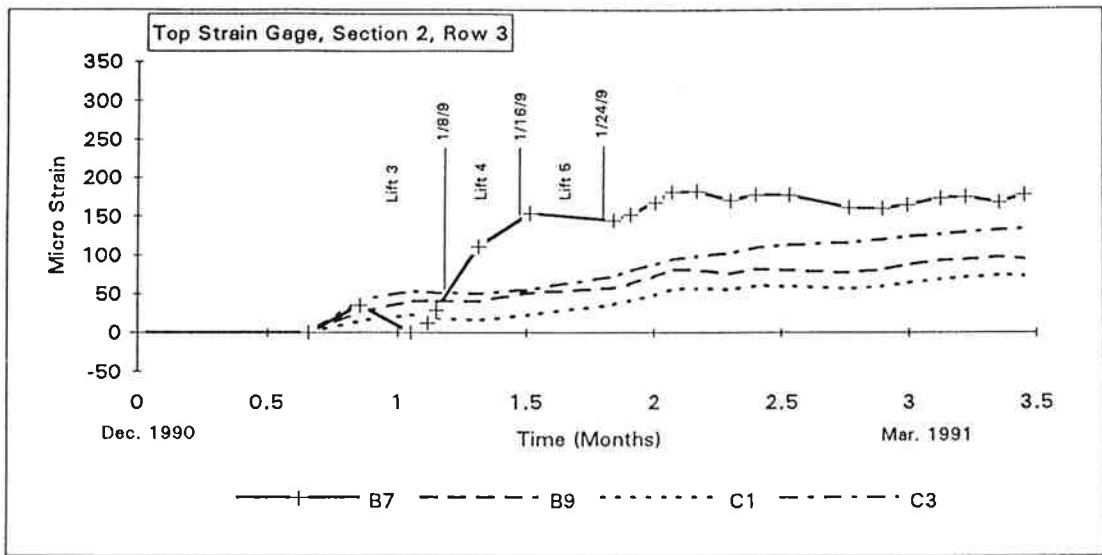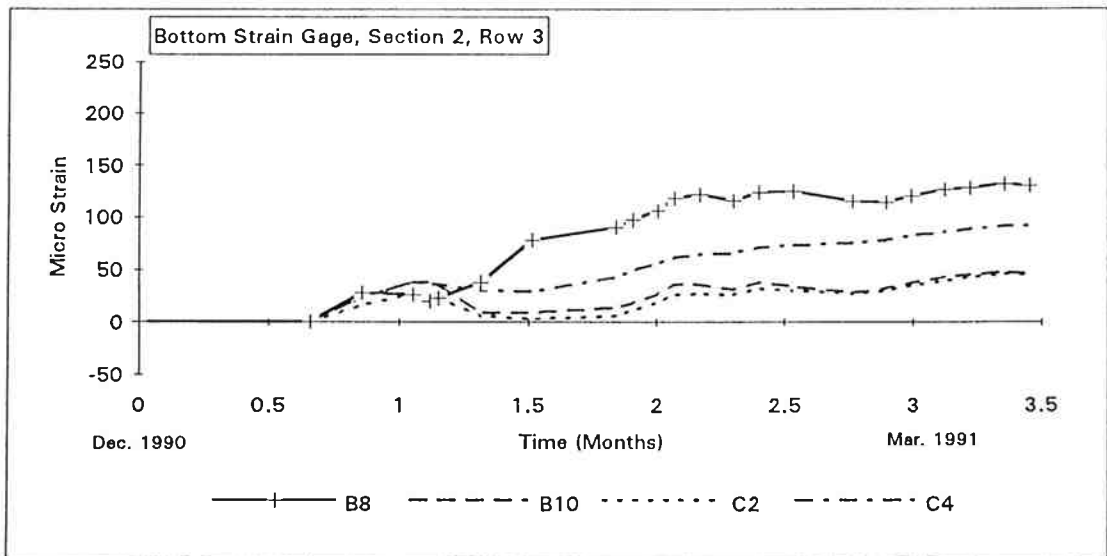
18

- Typical Short Term Readings of Top Strain Gage at Section 2

- Typical Short Term Readings of Bottom Strain Gage at Section 2
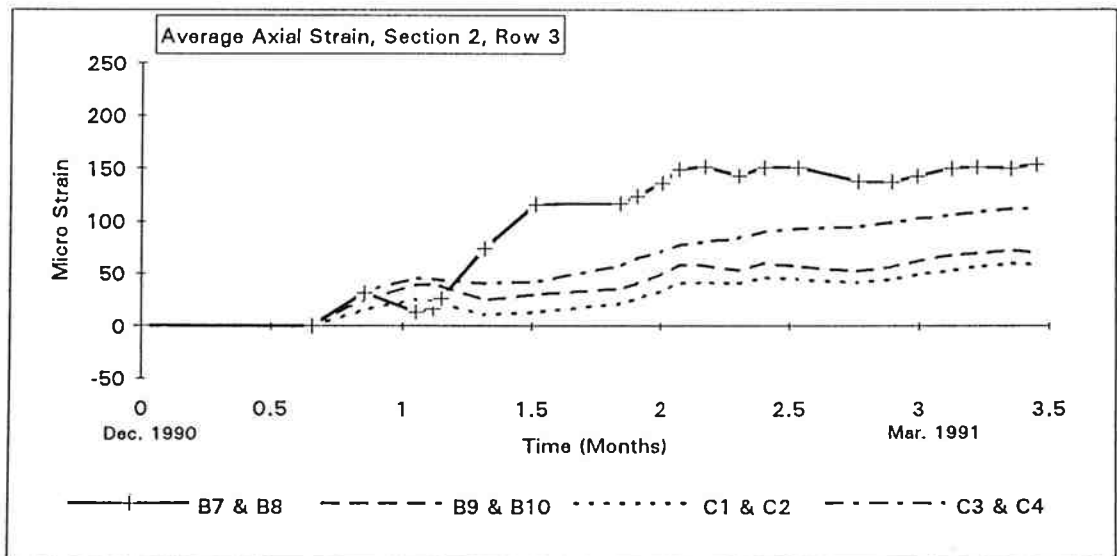
- Typical Short Term Average Axial Strain at Section 2

Figure 2.5 Short Term Nail Strain at S2
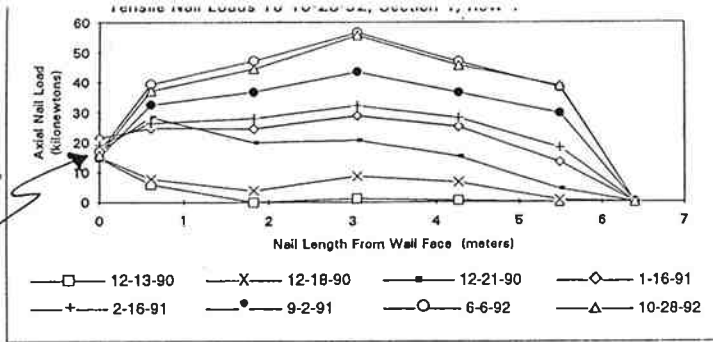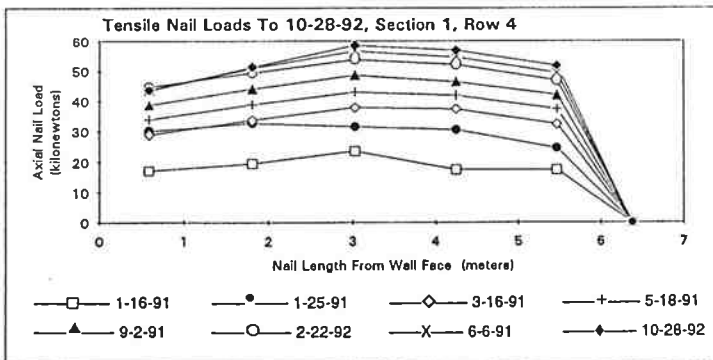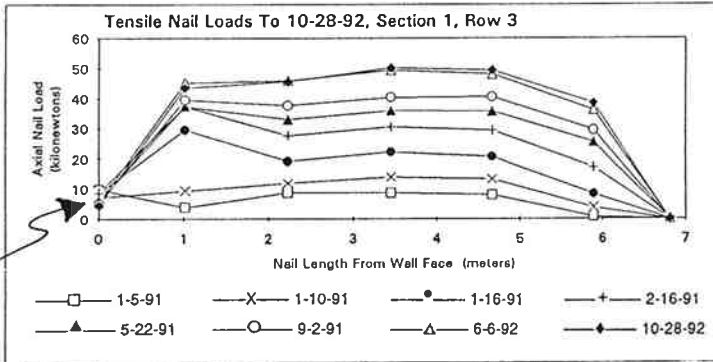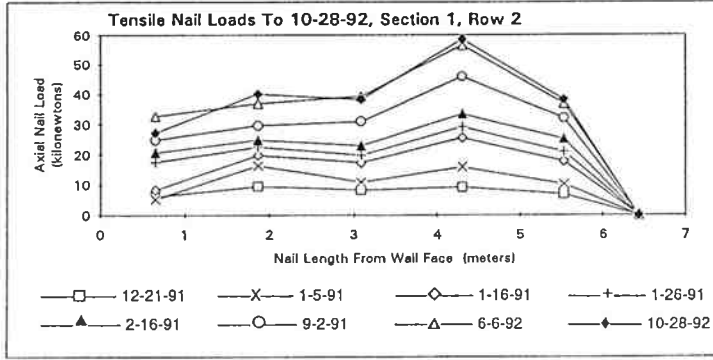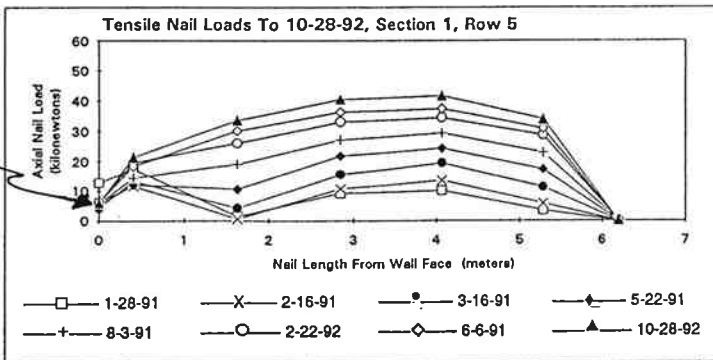
Figure 2.6 Calculated Nail Load, Row 3 at S1
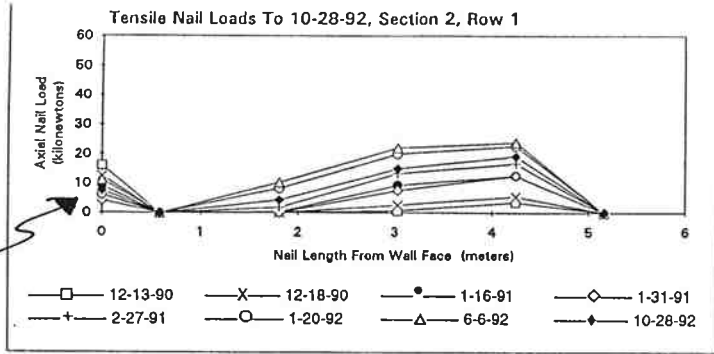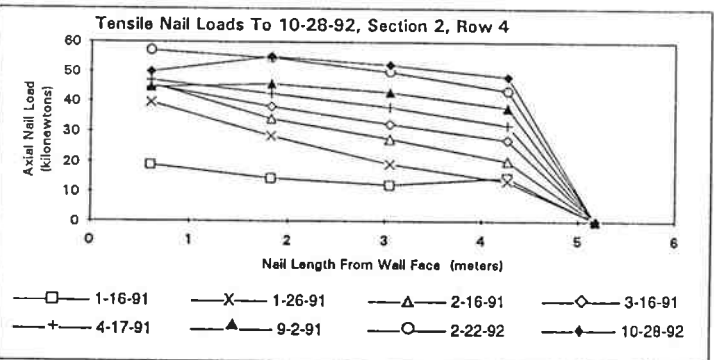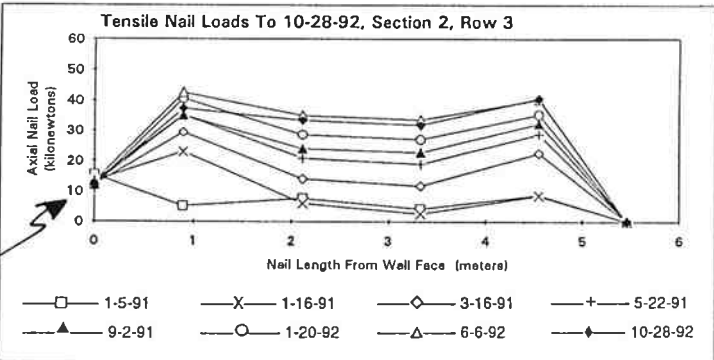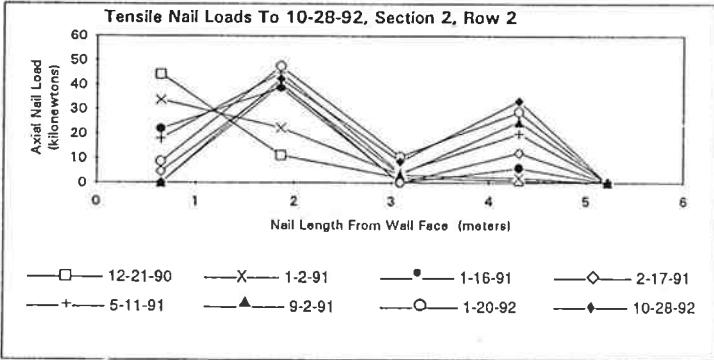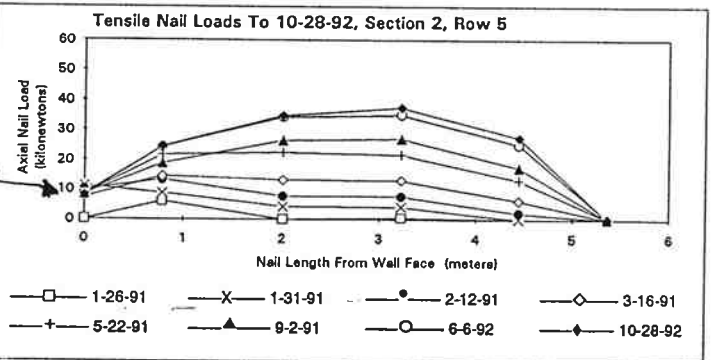
Figure 2.7 Calculated Nail Load, Row 3 at S2

21

Horizontal Single Point Extensometer @ Pile Cap
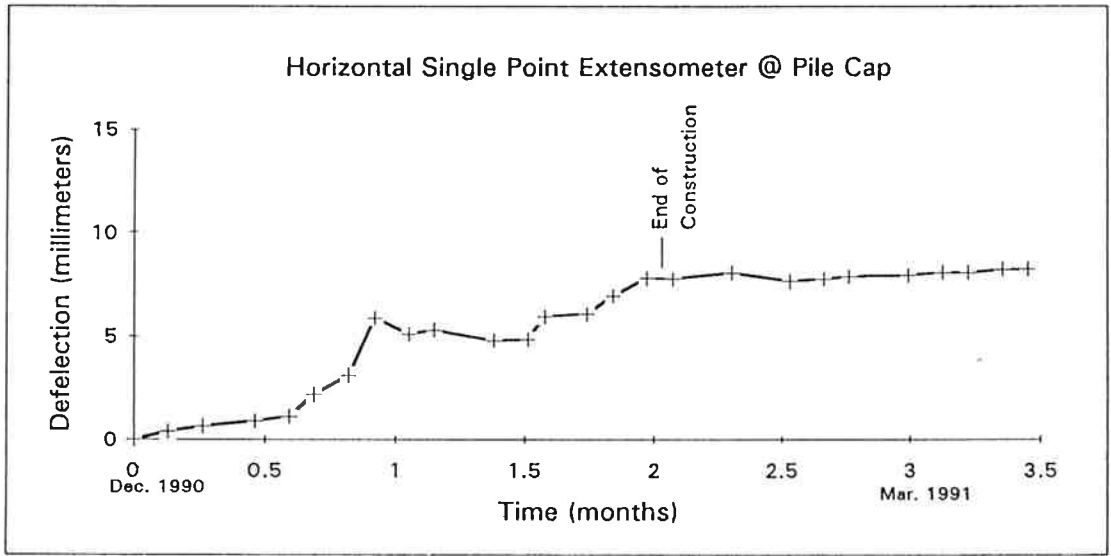
- Short Term Extensometer Readings

Horizontal Single Point Extensometer @ Pile Cap
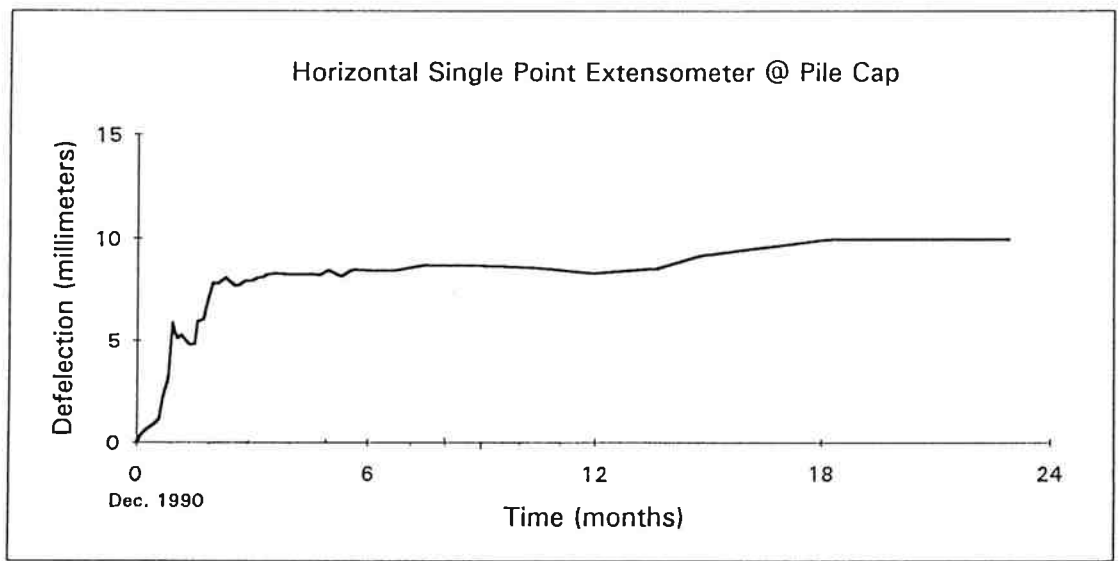
- Long Term Extensometer Readings

Figure 2.8 Short and Long Term Extensometer Data
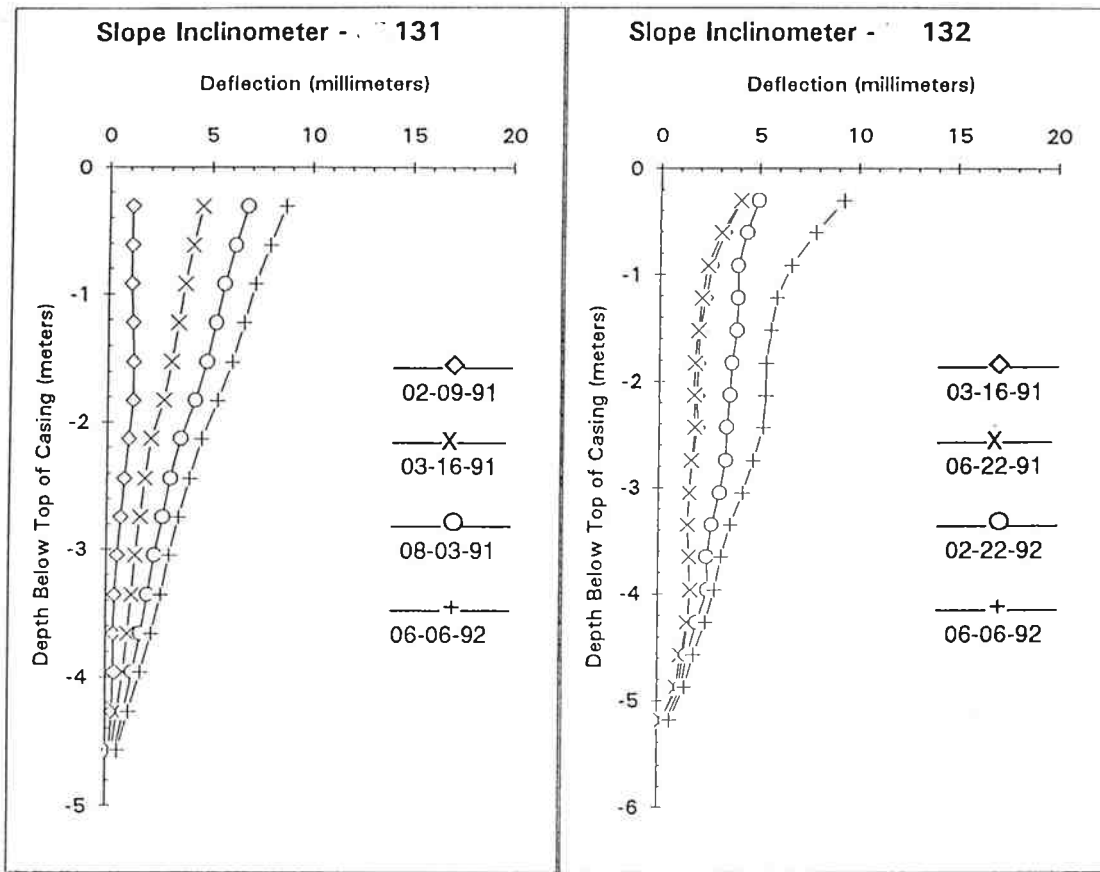
Figure 2.9 Inclinometer Data in wall at S1
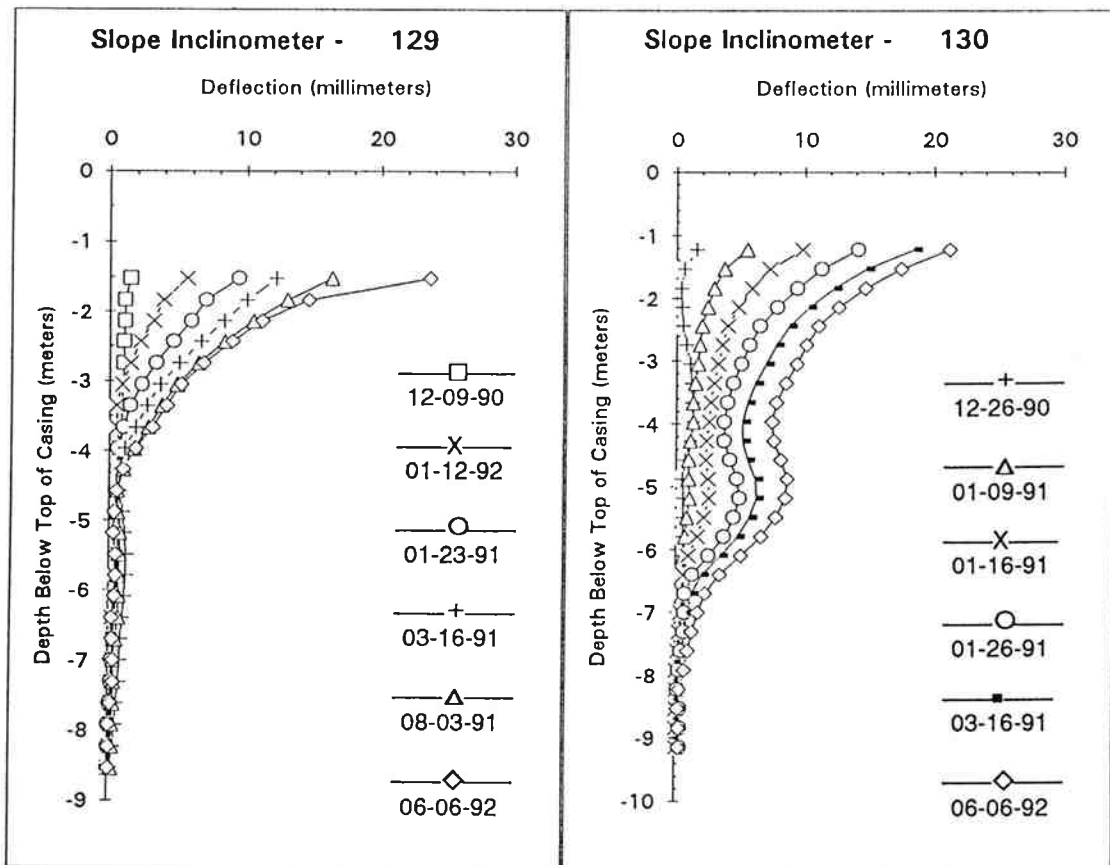
Figure 2.10 Inclinometer Data 1.0 m behind S2 shotcrete wall

THIS PAGE INTENTIONALLY LEFT BLANK.

3.0 NUMERICAL APPROACHES

3.1 INTRODUCTION

Design and analysis of soil nail wall projects in the U.S. typically use limit equilibrium slope stability analysis procedures, modified to include nail forces, Figure 3.1. The global safety factor expressed by these methods includes the effect of the pullout resistance of nails, but offer no understanding of the working behavior throughout the reinforced structural 'system'. The programs GOLDNAIL (1990) and SNAIL (1990) are of this type, the former in use for design by predicting nail loads, and lengths, with face pressures for a specified factor of safety, Figure 3.2. The latter code performs a factor of safety analyses for a prescribed wall by calculating critical failure surfaces and accompanying F values. These programs do not provide any understanding of the pile-soil-nail interaction present at Swift Delta. This category of problems, known as Soil-Structure Interaction problems, are most satisfactorily solved using true numerical approximation techniques, i.e. finite difference and/or finite element methods. However, the understanding of working level behavior cannot be obtained without additional engineering effort, and cost! The required input to completely describe the mechanical behavior of the soil, nail, pile, and shotcrete system increases almost exponentially. In this report the following finite difference (FDM) and finite element (FEM) codes have been employed, and are described below with their associated problem statement and computer platform. Each code is then more fully described.

3.2 FINITE DIFFERENCE SCHEMES

LPILE, COM624P: Pile deflection and bending studies to qualitatively assess the effects of excavation and soil to pile arching. DOS pc XT, 386.

BMCOL7: Derivation of idealized wall pressures from known nail loads. DOS pc XT, 386.

3.2.1 COM624P and LPILE

Both these codes are in use by ODOT for the deflection and bending moment analysis of a laterally and axially loaded vertical pile. COM624P was supplied by ODOT for use by the research group and contains techniques for the soil P-y spring response on both level and sloping ground. By way of feedback to ODOT a set of user comments on COM624P is provided in Appendix A. Following a study of valid wall pressures variations, given by matching nail loads with BMCOL7 nail output (see below), a variety of modeling scenarios were examined. These

include attempts to capture effects from slope removal, surcharge pressures and horizontal pressure arching from nails to the piles. Finite difference methods have no ability to follow the true chronology of boundary condition changes. Further, the absence of instrumentation data recording pile initial bending and deflections mean only a *qualitative* indication of pile distress can be made. Thus, statements on the 'relative' importance of the boundary condition changes, such as slope excavation, can be offered but little confidence in *quantitative* results is available. It is accurate to state both COM624P and LPILE give predictions of structural behavior only if the system had been constructed to a fixed, particular set of boundary conditions. Their use then for the nail-soil-wall-pile interaction problem is limited.

3.2.2 BMCOL7

The beam on elastic foundation models, so called Beam Column finite difference methods (FDM), solve the fourth order beam bending equations to arrive at deflection solutions for one dimensional structures that have normal loads and/or reactions (LPILE and COM624P are of this type). A single 356 mm (14 in.) diameter foundation pile behind the wall and a one unit (foot) length, along the wall, vertical section of the soil nail shotcrete wall, can both be studied by this method. BMCOL7 is a general purpose, menu driven, soil spring supported beam/column program (BMCOL7 1987) which allows nonlinear loads and soil supports at any point. The code is of most use in the equilibrium analysis of the completed shotcrete wall at S1 and S2 to establish possible earth pressure distributions. Detailed input and output are reported in Section 4.

3.3 FINITE ELEMENT SCHEMES

CAMFE: One dimensional analysis of a pressuremeter cavity to match the field measured data and help establish soil constitutive properties. DOS pc, 386.

ABAQUS: Three dimensional (3D) studies, reported in Section 7, of the full excavation sequence including pile, nail, soil, and shotcrete features. UNIX, SUN Workstation, CRAY-MXP.

FENAIL: Developed specifically for this project. Two dimensional plane strain and axisymmetric analyses are possible, with quad, beam, bar and interface elements for interaction analyses of pile and soil nailing. DOS pc 486(16MB RAM, minimum at 33 MHz, with math co-processor recommended).

The only previously reported FEM code written specifically for soil nail wall studies has been developed at University of Illinois, i.e. the code SNAP (Salama 1992), however, the code to date is not available yet for general distribution. In the absence of any other general FEM codes the research group was committed to the production of an entirely new code that contained the

specific features required for soil-nail-pile studies, FENAIL (1993). It is considered to be the most sophisticated FEM approach yet available for soil-nail-pile work on DOS machines.

3.3.1 ABAQUS

The ABAQUS package is a comprehensive well documented code (ABAQUS 1992) designed as a multi-purpose coupled static/mechanics/thermodynamic modeling modular set. A number of uncompiled modules, a wide array of element types and constitutive models, permit large extensive analyses to be attempted. The code can be leased only and resides on UNIX operating system machines, including a Cray-MPX supercomputer. This was available on the Geotechnical SUN workstations in Civil Engineering at PSU and through internet link to the Cray-MPX at the San Diego Supercomputer center to run the 3D problems. Access, manipulation and output from this code is accomplished by the PATRAN (PDA 1992) post processor code leased from PDA Engineering, Palo Alto, California. Example output is shown in Figure 3.4. The soil models employed in this Swift Delta study include: linear elastic isotropic, elastic anisotropic and Drucker Prager plasticity.

3.3.2 FENAIL

The code composition was contracted to Geotechnical Engineering Modeling (GEM). The framework for the FENAIL code was drawn from the Soil Analysis Code (SAC) written at University of California-Davis (Herrman and Mish, 1983) and is a second variant of the MADAM code (Smith 1992). The code is a 2D static plane strain program which models excavation and construction sequences for Soil-Structure problems. Soil nails are modelled by axial, truss or beam elements. The wall shotcrete facing is modelled as beam elements of zero thickness. Soil to structure contact face (interface) elements are also available. The range of constitutive models include linear elastic, anisotropic elastic and hyperbolic plasticity with c and phi frictional behavior for soil. Standard node and element output are produced, including load/time step files for post processing via TECPLOT code (TECPLOT 1993). This FENAIL/TECPLOT combination produced the cover of this report in color postscript and a gray scale is presented in Figure 3.3 of typical horizontal stress contours for the Swift Delta problem. FENAIL was written in FORTRAN 77 and compiled using a Watcom Fortran 77/386 for DOS systems on 386/486 personal computers. A DOS memory extender was used by the DOS 4GW memory manager. Larger models, using the multiple node features for interaction, require 16 MB of RAM and a minimum of 33 MHz to be available. A math co-processor is also required.

During the course of this research considerable time and effort was spent in debugging and attempting to define the practical limits of FENAIL.

3.4 SUMMARY

Full three dimensional (3D) nonlinear analysis, with complete chronological time scaling for gravity, slope, and six excavation nailed lifts is numerically possible. However, the enormous computational effort and time expended to reach a solution makes this impractical. The lack of quality comprehensive soil shear strength laboratory data further limits the confidence in this level of sophistication. The only available computing resources to handle large matrix inversions and track model nonlinearity are at the level of the supercomputer. Such a three dimensional nonlinear problem for Swift Delta cannot be attempted on the more readily available PC DOS 386/486 machine. Any three dimensional FEM approach is rarely attempted in Geomechanics, and only then linearly given the restricted access to supercomputers. This requires that the bulk of analyses be made assuming 2D plane strain conditions exist. As in any category of retaining wall structures, studies of soil nail walls, are well suited to the plane strain restriction with zero movement expected along the wall longitudinal axis. To understand the pile interference at Swift Delta, for a nail to pile center distance of 0.7m (2.25 ft.), there is a need to 'couple' the pile response through the soil to the nail response. This is described in Section 6 using the coupled node technique. However, description of the 'coupling' spring is not yet well understood, or defined. Three dimensional analysis of the behavior of Swift Delta are made in Section 7 for elastic, anisotropic and plastic models which contain a single nail (the top nail) to assess the piles contributions to global mass stiffness. Thus, only the 3D work can model the degree to which load transfer, by soil stress arching, may be occurring between the nail and pile. It can further explore whether the presence of the pile produces a significant increase in lateral stiffness of the soil mass and a reduction in expected soil displacements when compared to a soil nailed mass without piles.

Nail Tension Distribution - Limiting Equilibrium Analysis
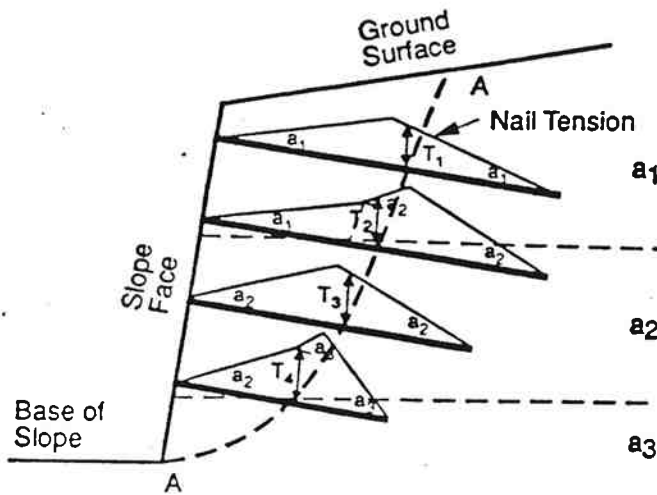
a = factored adhesion
(force/unit length)
A = ultimate adhesion
F = adhesion factor
F_p = pullout factor of safety

$a = A/F$ and $F \geq F_p$

$T_1 + T_2 + T_3 + T_4 \geq T_{Total}$
required to achieve specified
factor of safety for surface AA
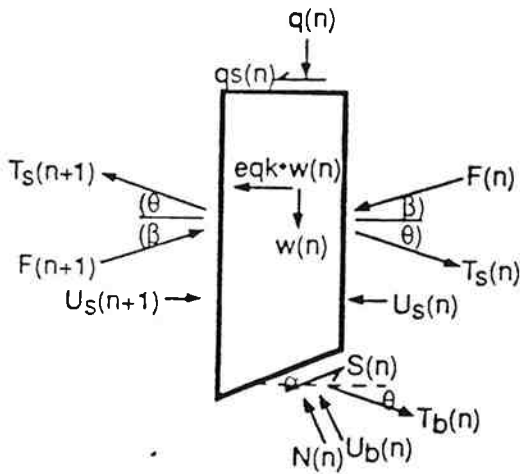
$w(n)$ = self weight
eqk = earthquake coefficient
$q(n)$ = normal surcharge
$qs(n)$ = shear surcharge
$U_S(n)$ = interslice water force
$T_S(n)$ = interslice nail force
$F(n)$ = interslice soil force
$U_b(n)$ = base water force
$T_b(n)$ = base nail force
$N(n)$ = base normal force
$S(n)$ = base shear force
   $= f[N(n)]/F_S$
F_S = soil factor of safety

Limiting Equilibrium of Typical Slice

Figure 3.1 Limit Equilibrium Force Assumptions

after Goldnail(1990)

TIE- BACK WALL

Facing

Tie -Back Strand & Grout

Failure Plane

Stress Distribution on Failure Plane

Stress on Tie Back Strand (Uniform)
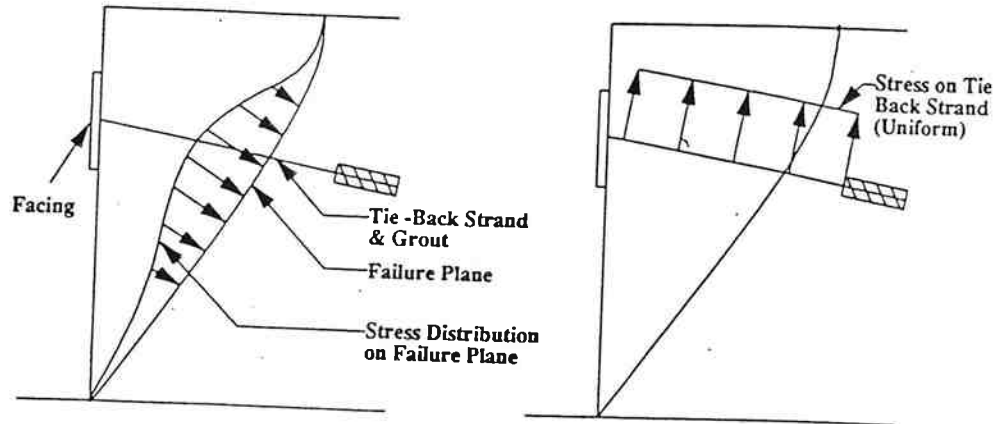
LARGE AND WIDELY DISTRIBUTED STRESSES ON ALL FAILURE PLANES DUE TO PRE-TENSIONING OF STRAND

SOIL NAIL WALLS

Fully Grouted Nail

Failure Plane
Stress Distribution on Failure Plane

Stress on Nail (Variable)
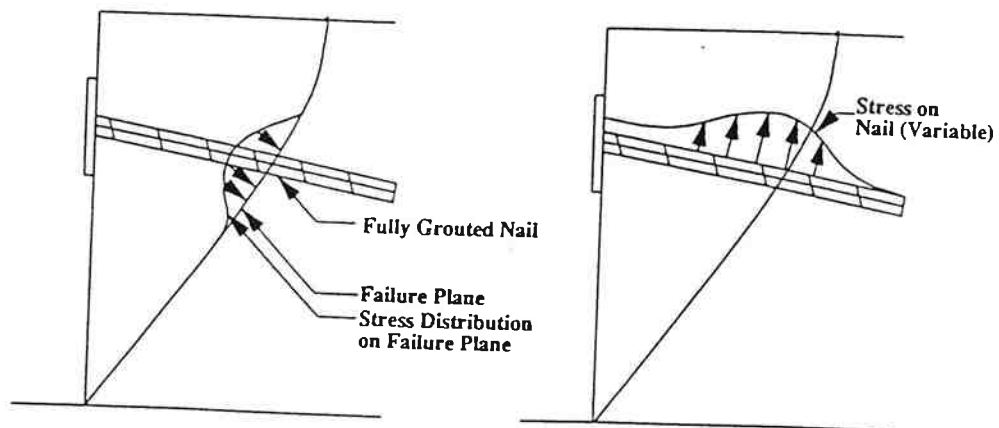
LOCALIZED AND SMALL TO MODERATE STRESSES ON FAILURE PLANES. NAIL TENSION DUE ONLY TO MOVEMENT OF SLIDING MASS ON INCLINED FAILURE PLANES. (NAIL BENDING AND SHEAR STIFNESS NEGLECTED).

Figure 3.2 Hypothesized Nail and Failure Wedge Stresses

after SNAIL (1990)

30
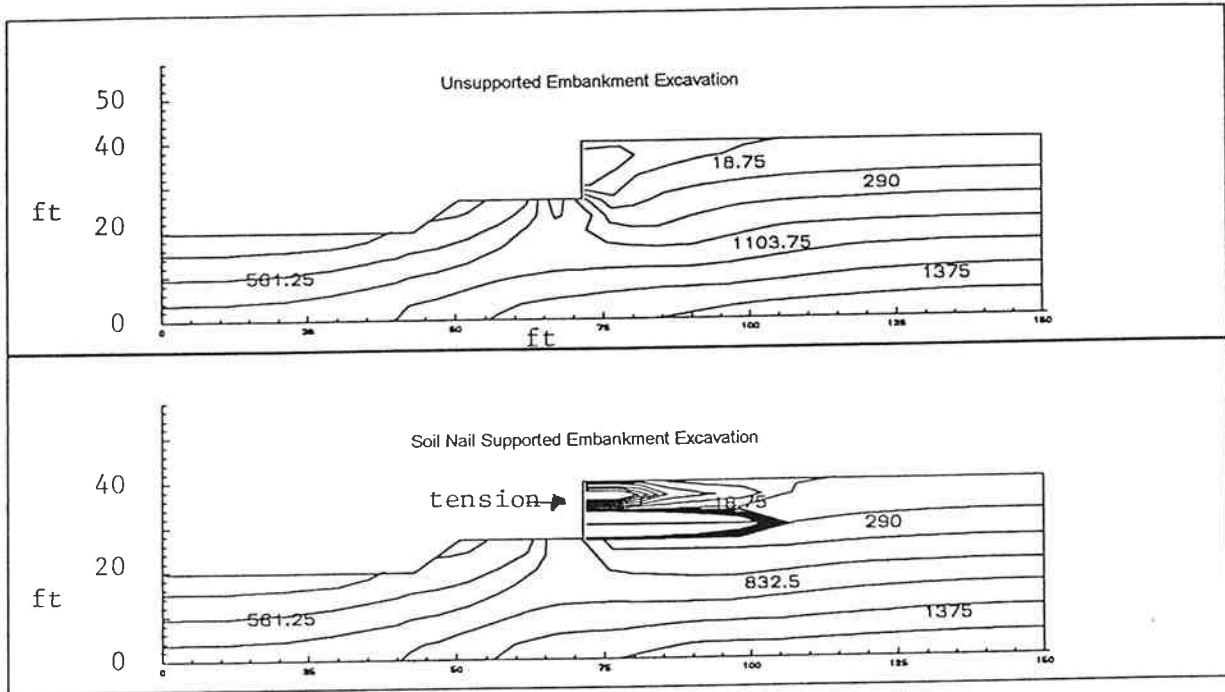
Horizontal Stress Contours For Embankment Excavation
13.33 ft. Removed, 2 Nails Installed

NOTE + compression, - tension (psf)
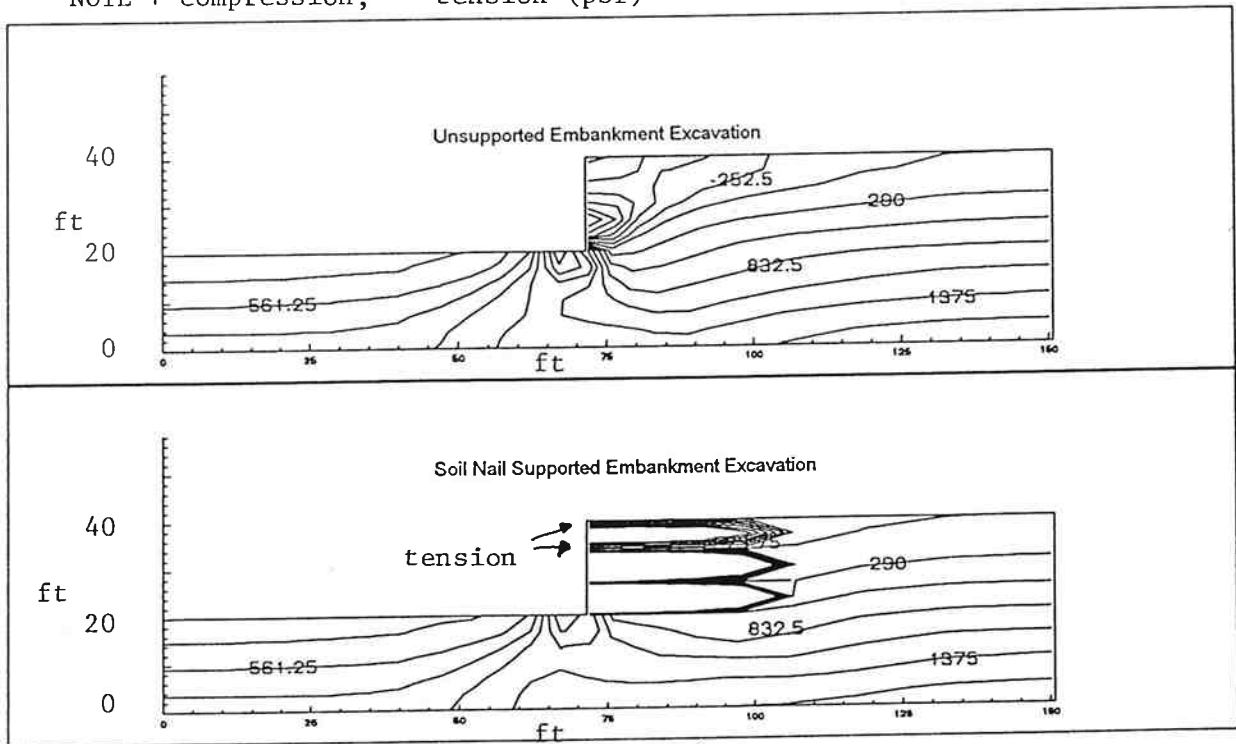
Embankment Excavation, Horizontal Stress Contours
20 ft. Excavation, 3 Nails Installed

Figure 3.3 FENAIL Stresses for Partial and Fully excavated cut, with and without nails

THIS PAGE INTENTIONALLY LEFT BLANK.
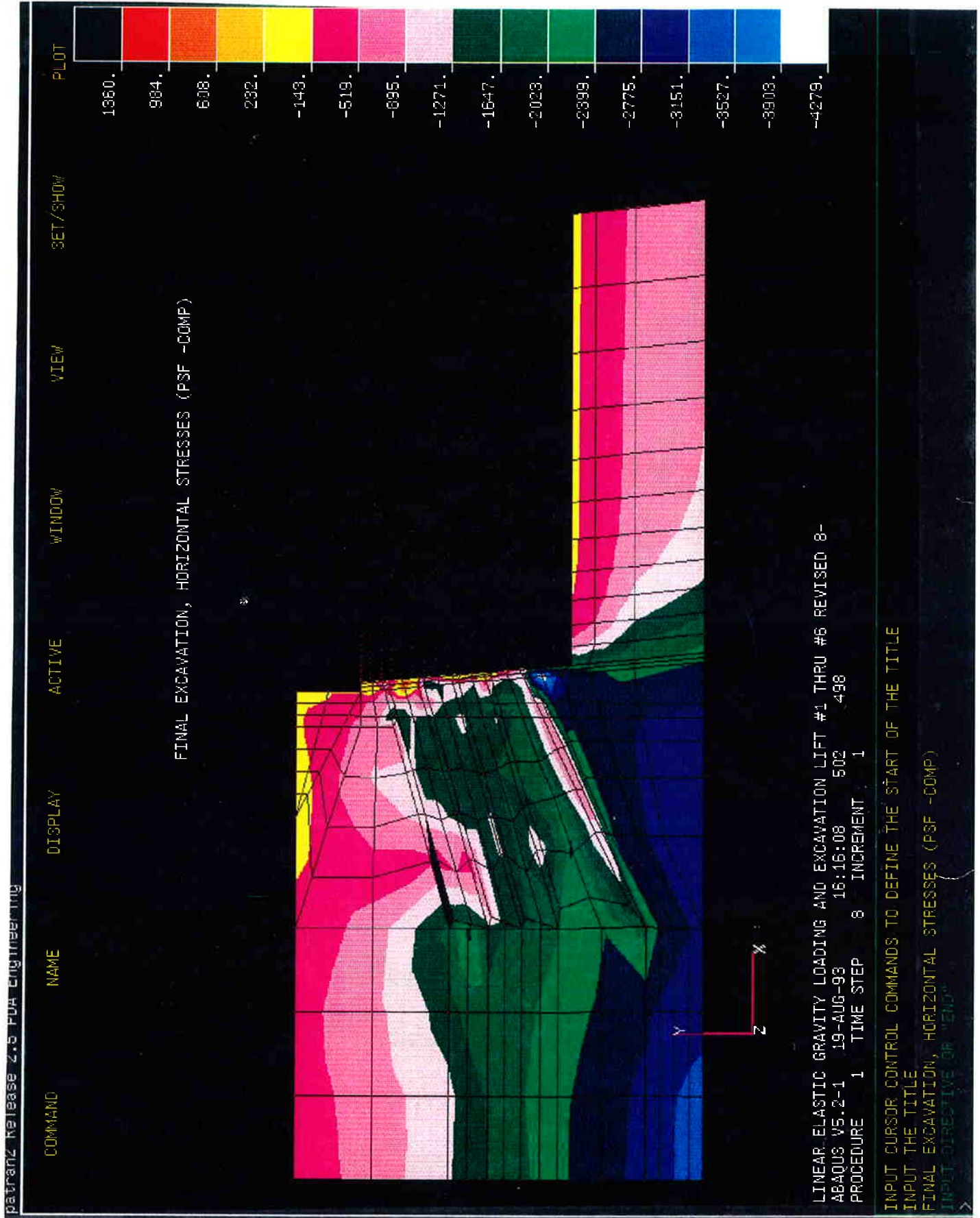
Figure 3.4 Typical ABAQUS Two Dimensional Horizontal Stress at Full Excavation

THIS PAGE INTENTIONALLY LEFT BLANK.

4.0 BEAM ON ELASTIC SUPPORTS FOR WALL AND PILE MODELS

4.1 BMCOL7

In order to make full use of the laterally loaded pile programs COM624P and LPILE some measure of the soil pressure distribution on the back face of the shotcrete wall is necessary. Earth pressure cells on the Swift Delta wall failed to provide this distribution. By the use of BMCOL7 models representing the shotcrete wall the input soil pressure distributions could be varied in a simple parametric study to match output nail loads (from the load cell) with those predicted by BMCOL7. These soil pressure distributions then provide a basis for making an estimate of the magnitude of wall pressures lost by possible arching to the piles. A 0.3 m (1 ft.) longitudinal length along the wall at S1 and S2 was modelled with node spacing of 15.2 cm (6 in.) by the BMCOL7 FDM technique. The nails and soil pressures were represented by linear concentrated springs and input pressures respectively. By repeated modification of the input soil pressure distribution, a close match could be found between the normal component of the BMCOL7 output nail loads and the measured loads. The October 1992 Load Cell measured nail loads were used with the missing second and fourth row nail load linearly interpolated from first, third and fifth row data. With the load cell on the outside of the initial 8.9 cm (3½ in.) shotcrete, and unknown bonding conditions between the nails and shotcrete face through the wall thickness, the exact interpretation of these measured loads is uncertain. Wall sections S1 and S2 are both taken as 5.36 m (17'-7") high with a nail longitudinal spacing of 1.37 m (4½ ft.). With the FDM model analyzing a 0.3 m (1 ft.) longitudinal horizontal length all input must be reconstructed to this base length and wall <u>normal</u> forces and reactions described. Thus nail spring stiffnesses in the model, and all loads, make use of the cosine θ component, where θ is the nail inclination.

4.2 WALL

Long term shotcrete wall flexural stiffness was checked by the pc program STIFF 1 (1992) for any bending induced nonlinearity. All program execution was performed with English customary units and these are given here to aid clarity without an SI equivalent. The input can be summarized as follows:

35

Table 4.1 Flexural Stiffness Parameters

Width	12.00 in
Minimum Assumed Concrete Compressive Strength	1.50 ksi
Welded Wire Mesh Yield Strength	36.00 ksi
Modulus of Elasticity of Steel	29,000 ksi
Number of Reinforcing Bars	4.00
Number of Rows of Reinforcing Bars	2.00
Cover Thickness	1.25 in

STIFF 1 output shows that the wall bending stiffness (EI) changes less than 3% up to bending moments of 20 kip-in. under zero axial load. Rapid loss in EI occurs at around 28 kip-in. All

BMCOL 7 models treat EI constant at the uncracked section flexural stiffness of 7,000,000 kip-sq. in.

4.3 NAILS

Based on the October 28, 1992 readings, Table 4.1 summarizes the normal component (equivalent per foot) of the nail loads, measured by the load cells, at the locations given. BMCOL7 modeling is made using a nail spring stiffness response of (Nail Area x Steel Modulus)/Length.

4.4 EQUILIBRIUM WALL PRESSURES

Wall input pressures were manipulated through successive BMCOL7 executions to arrive at nail (spring) normal load predictions that closely match those measured in Table 4.1. Ten control points were specified to describe the magnitude and location of the soil pressure profile. The final acceptable predicted normal nail load component results are shown in Table 4.2 for both S1 and S2 and are compared to the measured Table 4.1 loads. Figure 4.1 illustrates the input soil pressure profile from these correct solutions and is used in the COM624P models described in the following section.

Table 4.2 Measured Nail Normal Load Components

S1 UNDER BRIDGE DECK

BMCOL7 Nail Position	Nail Measured Load	Nail Measured Load/1ft.	Measured Normal Load Component
2.5 ft	3.57 kips	0.808 kips/ft	781 lb/ft
5.5 ft			496 lb/ft (interpolated)
8.5 ft	0.96 kips	0.217 kips/ft	210 lb/ft
11.5 ft			247 lb/ft (interpolated)
14.5 ft	1.33 kips	0.301 kips/ft	283 lb/ft

S2 OUTSIDE BRIDGE DECK

BMCOL7 Nail Position	Nail Measured Load	Nail Measured Load/1ft.	Measured Normal Load Component
2.5 ft	1.68 kips	0.380 kips/ft	367 lb/ft
5.5 ft			480 lb/ft (interpolated)
8.5 ft	2.71 kips	0.614 kips/ft	593 lb/ft
11.5 ft			490 lb/ft (interpolated)
14.5 ft	1.82 kips	0.412 kips/ft	387 lb/ft

4.5 COM624P AND LPILE

It is recognized the state of the practice lateral load pile analysis codes are the FDM based COM624 and LPILE. Both are available from Ensoft, Inc. of Austin, Texas. The more recent COM624P code distributed throughout the State Department of Transportations network by the Federal Highway Administration (FHWA) contains adjustments to the soil response P-y curves for sloping ground. (Some difficulty was experienced by the Research group in using COM624P and a summary of these user comments appear in Appendix A). Finite element methods do not directly give bending moments and fibre stresses and strains for laterally loaded piles within the continuum model. Thus it is desirable to attempt some study of S1 using COM624P to evaluate the limits of these FDM programs for the more complex boundary conditions at Swift Delta. The study also provides an interpretive aid to the later FEM work by providing the likely relationship between predicted deflections from FEM models and bending moments. However the models described below do not represent routine use of COM624P and the validity of some boundary conditions is open to question.

A total of 4 pile model scenarios were assembled to study: slope effects, changes in P-y conditions due to excavation and possible soil arching, plus the maximum AASHTO 0.92 m (3 ft.) of permitted soil additional lateral surcharge live loads, Figure 4.2. The BMCOL7 predicted soil pressures from nail loads includes existing soil surcharge depths effects. The 36 cm (14 in.) diameter pipe pile with 6.35 mm (.25 in.) thick walls gave an I value of 10,626 cm^4 (255.3 in.^{4}) and yield moment of 141 kNm (1250 kip-in.) for 35 ksi steel. The concrete infilling is neglected

since this is unreinforced and is unlikely to contribute to bending stiffness. The 2H:IV embankment slope prior to wall construction was rejected on input by COM624P for unspecified reasons and a maximum of 18° was used to give a successful execution. The soil profile used for P-y generation is given on Figure 1.3. Recall *FDM have no capability to chronologically (time scale) modify input boundary conditions.* It was the intent of this FDM study to attempt to evaluate what additional bending stress and deflection is produced by the wall construction. The only meaningful deflection study is therefore to evaluate post-construction models to an original reference condition, and then attempt to interpret changes in deflection and moment.

Table 4.3 Predicted BMCOL7 Nail Normal Load Components

S1 UNDER BRIDGE DECK

Measured Normal Load Component	BMCOL7 Model	Load Difference
781 lb/ft	796 lb/ft	+1.9%
496 lb/ft	491 lb/ft	-1.0%
210 lb/ft	215 lb/ft	-2.4%
247 lb/ft	257 lb/ft	-4.1%
283 lb/ft	276 lb/ft	-2.5%

S2 OUTSIDE BRIDGE DECK

Measured Normal Load Component	BMCOL7 Model	Load Difference
367 lb/ft	340 lb/ft	-7.4%
480 lb/ft	490 lb/ft	-2.1%
593 lb/ft	566 lb/ft	-4.6%
490 lb/ft	491 lb/ft	-0.2%
387 lb/ft	399 lb/ft	-3.1%

4.5.1 Model 1 Reference Condition

Model 1 is a pre-construction geometry input state with soil slope, internal P-y curves and the use of 3 feet AASHTO live soil surcharge on a 20-ft x 20-ft plan pattern to 'excite' the model to give lateral loadings. This pattern was selected to generate lateral pressures from elasticity below the ground surface by the GEOTEK-PRO (1991) software, which load the pile. Output indicates around 0.25-in. of pile top deflection.

4.5.2 Model 2 & 2a P-y Curve Removal

Full excavation of the soil ahead of the pile is represented in Model 2 by removal of all lateral resistance P-y curves down the wall height 5.3 m (17½ ft.), preservation of the remaining boundary conditions is made from Model 1. The restraint offered by the pavement slab in front

of the wall prevents any critical depth effects to the P-y curves below the wall depth. Model 2a has the addition of soil wall BMCOL 7 pressures from S1, given in Table 4.2, and the total pressure is given in Figure 4.3. This effectively models the piles as a diaphragm wall with soil arching effects. COM624P is unable to model the restraint offered by the bridge superstructure after closing of expansion joints. Clearly the unreasonable level of deflection reached (in inches) from Figure 4.3 demonstrated these load levels cannot be felt by the piles.

4.5.3 Model 3 & 3a Full K_a Soil Pressure Arching

Model 3 input removes the AASHTO 0.92 m (3 ft.) of soil surcharge live pressure and the BMCOL7 load, and follows the hypothesis that 100% soil arching is present, with classic retaining wall K_a condition pressures, shown in Figure 4.4. Model 3a shows the effect of the addition of the AASHTO live surcharge. Given the resulting excess deflections from the K_a state the full 100% arching condition is not mobilized at Swift Delta.

4.5.4 Model 4, 4a & 4b S1 and S2 Pressure Differences

A more defensible assumption for any pile additional load from soil nailing is to consider the difference between S2 and S1 BMCOL7 wall pressures, Table 4.2, shed to the piles across the full 1.37 m (4½ ft.) width. Thus Model 4 has Model 2 P-y curves without AASHTO live surcharge. Model 4a has the addition of AASHTO live surcharge. Both Model 4 and 4a have the net difference in the BMCOL7 pressure profiles from Figure 4.1. Following the rationale that pile lateral restraint in front must be present (from the nails) would suggest the final reaction transfer is shed back behind the piles through soil nail restraint, provides Model 4b input. Full COM624P P-y curves are again reacting against pile movement over the full wall height in Model 4b. Pile deflection and net pressures profiles appear in Figure 4.5 for the Model 4 series. The apparent anomaly of the pile negative deflection is the result of slightly higher S1 pressures compared to S2 at the near surface.

4.6 DISCUSSION SUMMARY

The pile deflection results of the COM624P investigation rules out a *quantitative* interpretation of the Swift Delta Interchanges soil-nail wall performance, for the reasons discussed in Section 3, a *qualitative* interpretation only is possible. Site instrumentation indicates that maximum pile top deflection is on the order of 8 mm to 13 mm (1/3 to 1/2 in.). Model deflections on the other hand, ranged from 75 mm to 630 mm (3 to 25 in.). To develop a more accurate model of the S1 conditions would require a more detailed description of the soil conditions under the bridge deck and behind the wall (eg. soil layers, relative densities, moisture content, etc.). Also the geometric ground profile has distinct differences from S1 to S2 aside from the pile presence. Therefore, S2 conditions and the measured data at S2 are not necessarily those that would be

produced at S1 if the piles were not present. A qualitative discussion of the results therefore yields the only contribution to understanding the nature of the wall-pile-soil interactions.

To provide a more complete understanding of the input model variations, the COM624P generated P-y curves are shown in Figure 4.6. This full set of soil restraint curves were present for Models 1 and 4b only. All other models have the P-y curves shown in upper plot of Figure 4.6 removed for the top 6.1 m (20 ft.), i.e. over the wall height. This would produce a worst case scenario by removing the significant surface restraint to the piles moving laterally. In reality this restraint is present, in some form, from the soil nail wall immediately ahead of the piles.

Table 4.3 provides a summary of input conditions and output peak deflection and bending movement for each of the four model scenarios studied. The units are left in the COM624P output English form for clarity.

Table 4.4 COM624P Model Summary

Model	P-y Condition over Wall Height	AASHTO 3 Feet Surcharge as Live Load	BMCOL7 Pressure Condition	Peak Pile Deflection (in)	Peak Pile Bending Moment Kip-in	Comments
1	All Present	On	None	0.25	116.0 @ 12 ft. deep	Precon- struction Reference
2	Lower P-y only	On	None	4.5	3250.0 @ 21 ft. deep	Soil Arching to Piles
2a	Lower P-y only	On	Full S1	15.0	1060.0 @ 18 ft. deep	
3	Lower P-y only	Off	Off	13.5	3210.0 @ 21 ft. deep	K_a Retaining wall Pressure
3a	Lower P-y only	On	Off	25.0	5360.0 @ 21 ft. deep	
4	Lower P-y only	Off	S1-S2 difference	-0.8	227.0 @ 12 ft. deep	Use of S1-S2 Pressures on Pile
4a	Lower P-y only	On	S1-S2 difference	3.7	1250.0 @ 18 ft. deep	
4b	All Present	On	S1-S2 difference	0.1	38.7 @ 15 ft. deep	Pile Restraint From Wall

Given the unreasonable high level of predicted deflections it does seem clear that Model Sets 2 and 3 are invalid. Under Model 1 and Model 4b conditions deflections of 84.2 mm (3.37 in.) and 134 mm (5.31 in.) were required to bring the pile moment up to a yield of 141 kN-m (1250 kip-in.). This was established from COM624P with pile top lateral loads of approximately 40 kN (9 kips) and 4.5 kN (1 kip) in Model 1 and 4a respectively. These loads were not intended to represent a true field condition but only to generate the necessary deflection.

In Model Set 2 and 3 the most notable effect is the loss of the stabilizing force from the soil given by the upper 6.1 m (20 ft.) of P-y curves. Model 1 and Model 2, which are both subject to the same horizontal distributed load, have a difference in pile top deflection on the order of 18. All the excessive deflections given by Models 2 and 3 confirms that the pile's response to the pressure changes from wall construction should not be analyzed as a simple retaining wall.

Model 4 begins an investigation of the components of the loads seen by the wall and the pile based on earlier reported BMCOL7 work using measured nail loads. By first separating those parts of the load that are a result of the geometry unique to S1, a 'feel' for the nature of the difference between S1 and S2 is found. In Model 4a and 4b the resultant soil pressure has the AASHTO live load surcharge placed in addition to S1-S2 differences and the result should be as close as FDM can come to the as measured workings of the soil-nail wall. Excavation 'lifts' removes laterally prestressed soil ahead of the pile and for the lower lifts the top nails would be expected to pick up this load. This suggests that the pre-existing pile loads at S1 before wall construction has an effect on the behavior of the wall by influencing nail performance. This may account for the peak BMCOL7 pressure on Figure 4.1 which is 1.27 m (50 in.) deep on S1.

Model 4b replaces the previous deleted P-y curves offered from the soil excavated in front of the pile for wall construction. Comparing the pile deflections of Model 4a and Model 4b the significance of the soil response in front of the pile again is reinforced. Following the hypothesis that nail loads contain a load component from offering restraint to the pile, the peak deflections are reduced by almost 98% to only 0.63 cm (0.025 in.).

Down the pile, there is a further peak in the resultant pressure difference between S2 and S1 distributed loads shown on Figure 4.5. Using elasticity, Boussinesq solutions confirm any influence of the surcharge diminishes rapidly down the pile. However, as the Swift Delta granular soil stiffens with depth, from overburden pressure, the ability of the soil to support arching across the piles and nails will increase.

Given the frequent excessive FDM predicted deflections, when compared to the field expected 'total' of something between 8 mm to 13 mm (1/3 to 1/2 in.) the most refined Model 4b prediction is surprisingly good. All other scenarios confirm the full influence of slope removal by excavation and soil arching is not carried by the Swift Delta piles.

Estimated Pressure Distribution
Section 1 (at Bridge Deck) using BMCOL7
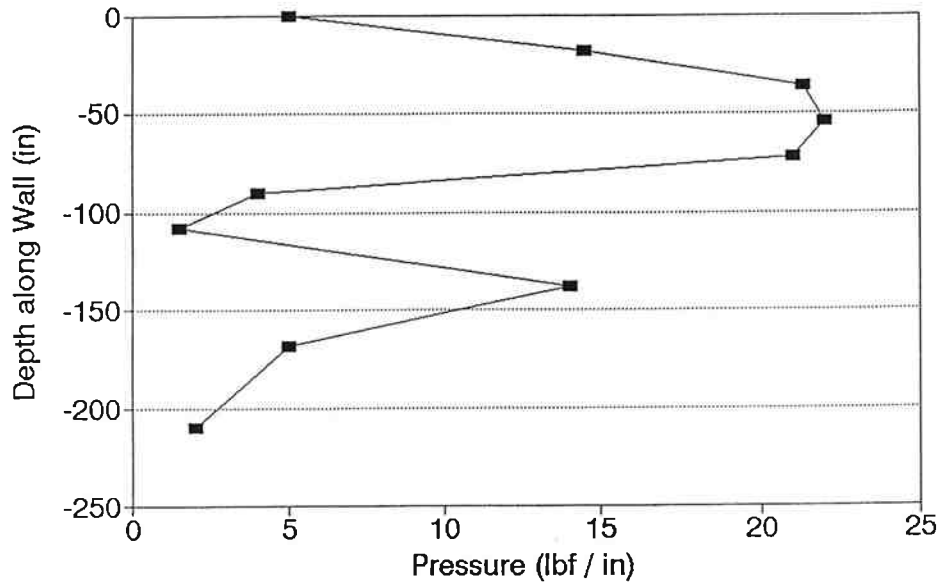
Estimated Pressure Distribution
Section 2 (at Bridge Abutment)
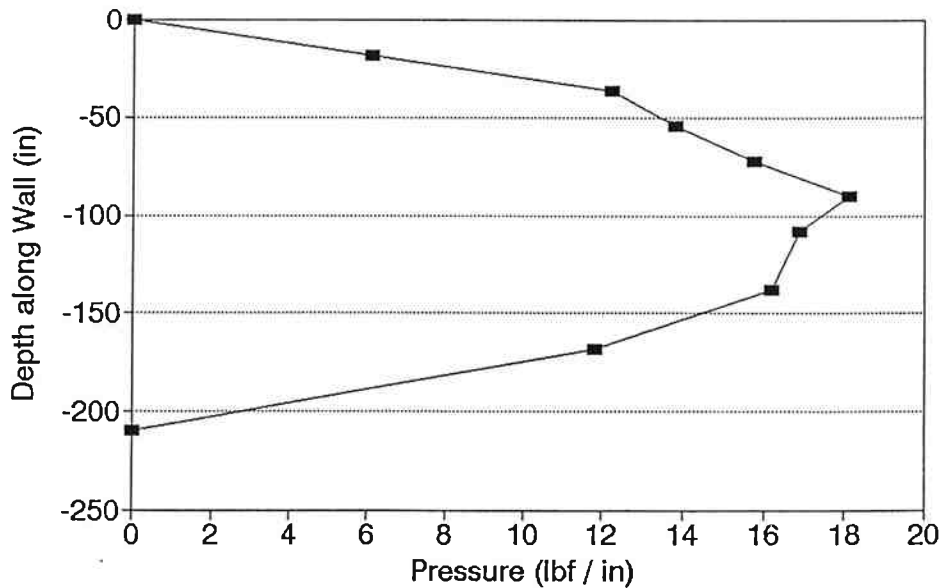
Figure 4.1 BMCOL 7 Pressure Down the Back Wall Face

APPLIED LOAD
Model 1
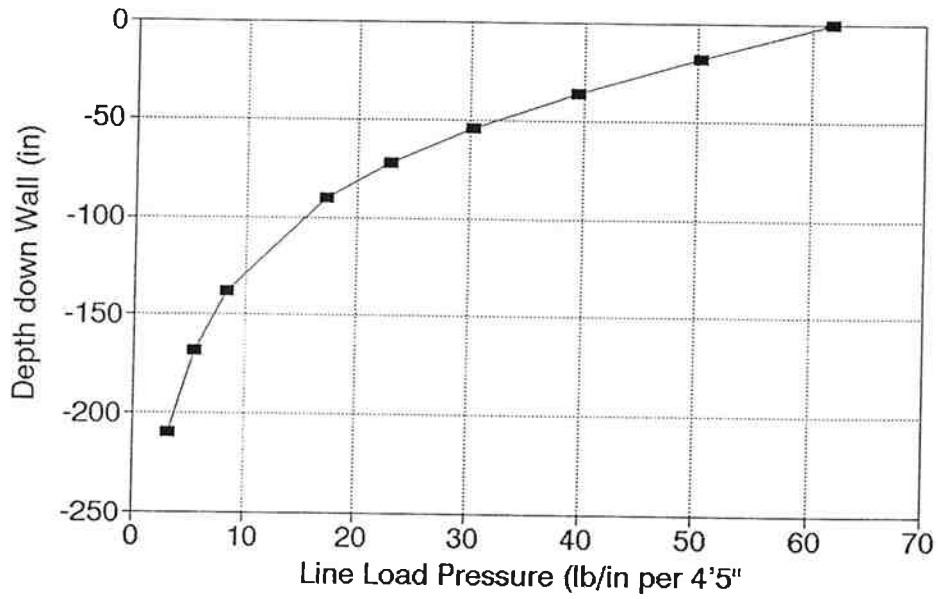
Figure 4.2 AASHTO Surcharge Load to Wall from GEOTEK-PRO

APPLIED LOAD
Model 2a
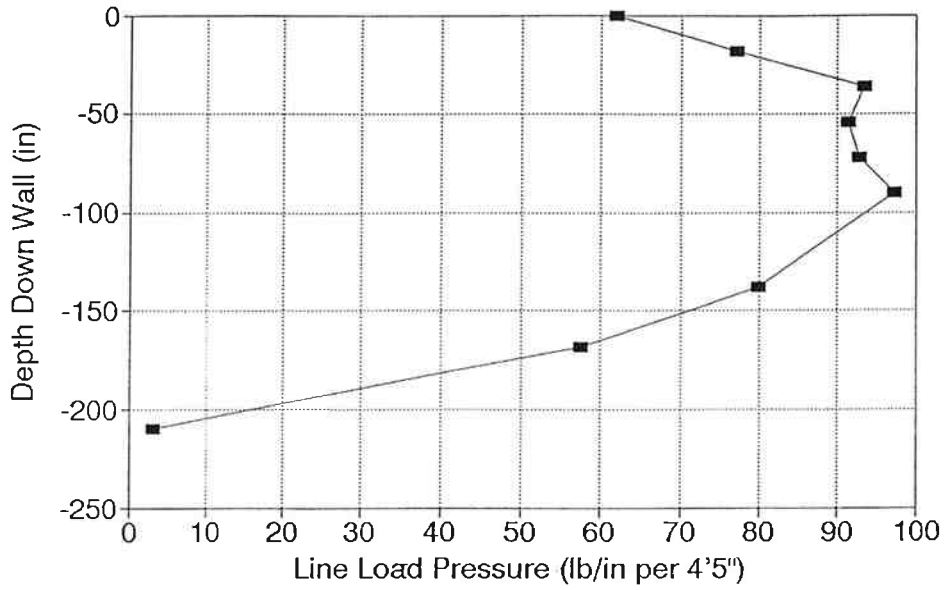
Pile Deflection
Model Set 2
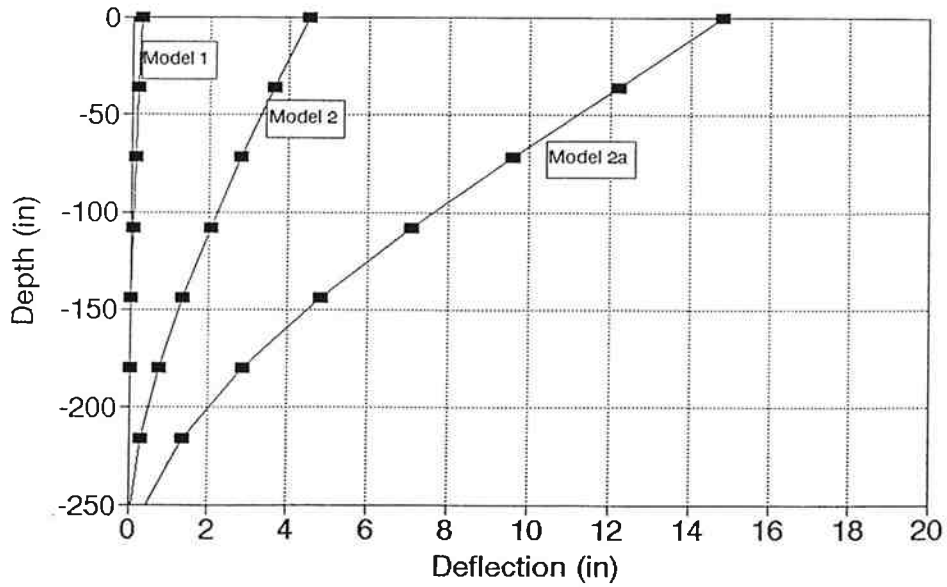
Figure 4.3 Boundary Condition Load and COM624P Deflections for Model 2 Series

APPLIED LOAD
Model 3
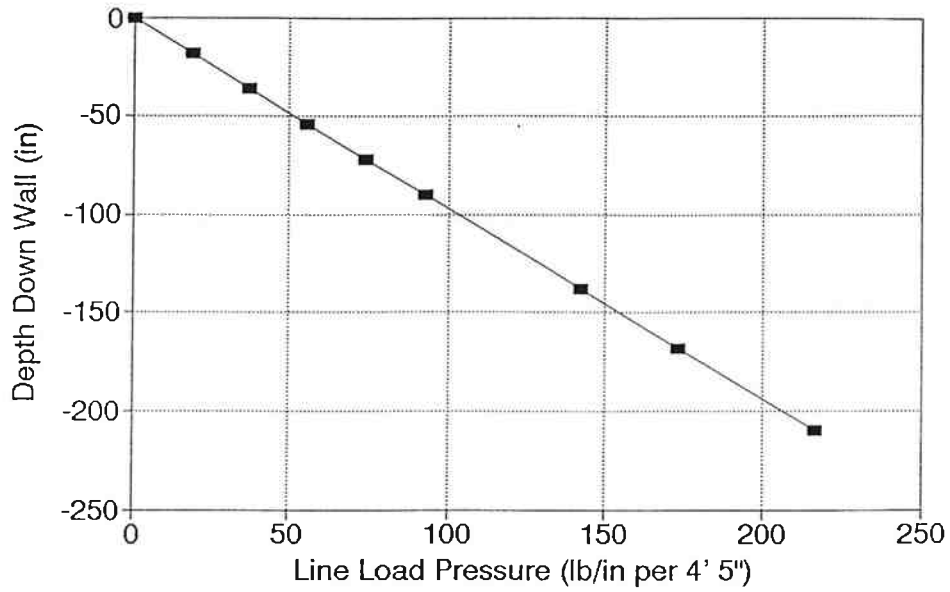
Pile Deflection
Model Set 3
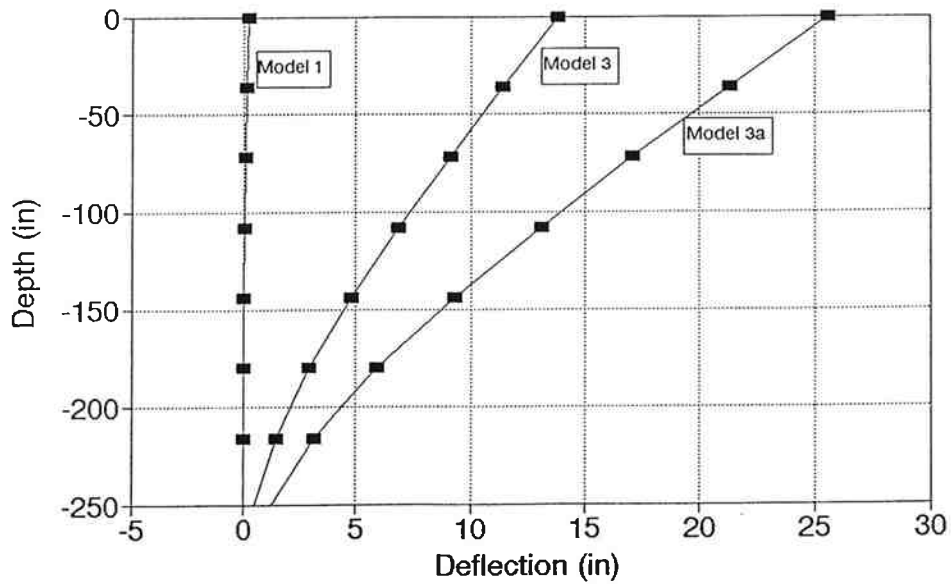
Figure 4.4 Boundary Condition Load and COM624P Deflections for Model 3 Series

APPLIED LOAD
Model 4

Line Load Pressure (ib/in per 4'5")
Depth Down Wall (in)

APPLIED LOAD
Model 4a

Line Load Pressure (lb/in per 4'5")
Depth Down Wall (in)

Pile Deflection
Model Set 4

Model 4   Model 1
Model 4b   Model 4a

Depth (in)
Deflection (in)
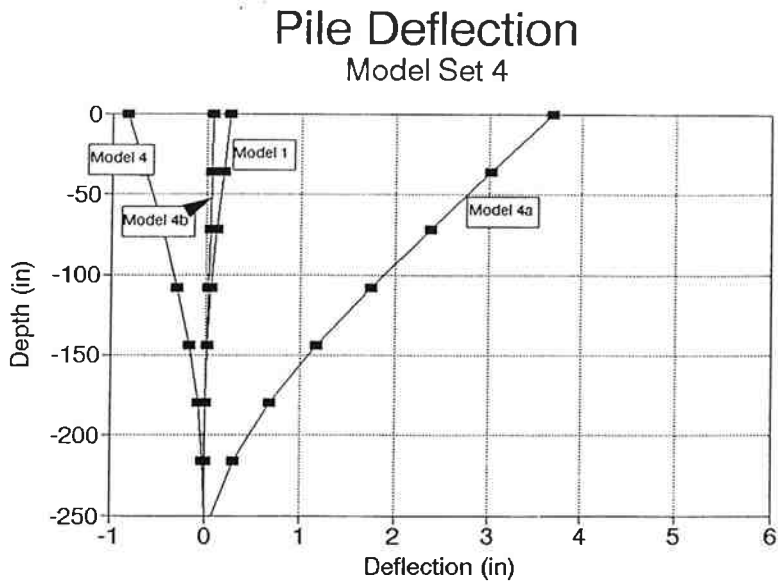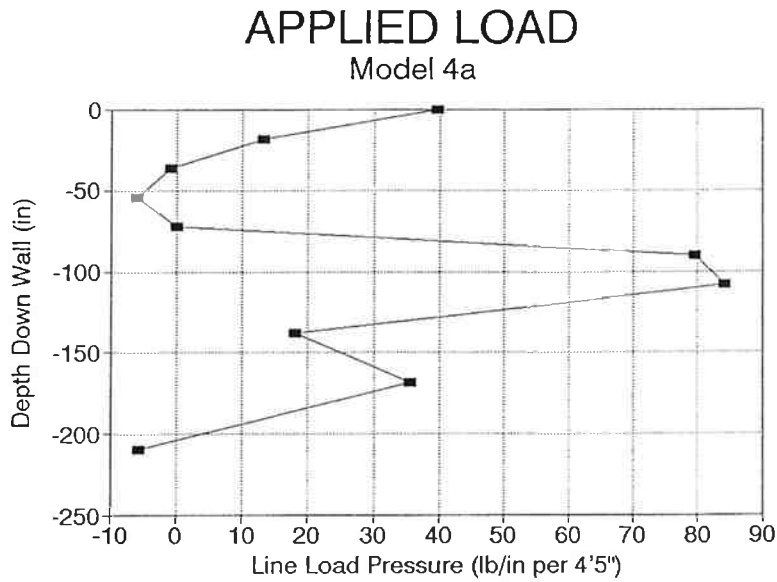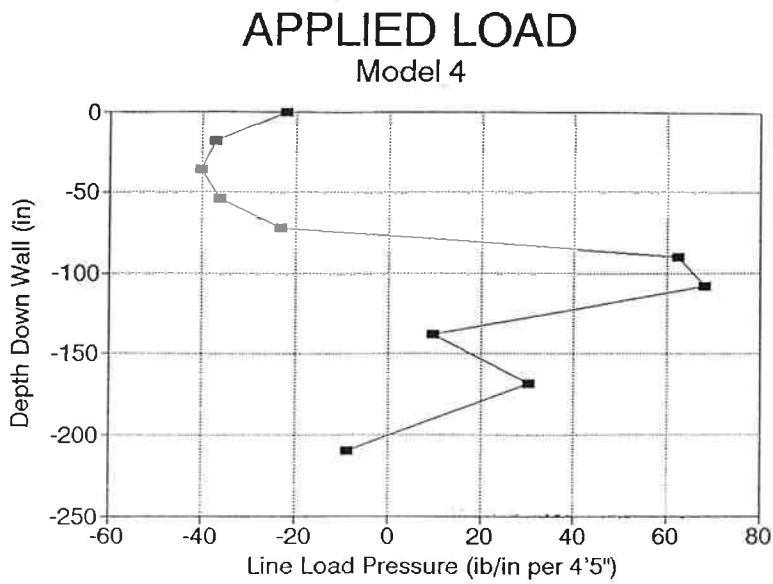
Figure 4.5 Boundary   Condition   Load   and   COM624P
Deflections for Model 4 Series

P-y Curves
Model 1: Within Wall Height
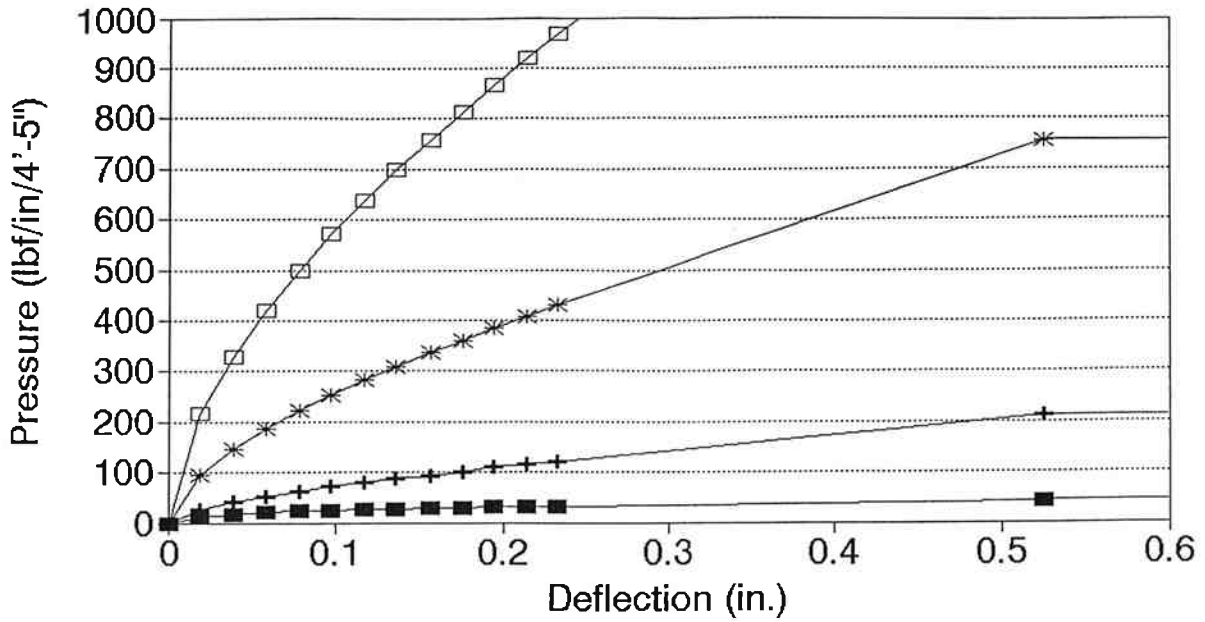
Legend: 60-inches, 120-inches, 180-inches, 240-inches

P-y Curves
Model 1: below wall
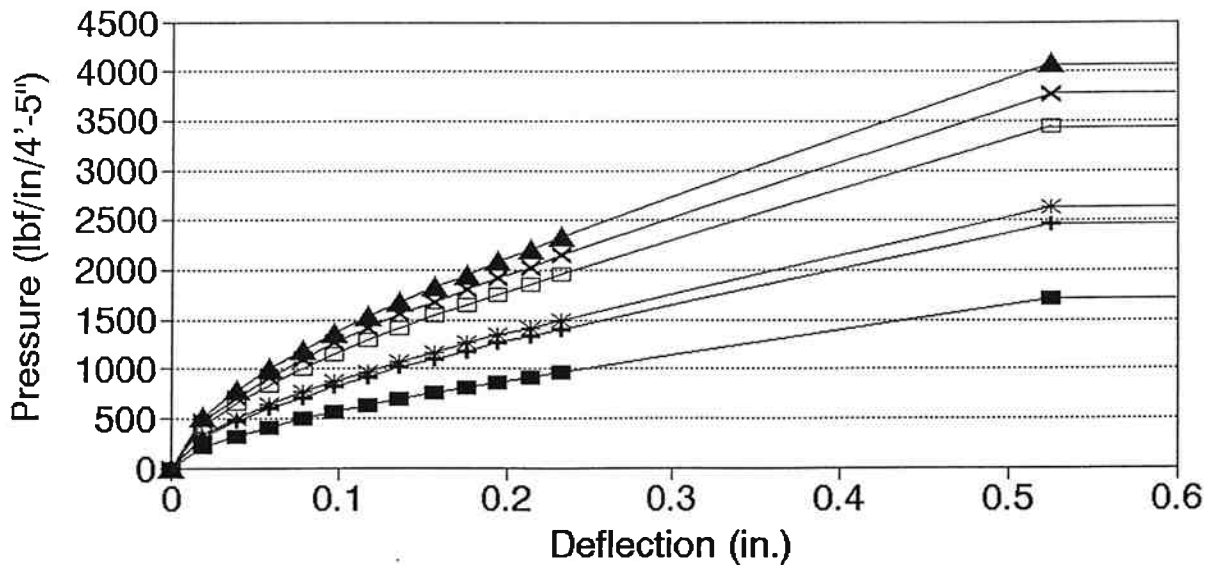
Legend: 240-inches, 300-inches, 360-inches, 420-inches, 480-inches, 540-inches

Figure 4.6 Lateral Restraint P-y Curves

THIS PAGE INTENTIONALLY LEFT BLANK.

5.0 FEM AND SWIFT DELTA SOIL MODELING

One key advantage in using numerical techniques to study Soil-Structure interaction problems is the ability to track material behavior at stress states prior to failure. Predictions of material stress strain behavior permits an equilibrium solution for Swift Delta to be reached without *apriori* failure mechanism assumptions on the soil nail wall being made. These solutions permit full predictions of deflection, strain and all states of stress to be made from a known strain to stress soil input relationship. It follows then that acceptable and reasonable deflection patterns must be found before strain and stress levels are credible, since they follow from the direct calculation of deflections. The ability to theoretically track the nonlinear, stress dependent, behavior of the SP sand at Swift Delta, now becomes of fundamental importance. Often, in the absence of quality laboratory data, dependence upon *back analyses* using measured data is made to calibrate the soil constitutive parameters for the numerical study of a case history. This back analyses approach can significantly weaken a predictive models validity. This has <u>not</u> been done at Swift Delta. Independent material nonlinear predictions were made using pressuremeter data, published parameters and engineering judgement. It should be understood that model boundary conditions such as excavations, which bring large zones of soil close to failure, either by minor principal stress relief or high states of shear stress, are interpreted with less confidence since most FEM nonlinear analyses are pseudo-linear by their piecewise iterative process. Often the change in the geometry of the soil surface can increasingly invalidate the early chronologic prediction of the stress changes that accumulate later in the analyses. The problem, then, of the FEM for soil nail walls is particularly difficult, with the soil nonlinearity, soil to structure interaction and three dimensional aspects, all compounded by repetitive excavation modeling.

5.1 CONSTITUTIVE MODELING

The FENAIL code employs isotropic, anisotropic, linear elastic models for linear work, and a Hyperbolic Plasticity (HP) model for nonlinear work. The interface, membrane and boundary spring elements add additional nonlinearity and are very difficult to quantify at the present time. Research has only recently begun on interface modeling for soil-structure problems (Desai and Mugtadir 1986). The hyperbolic model in FENAIL follows the expression of Konder (1963), which states the soil's deviator stress can be approximated in hyperbolic form where the initial stiffness is made a function of confining stress. It forms the origin of the, so called, Duncan & Chang hyperbolic FEM model which grew to require eleven input parameters. FENAIL's simpler version was designed to preserve numerical stability, keeping yield related by common Mohr-Coulomb (c-phi) criteria, and requires the user to identify the nondimensional hyperbolic input 'K', and power 'n'. Advantage was taken of the observation from the ODOT direct shear test series that no volume change, either contractive or dilatant, was observed. Hence no model is incorporated in FENAIL's early version for Swift Delta to permit volumetric changes, under either isotropic or deviatoric stresses. Given the lack of a testing base for the SP sand at Swift

Delta, using the hyperbolic formulation gave access to the well published data base of parameters. A good review is presented by Marin, Kiefer and Anderson (1993).

5.2 HYPERBOLIC AND YIELD PARAMETERS

The SP fill sand is shown by the boring logs, blow count and direct shear testing to be a medium sand at, or around, critical void ratio, with a phi angle of 33°. Given the moist condition above the water table apparent cohesion was also present in the short term in stable 4-5 feet observed vertical cuts.

CAMFE, Carter (1978), is a one dimensional FEM code that permits elastic-plastic simulation of a PMT cavity expansion. A simple parametric study was conducted by varying the input plastic constitutive parameters, c and phi, employing an elastic - plastic soil model. It was hoped this might both confirm for FEM input the single direct shear test measurement of phi, and also provide an estimate of the apparent cohesion. CAMFE does have the ability to track pore water pressure changes, with an input coefficient of permeability, k. Volume change in drained, or partially drained, conditions is only possible with the 'Critical State' model in CAMFE. No constitutive parameters are available for the SP Swift Delta sand using Critical State techniques which demands Triaxial testing. Therefore the real time loading rate, permeability k, and the restriction of the elastic-plastic model, influence the accuracy with which the parametric study can estimate c and phi. Input elastic stiffness for each test has been taken from the measured pressuremeter (PMT) test result (which is well understood to be of the order 30% to 50% of the soil's true elastic undisturbed compressive stiffness), and the initial horizontal and vertical effective stress state calculated using an effective unit weight of 17.6 kN/m^3 (110 pcf). Examination of Figure 1.5 and Figure 1.6 shows that the PMT tests 3, 4 and 5 provides the best quality data to match with the CAMFE code. CAMFE's plastic response is governed by the c-phi criteria, where the cohesion and initial stress state strongly influence the yield point of the curve, i.e. where pseudo elastic behavior moves to a nonlinear response. Successive CAMFE models of 99 elements (198 nodes) radiating out from the borehole centerline to a maximum distance of 2.53 m (8.3 ft.) for the 32 mm (1.25 in.) radius EX size cavity, were executed. CAMFE makes no iterations but modifies stiffness based on the new stress state at the commencement of each incremental time step, i.e. "tangent stiffness" method is used. Selected results of the best match are shown in Figure 5.1 to the measured PMT Test number 3. Based on modeling of all tests, 3, 4 and 5 around the expected phi of 33° shows maximum predicted cohesion in a likely range 24-38 kPa (500-800 psf). This is highly unreasonable for the Swift Delta sand and is in error for the following reasons:

- The sand stiffness is not stress dependent in CAMFE and it is in the field,

- No effects of borehole unloading (from the auger), reloading and disturbance are present in CAMFE,

- No volume change has been modelled, which strongly influences phi

50

It is much more reasonable that the apparent cohesion is only of the order 4.8 kPa (100 psf) to 7.2 kPa (150 psf).

An alternative approach is to follow the recommendations of Neumann (1987) for a direct correlation between Konder's hyperbolic approaches and the PMT tests by suggesting:

$$E_o = KP_a \left(\frac{\sigma_r}{P_a} \right)^n$$

where E_o = PMT modulus

P_a = atmospheric pressures

σ_r = initial radial stress

K,n = Nondimensional hyperbolic parameters

This hyperbolic approach better fits the FENAIL hyperbolic model but may not be relevant for ABAQUS modeling. For a constant volume soil Poisson's ratio was set at 0.45 and stresses found with unit weight, γ, at 17.6 kN/m³ (110 pcf), and K_o = 0.46.
It follows that:

$$\log \left(\frac{E_o}{P_a} \right) = \log K + n \log \left(\frac{\sigma_r}{P_a} \right)$$

and a linear best fit line reveals the slope 'n' and intercept 'K' shown in Figure 5.2.

PMT modulii are recognized to be significantly below intact, compressive, Young's modulus values for classic elasticity work. This is due to borehole disturbance, unloading in the circumferential direction where soil stiffness is very low, and the large strain range throughout the PMT test. The well documented rheologic factor, λ, is used in practice to move the measured PMT modulus , E_0, up to the Young's modulus, E. The same argument holds to the previous derivation of the nondimensional parameter K, and with a sand λ is in the range ⅓ to ¼ gives a value for K of the order 150-200, with n of 0.27. Both are acceptable when compared to published data.

5.3 ABAQUS DRUCKER PRAGER

The only plasticity model in ABAQUS most suitable to employ for frictional material is the Drucker Prager (DP) set, calibrated from a c phi match in compression using plane strain

51

restrictions. The model is suitable for cohesive granular materials and originally was designed for pressure dependant metal yield. Unfortunately, it is not widely used for soils, and is shown to be numerically very sensitive under typical soil structure problems, particularly granular soils. The features of the DP model are (ABAQUS 1992):

- There is a regime of purely elastic behavior, followed by nonrecoverable strain, which can be described as plastic.

- Following the initial isotropic behavior yield is governed by hydrostatic pressure, and a dependency on the intermediate principal stress.

- Inelastic behavior is generally accompanied by volume change.

Unfortunately, model calibration must come from standard Triaxial compression/tension tests, and these results are not available for the Swift Delta fill sand. By forcing both c phi and DP to predict the same yield in the Triaxial state we have:

$$\tan\beta = \frac{6\ \sin\ \phi}{3\ -\ \sin\ \phi}$$

$$\kappa = \frac{3-\ \sin\ \phi}{3+\ \sin\ \phi}$$

and

$$\sigma_c = 2c\ \frac{\cos\ \phi}{1\ -\ \sin\ \phi}$$

for the yield surface to remain convex requires $K \geq 0.778$. Furthermore, when ϕ is significantly larger than $22°$ a poor match is found. In drained conditions granular soils typically have $\phi > 30°$. Finally, for nondilatant flow in plane strain additional restrictions arrive which set $\kappa = 1.0$ and $\tan \beta = \sqrt{3}\ \mathrm{Sin}\ \phi$. Thus it can be seen the DP modeling in any 2D or 3D ABAQUS work is of limited use without quality Triaxial data. Plane strain parameter fitting matches true 2D work, and may also be a reasonable match to Swift Delta Soil Nail 3D work, since principal displacement vectors stay close to 2D. For a realistic use of this match significant cohesion must be proposed (however unreasonable) and for c = 500 psf and ϕ = $32°$, the DP parameters become:

$$
\begin{aligned}
\Psi &= 0 \\
\beta &= 42.5° \\
E &= 200\ \mathrm{psf} \\
d &= 735\ \mathrm{psf} \\
\kappa &= 1.0 \\
\text{and}\quad \sigma_c &= 1058\ \mathrm{psf\ for\ compression\ matching}
\end{aligned}
$$

5.4 GEOSTATIC CONDITIONS

Significant differences also exist between FENAIL and ABAQUS in their establishment of a realistic gravity stress state. The Swift Delta slope, and fill behind the proposed wall, must be initially stressed by the soil's unit weight and K_o conditions. For ABAQUS, these unit weight (body forces) in the vertical direction must be 'reconciled' to the vertical and horizontal initial stresses which are user defined. Calculation of nodal forces in the ABAQUS mesh expose out-of-balance stress states which distort the mesh arbitrarily to bring about initial equilibrium conditions. Thus a deformation pattern is created under the restriction that horizontal stresses require all nonhorizontal boundaries (i.e. the 2:1 slope) be fixed in the horizontal direction. FENAIL, in common with most other geotechnical FEM codes, establishes equilibrium by a true gravity 'turn on' where mesh displacements deform downward and outward under body loads. Thus ABAQUS and FENAIL predicted total displacements, even in elasticity, will not correlate well. Stresses, which set the soils response to further loading or unloading, do correspond however.
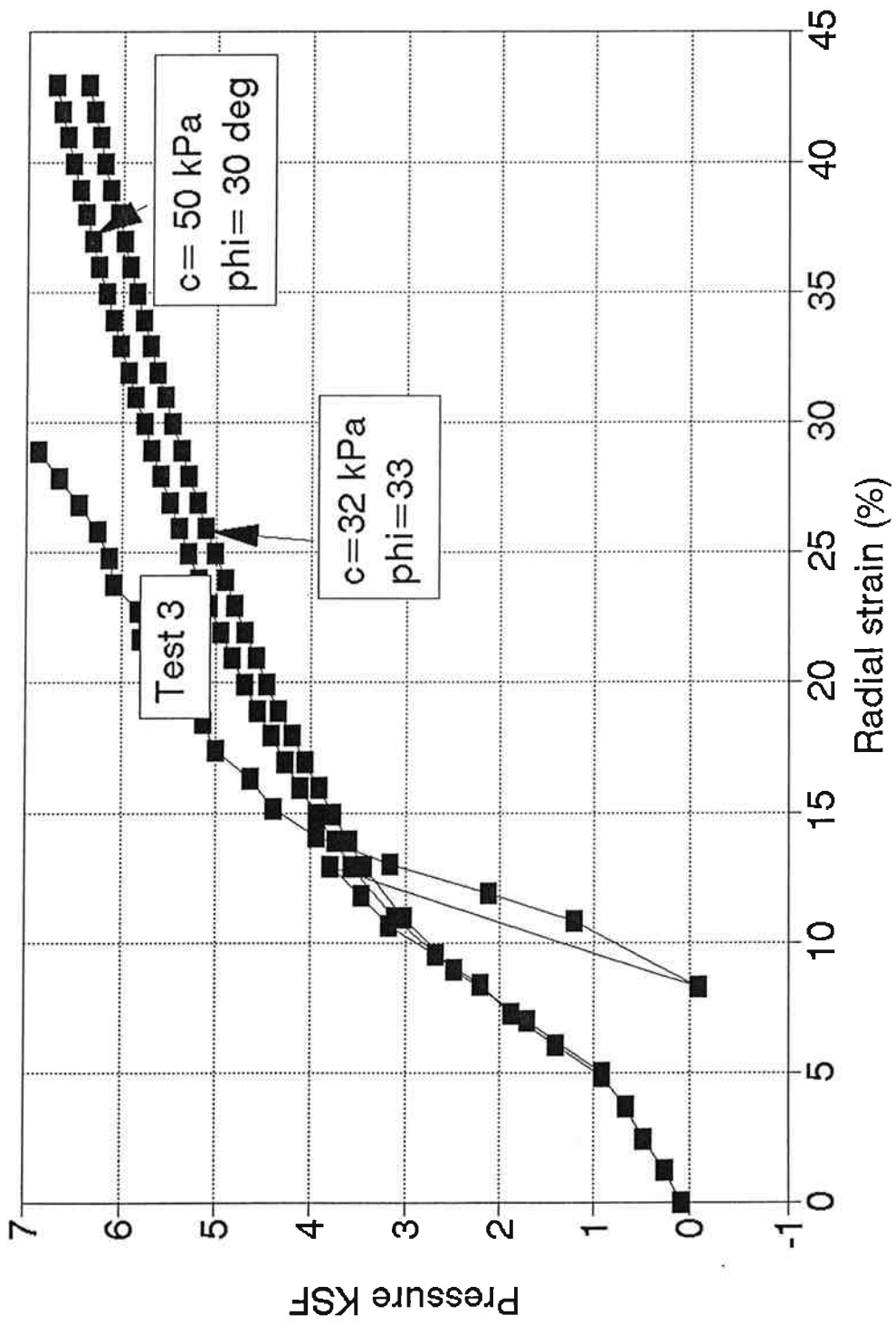
Figure 5.1 Example CAMFE Predictions and Test Result for PMT Test #3
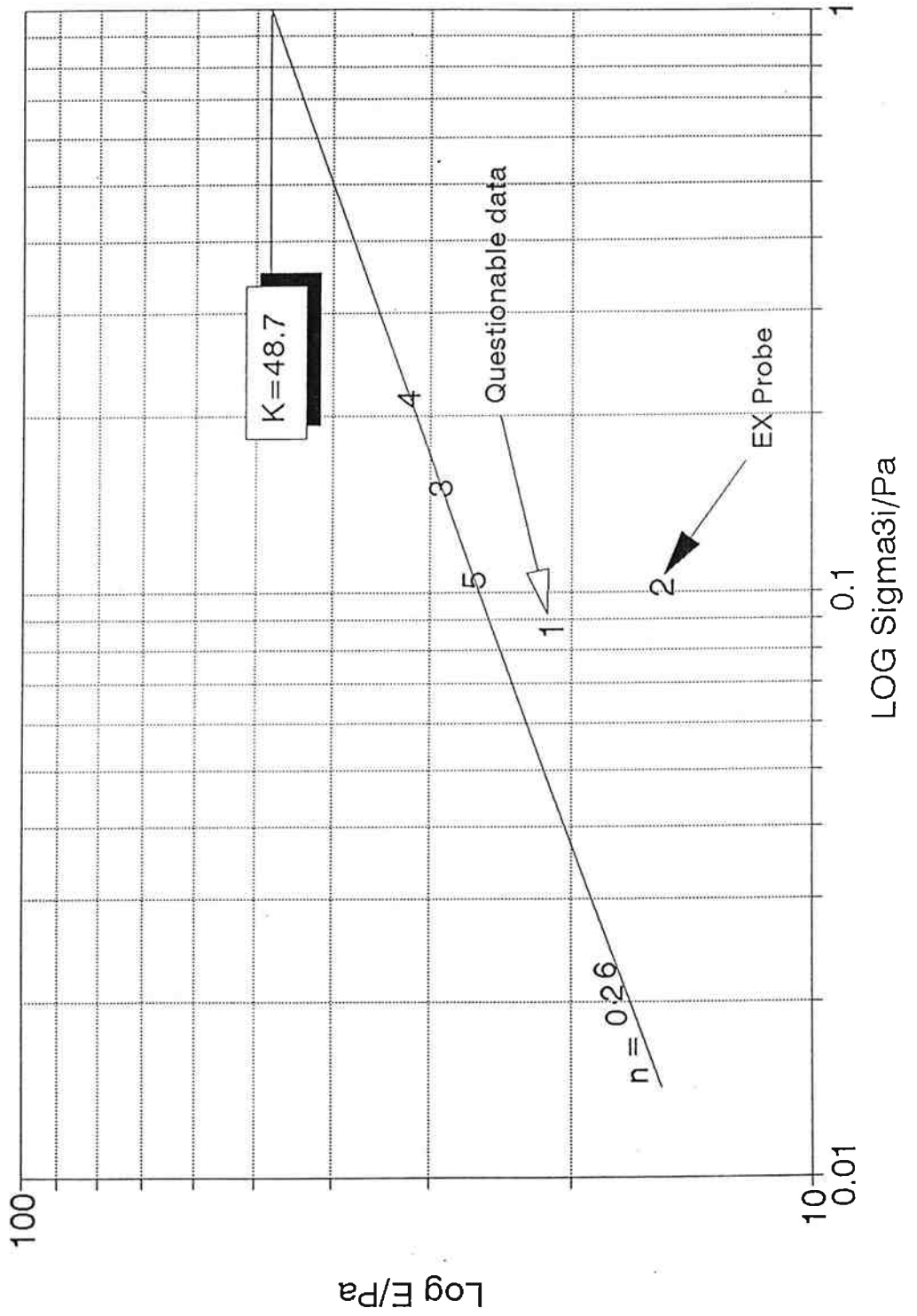
Figure 5.2 Hyperbolic Parameters from PMT Data

THIS PAGE INTENTIONALLY LEFT BLANK.

6.0 FENAIL TWO DIMENSIONAL STUDIES

The Finite Element Soil NAIL code (FENAIL) was introduced and discussed in Sections 3 and 5. The code represents a very significant portion of the research effort during this study as no other DOS based codes to study nail to pile interaction were available. It should be recalled that a period of years is necessary to fully validate all new features of such a code, in a wide group of soil-structure problems. Additionally, some of the challenging numerical modelling issues regarding the focus of this research should be noted. Some of these issues were acknowledged at the outset. Others surfaced as the research progressed. They included:

- The desire to examine the structural interaction of a soil nail wall/pile supported bridge abutment,

- The realization that the nature of this interaction is a three-dimensional problem,

- The acknowledgement that numerical techniques are dependant upon the ability to develop mathematical relationships which describe soil behavior, as well as soil structure interaction,

- The inability to apply three-dimensional soil constitutive relationships based on currently available laboratory testing, or in situ testing, of soils,

- The concession that the practical engineer does not necessarily have access to the computational resources necessary to evaluate three-dimensional numerical models, and therefore a two-dimensional approach would be desirable,

- The difficulty in development of a finite element code capable of predicting the stress states developed by excavation of soil overburden. This is an area which demanded considerable effort, since available finite element codes for soils have concentrated on *adding* elements to a mesh (thereby increasing stress on the system), rather than removal of elements from the mesh. Excavation sequence modeling presents formidable numerical issues that must be addressed due to the removal of stressed and deformed portions of a continuum.

- And finally, the realization that the Swift Delta measured data simply did not provide the three dimensional interaction quantities necessary to validate a numerical model of soil nail/pile interaction, either two- or three-dimensional. This is a function of available technology rather than the implementation of the instrumentation program itself or the numerical modeling approach used here.

The Rational Systems International DOS4GW memory manager is employed for 80386 and 80486 machines (math co-processor essential) to execute FENAIL. The most satisfactory, and preferred, platform is the 80486DX machine with 16 MB RAM, operating at 33 MHz or faster. As with any new code, and especially with the limited time and resources available for this study, the results should be viewed with great care and emphatic conclusions avoided. The available Swift Delta instrumentation data, however, does aid validation of FENAIL. A separate User Manual is also available.

Only experienced FEM modelers should attempt analysis of soil nail walls with FENAIL. Substantial engineering judgement is necessary to interpret, validate and apply the results.

6.1 FENAIL MODELING APPROACH

The issues mentioned above led to the following research goal:

> 'Develop a two-dimensional finite element numerical code and associated numerical modelling scheme, which would be capable of capturing some three-dimensional behavior, and that would be executable under DOS personal computer architecture.'

The issues of developing full validation data for the numerical model will take some time. Further, such a model can only be validated by full-scale experiments such as the Swift Delta wall, since decades of the development of numerical constitutive models, based on in-situ and laboratory testing techniques, have inadequately captured "true" three-dimensional behavior of soils.

The Swift Delta wall analysis scheme incorporated the following components and features:

- A basic, two-dimensional mesh which was generated using ABAQUS and utilized by both codes (FENAIL and ABAQUS) to provide preliminary verification checks to simple elasticity models for which closed form solutions were available. A nominal strip footing load was applied with linear elastic properties with both codes employing the same mesh.

- The two-dimensional mesh geometry incorporated the ability to model the soil, the nails, the shotcrete and the piles.

- No frictional "slip" or any other effects of frictional movement for the behavior between the nails/soil/piles is captured by a unit-thickness (i.e. plane strain) two-dimensional model. Thus, all elements would occupy the same two-dimensional space. Due to the necessity of continuity, no differential movement between the soil nail wall and the piles at S1 could be modelled in the third dimension (parallel to the pile line and cap). The concept of overlain two-dimensional meshes was employed to model the response in the "out-of-plane" third direction. The second mesh consisted only of those nodes needed to model the "out-of-plane" pile. The soil, nails and shotcrete remained in the "in-plane"

58

mesh which is depicted in the FENAIL output at S1. The second mesh contained nodal points which exactly matched the coordinates of their counterparts in the "in-plane" mesh at the beginning of modelling. Both the top and bottom of the pile (away from the soil nail wall, vertically) was placed within the large, "in-plane" mesh. The nodes within the area of the soil nail wall were connected with "*interference*" elements to the pile nodes which modelled soil/nail/pile interaction as a spring, with no actual thickness. This concept is herein referred to as the "quasi-3D approach."

- The soil was modelled using a relatively simple hyperbolic constitutive relation employing six parameters, as discussed in Section 5.

- The nails were modelled as a transformed section of the steel tendon and encapsulating grout by beam elements, described with steel properties and transformed section geometry.

- The shotcrete facing was modelled as beam elements of zero thickness which were added to the mesh incrementally following excavation of soil. The facing response was not expected to dramatically impact the soil/nail/pile interaction based on current notions of the behavior of reinforced soil masses. The gain from this simplistic approach was that soil elements did not need to be removed and replaced with elements of very different material properties (thus causing stress continuum problems). The loss was that the effects of the weight of shotcrete hanging on the heads of the nails and adhering to the vertical soil cut were lost since the beam elements occupy no thickness and are weightless in the numerical model.

- The piles were modelled as beam elements with elastic steel properties, based on the dimensions of the piles. The pile nodes were connected to the nodes of the large mesh (containing the soil, nails, shotcrete and pile cap) using interface elements. Since the soil nail/pile interaction behavior is not actually a true contact interface, these elements are better referred to as "interference" elements which will allow slippage of the large mesh past the attached pile mesh.

All work with FENAIL was accomplished in English customary units, which include all post processed plots. Metric equivalencies are reported but all outputs remain plotted in English units. On all color TECPLOT figures the **axis scales are in feet, stresses in psf and deflections in feet**.

6.2 FENAIL VALIDATION

By way of elasticity performance checks using the mesh in Figure 6.1 the output x and y displacements (hereafter referred to as just x and y) for a 0.048 kPa (1 psf) surface vertical line load, 5.03 m (16.5 ft.) long behind cap, are shown in Figures 6.2 (x) and 6.3 (y) for a weightless soil. Visual superposition of these figures demonstrate surface "dishing" and peak

vertical (y) settlement of 4.5 cm (0.18 ft.), which compares well to the ABAQUS prediction of 4.8 cm (0.19 ft.), and to elasticity plane strain solutions. Horizontal displacements within the soil mass predicted by both codes also compare to within 5%.

6.3 MESH AND MODEL DETAILS

To aid direct comparison to ABAQUS for two dimensional work, and assist in studying both S1 and S2 instrumentation sections, a single mesh was produced. The full mesh for S1 is shown in Figure 6.1 with the pile, nails and shotcrete wall elements as beams are indicated, and modelled as described above. The S2 model employs essentially the same mesh, but with a 2:1 slope atop the excavation, indicated in Figure 6.1, in place of the pile cap and soil surcharge. The largest model has a total of 505 elements, with 3 degrees of freedom per node. Both left and right vertical boundaries are free to translate vertically only, with the base being fixed. The mesh principally follows the characteristics of ABAQUS-PATRAN styles and does not make use of FENAIL's mesh generator. This makes revised versions of the mesh relatively inefficient, but is desirable since it allowed more models to be studied in less time.

Of the modeling scenarios attempted, four (4) are deemed significant to report here. The model names and attributes are listed below. The element types and other associated input parameters are summarized in Table 6.1.

5EXC: Full height excavation of the S1 mesh with gravity effects for a linear elastic soil. No pile, shotcrete or nails are present.

1XNB: Full height excavation of the S1 mesh (under the bridge), using a hyperbolic, nonlinear soil with nails and shotcrete wall. No piles are represented. This may be compared to the S2 model, 2XNB, and the S1 model with pile response included, 5NPS.

2XNB: Essentially the same model as 1XNB, except the mesh geometry is revised to account for the 2:1 soil slope present above the wall, away from the bridge. Model results may be compared to the Swift Delta Section 2 instrumentation data.

5NPS: This is the 1XNB model revised to add the second, overlain mesh comprising the pile elements. The soil nail/pile interaction is now represented through "interference" links between common nodal coordinates where the vertical pile (beam element) column passes the nail (beam element) within the large mesh. This is the quasi-3D model.

Since reference is made to the TECPLOT outputs in English units the metric equivalents are omitted for clarity.

60

The results from these models are discussed below in general terms. More specific pile and nail behavior predictions are lifted from the output and given in the Pile, Nail and Wall Behavior Summary subsection, and Table 6.2, at the end of Section 6. The figures at the end of Section 6 are color, postscript processed representations of the FENAIL output for the various models. Many of the output files are plotted in terms of both x and y displacements as well as associated stresses. Displacements have been used primarily for comparisons of the model results to the instrumentation data.

6.4 MODEL 5EXC-FULL S1 EXCAVATION, LINEAR ELASTIC SOIL.

A linear elastic soil of E = 23.94 MPa (500,000 psf), Poisson's ratio = 0.3, which may be compared to ABAQUS work with the same elastic parameters is used in this model. The modulus value is derived from the pressuremeter work presented previously in Section 5. No piles, nails or shotcrete are active. Gravity stress states are well demonstrated with γ = 15.7 kN/m³ (100 pcf), and the excavation modeling abilities of the FENAIL code are shown in Figures 6.4 to 6.7 for the first cut of excavation and Figures 6.8 to 6.11 for the last cut. Input parameters are listed in Table 6.1. The following observations are made:

- Total lateral deflection of only about 0.01 inch indicates that in order to develop a model which compares with measured deflections in the Swift Delta wall, a nonlinear, hyperbolic soil model should be used. This approach is carried through all subsequent modeling efforts.

- Excavation rebound of about 1.0 mm (0.04 inches) at the cut base is evident as the relief in load can be interpreted as a 'suction' response (stress relief) to the exposed cut in elastic soil.

- The wall moves up about 1.0 mm (0.04 inches) under rebound and shows noticeable rotation of about 0.02 inches back into the slope. The y movement dominates as vertical gravity stresses are higher than horizontal and no removal of horizontal restraint is present in the overall model.

- Vertical σ_y stress begins to drop off during the last .9m-1.22m (3-4 feet) approaching the free cut face.

- Local stress "spikes" show up which do suggest some compromise in TECPLOT's interpolation routines, as well as highlighting some of the irregular element geometries in the mesh. The smoother x and y distributions reflect the more "comfortable" zero initial state. Mesh element geometric irregularities also produce local spike anomalies.

61

Table 6.1 Summary of FENAIL Input Parameters

	MODEL			
ELEMENT TYPE OR PARAMETER	**5EXC**	**1XNB**	**2XNB**	**5NPS**
Soil Constitutive Model	Linear elastic	Hyperbolic elasto-plastic	Hyperbolic elasto-plastic	Hyperbolic elasto-plastic
c (psf)	N/A	100	100	100
ϕ (degrees)	N/A	32	32	32
γ (pcf)	100	110	110	110
K (no units)	E=500,000 psf	300	300	300
n (no units)	N/A	0.5	0.5	0.5
ν (no units)	0.3	0.45	0.45	0.45
Shotcrete	None	Beam element	Beam element	Beam element
Area (ft^2/ft. of wall)	N/A	0.667	0.667	0.667
I (ft^4/ft. of wall)	N/A	0.0247	0.0247	0.0247
E (psf)	N/A	500000	500000	500000
Soil Nails	None	Beam element	Beam element	Beam element
Area (ft^2/ft. of wall)	N/A	0.0187	0.0187	0.0187
I (ft^4/ft. of wall)	N/A	3×10^{-5}	3×10^{-5}	3×10^{-5}
E (psf)	N/A	4×10^9	4×10^9	4×10^9
Pile	None	None	None	Beam element
Area (ft^2/ft. of wall)	N/A	N/A	N/A	0.075
I (ft^4/ft. of wall)	N/A	N/A	N/A	0.013
E (psf)	N/A	N/A	N/A	4×10^9

Note: Metric equivalents are omitted for clarity.

6.5 MODEL 1XNB-S1 MODEL WITH HYPERBOLIC SOIL NAILS AND SHOTCRETE, NO PILES.

Most FENAIL features pertinent for comparison with instrumentation section S1 beneath the bridge deck are present in this model, with the exception of the piles. This is a plane strain section of nonlinear, hyperbolic soil, beam element nails and wall, with a 'soft' concrete cap to prevent cap stiffness dominating the output. Input parameters are listed in Table 6.1.

Again full gravity is employed and each of the six excavation steps modelled. Selected output for the final end of construction step follows in Figures 6.12 to 6.14. The following observations are made:

- Maximum x movement at the end of construction is 10.4 mm (0.41 inches) (Figure 6.12), which compares remarkably well to the field observed movements of about 7.6mm (0.3 inches) in the extensometer at the end of construction. When compared to the 5EXC model, the larger x displacements seem to indicate that the switch to a hyperbolic, elasto-plastic soil model is warranted, and that noticeable nonlinear soil behavior is predicted by FENAIL. Comparison of predicted to measured wall deflections over the full height of the wall is not possible, since inclinometer data at S1 is only available post-excavation.

- The nail influence throughout the mesh is shown, particularly with the x displacement 'spikes' on Figure 6.12, Also, by comparing the horizontal stress fields in Figure 6.9 (elasticity model) and Figure 6.13, the drop in σ_x toward the wall face seems to indicate that a distinct 'reinforced' soil mass condition is being produced by the nails.

- Horizontal σ_x stresses at the wall backface indicates a range 2.4 kPa-21.5 kPa (50-450 psf), with horizontal stresses increasing toward the bottom of the wall (Figure 6.13). The contour subroutine for TECPLOT does not allow precise interpretations of predicted wall facing pressures, but horizontal stresses are clearly predicted to be up to 50 percent less than the Rankine active lateral earth pressures (with $K_a = 0.3$), over most of the wall height.

- Without any description of shotcrete wall weight (shotcrete elements are modelled as weightless beam elements) the elastic rebound of the soil is not suppressed. Vertical downward wall movement does slightly raise σ_y locally in compression (Figure 6.14).

6.6 MODEL 2XNB-S2 MODEL WITH HYPERBOLIC SOIL, BEAM ELEMENT NAILS AND SHOTCRETE.

This model is the most appropriate for comparison with the instrumented section S2, outside the bridge deck. The model is a direct follow on to the 1XNB model, with a plane geometry

63

modification to account for the 2:1 slope above the wall, away from the bridge. Input parameters are shown in Table 6.1.

Given this model's direct relevance to the instrumented section S2, a more comprehensive series of plots are shown in Figures 6.15 to 6.24. These plots follow the changes in displacements and stresses through the excavation sequence to the end of construction. The following observations can be made:

- As may be expected, the surface slope 'bench' affects the σ_x and σ_y fields below this surface feature (Figures 6.15 to 6.17).

- The shear stress, τ, maximum plot of Figure 6.16 reveals patterns of maximum shear stress which have direct analogy to classic limit equilibrium slope stability mechanisms. This can be seen by noting the locally higher shear stresses developed at the toe of the slope. However, for the Swift Delta model, stresses have not reached a shear failure level.

- Initiation of wall excavation in a hyperbolic soil quickly reveals the expected outward x movement (Figure 6.18). The magnitude of approximately 2.5 mm (0.1 inch) agrees with observed movement in slope inclinometer SD-130 for about this same time during construction. The amount of work undertaken by the top nail row can be inferred from Figure 6.18 by noting the significant reduction in x displacement in the soil mass around the top nail. In a sense the soil mass is 'pinned' back which, of course, it is by the nail.

- Locally high τ maximum at the wall base must reflect the high stress relief at the time of element removal, which numerically is instantaneous (Figure 6.19). This may be considered analogous to the locally high shear stress observed at the toe of conventional gravity wall structures.

- The end of construction predicted response for x displacements (Figure 6.20) show the center 50 percent of wall dominating movements, to a maximum of 9.4 mm (0.37 inches). This deflection data is plotted against the observed movements for slope inclinometer SD-130 at the end of construction, and is shown in Figure 6.21. The displacements plotted from the FENAIL predictions are from a horizontal distance back away from the wall face equal to that of the field inclinometer casing. Note that the peak x displacements predicted in the middle of the wall are obscured at this distance into the slope and that the overall prediction of deflection magnitude is very close to the observed data.

- The model predicts a general translation of the wall face rather than a 'tilted' rotation pattern. Some case history wall deflections presented in published literature also show a translation response.

- σ_y stresses at the wall face again show a slight increase, since no unit weight of shotcrete can be assigned to suppress movement.

- The resulting increase in predicted σ_y at the wall toe generates a prediction of τ maximum which is higher than expected ($2\tau = \sigma_1 - \sigma_3 \approx \sigma_y - \sigma_x$), and also suggests an active wedge mechanism trying to form from the wall base.

- A realistic range of wall pressures is predicted from the distribution of σ_x at the wall face in Figure 6.22, on the order of 4.3 kPa - 9.6 kPa (90-200 psf). Over the average nail spacing, this distribution gives nail forces at the facing connection ranging from 1.8 to 4.0 kips per nail, which matches well to the load cell readings at S2.

- A localized x displacement 'spike' at the tail of top nail is present throughout the model excavation sequence (Figures 6.18 and 6.20) This 'spike' is unique and not repeated for the remaining four rows below. The cause or significance for this result is not understood, but a similar 'spike' has been reported by other researchers who have numerically modelled soil nail walls (Cardoso and Carreto, 1989).

- The maximum tensile loads in the beam elements representing the nails are located near the end of the nail, farthest from the face. Limit equilibrium theory would place the potential failure surface near this location, and this result therefore seems reasonable. Although the maximum tensile loads in these beam elements (nails) are in the range of 3.14 - 7.6 kN (0.7 to 1.7 kips), which is about 25 percent of the load interpreted from the measured Swift Delta data, the reduction in maximum load from the top nail to the bottom nail is of roughly the same order. These results have been extracted from the voluminous output file from FENAIL. These files are up to 1.2 MB (well over 300 pages) in size and are therefore not reproduced here.

6.7 MODEL 5NPS-S1 MODEL WITH HYPERBOLIC SOIL, BEAM ELEMENT NAILS AND SHOTCRETE, AND OVERLAIN MESH PILE BEAM ELEMENTS CONNECTED BY 'INTERFERENCE' ELEMENTS.

As described above, this model is the application of all available FENAIL features to date to predict the response of instrumented section S1, beneath the bridge deck at Swift Delta. In addition to all the properties and features described in Model 2XNB, there is present an 'interference' nodal connection element to model the nail-to-pile interaction. The FENAIL interface element is employed for this technique, but its constitutive relationship must describe the possible load transfer from the soil nails to a pile face which exists approximately 381 - 432 mm (15 to 17 inches) from the nail grout. Thus it is not a true interface, and is therefore referred to as 'interference.' Input parameters are listed in Table 6.1 for soil, shotcrete, nails and pile, and below for the 'interference' elements.

Again full gravity is applied to the model, followed by the five excavation steps, nail installation and wall construction. The nail to pile interference properties are:

Penalty number to model contact $= K\infty_{(n)} = 0.0$
Coefficient of friction $= f = 1.0$
Penalty number to model no slip $= K\infty_{(t)} = 0.0$
Penalty number to model flow across interface gap $= K_p = 0.0$
Angles defining the normals at the ends of the interface are:
$\theta_1 = 90$ degrees
$\theta_2 = 90$ degrees
The interface spring and shear coefficients are:
$K_{sn} = 2,920$ kN/m (200,000 lb/ft)
$K_{st} = 73,000$ kN/m (5000000) lb/ft
$S_{sn} = 0.0$
$S_{st} = 0.0$

and it should be noted that zero shear stress, S_{sn} and S_{st}, indicates elastic behavior.
The interface spring coefficients used were selected such that predicted stresses, as well as wall and pile cap movements, were comparable to those observed by the Swift Delta instrumentation. There is no basis in theory for selection of these values, and no instrumentation data provided for a direct measurement of the load transfer from the nails, through the grout, through the soil, and to the pile.

The following Figures 6.25 to 6.30 pick up this sequence after the third excavation lift through to end of construction. The following can be observed:

- By the third excavation lift, as seen on Figure 6.25, predicted pile cap movements of 3.8 mm (0.15 inches) compare well to extensometer movements corresponding to this construction stage of about 5.0 mm (0.2 inches). Predicted maximum wall movements are about 5.0 mm (0.2 inches) at this construction stage, with a general horizontal bulge predicted in the lower third of the intermediate wall height. Instrumentation data is not available to compare the distribution of wall movements during construction under the bridge.

- Similar to models 1XNB and 2XNB, locally high τ maximum zones are predicted at the free face excavation base following each incremental excavation (Figures 6.26 and 6.30). As expected from the successful long term performance of the Swift Delta wall, no shear failure is predicted due to any upward propagation of shear failure stresses (progressive failure) behind the wall. However, the local high τ maximum at the toe of the excavation may be an accurate prediction of the local, single lift height, face instability (sloughing) observed during construction.

66

- From the third to final excavation, the wall peak x deflection increases by nearly 100 percent (Figure 6.27). At the same chronologic interval the predicted pile cap movement changes only 30 percent, demonstrating the pile stiffness. When deflections between 1XNB (no piles) and 5NPS (with piles) are compared, the stiffness of the piles, and the load transfer from the nails to the piles, appear to have minimum influence in preventing wall movements.

- Figure 6.28 depicts σ_x distribution for the final excavation step and shows that nail interaction is difficult to interpret, but appears in the range of 0 - 9.6 kPa (0-200 psf) for the wall similar to the 1XNB and 2XNB models.

- Both the σ_x and σ_y at the end of construction (Figures 6.28 and 6.29) show rapid changes at the excavation toe. Coarse element construction at this point in the mesh does not adequately model this change well.

- Similar to models 1XNB and 2XNB, upward wall y movements are observed due to the zero shotcrete weight, resulting in a disturbed local σ_y plot as shown on Figure 6.29.

- The weight of the pile cap, is supported on the pile beam elements, thus locally reducing σ_y, relative to the 1XNB model with no piles (Figure 6.14 and Figure 6.29).

- As in 2XNB, the maximum tensile loads in the beam elements representing the nails are located near the end of the nail, farthest from the face. Again, the maximum tensile loads in these nails are about 25 percent of the load interpreted from the Swift Delta data, (FENAIL predicted range of 3.0 kN - 8.5 kN (0.67 to 1.9 kips). The trends in distribution and magnitude of forces are similar to the 2XNB model. Also, again due to the size of the output file, these full results are not reproduced here.

6.8 PILE, NAIL AND WALL BEHAVIOR SUMMARY

A summary of key FENAIL predicted results and Swift Delta instrumentation data is presented in Table 6.2.

Table 6.2 Summary of Key FENAIL Results
(All results at end of construction)

Result or Measurement	Swift Delta Instrumentation	MODEL	
		5NPS Section 1 (S1)	2XNB Section 2 (S2)
Pile Cap x Deflection (in.)	0.3	0.22	Not Applicable
Maximum Wall Face Deflection (in.)	S1 - unknown S2 - 0.7	0.36	0.38
Range of Maximum Nail Loads (kips)	S1 - 4 to 8 S2 - 3.5 to 10	0.67 to 1.9	0.7 to 1.7
Range of Wall Facing Pressure (psf)	S1 - 50 to 150 S2 - 60 to 150	0 to 200	90 to 200

Collecting the foregoing comments together and restating observations more directly for the Swift Delta model the following emerges:

- When comparing the best S1 modeling (5NPS) with the best S2 modeling (2XNB) the pile contribution shows up in 3 areas:

  1) A nominal increase in x deflection maximum from 9.2 mm (0.36 inches) (5NPS) to 9.6 mm (0.38 inches) (2XNB), but a more pronounced wall bulging pattern is seen without the piles in 2XNB at S2.

  2) A significant drop in σ_x against the wall. The S1 model even moving into tension at various locations up and down the entire wall face as some horizontal stress is shed to the pile. A close to linear distribution of σ_x is predicted in S2, but the distribution is less clear in S1.

  3) If significant lateral load carrying capacity was taken by the piles, it would be expected that nail loads would be lower at S1 than S2. FENAIL does not predict this. Rather, very similar nail loads were predicted in S1 and S2, which compares with the instrumentation strain gage data from both sections. FENAIL predicted wall pressures, however, for S1 are in the range 0 - 9.6 kPa (0-200 psf), and for S2 in the range 4.3 kPa - 9.6 kPa (90-200 psf), indicating that load transfer to the wall facing (irrespective of load carried by the nails) may be affected by the close proximity of the piles to the wall facing.

68

- Based on the FENAIL modeling results, soil nail wall deflections and stresses do not seem highly sensitive to the presence of the piles.

- In the FENAIL model 5NPS, the piles are stressed as a result of soil nail wall deflections through the "interference" element. In reality, this load transfer, by soil arching, from the nails to the piles, is a result of normal expected soil nail wall movements.

- The FENAIL models which incorporate the effects of soil nails indicate that the in situ reinforcement provided by the nails causes the soil stress fields (magnitudes and locations of σ_x and σ_y) to remain basically the same, before and after excavation. That is, the stress induced by excavation in front of the retained soil mass is accommodated by the passive inclusion of the nails. This would seem to validate the general assumptions of the behavior of reinforced soil structures. This preservation of stress fields may be seen by comparison of Figures 6.15 and 6.17 to Figures 6.22 and 6.23 which show the σ_x and σ_y stress fields, respectively, before construction (under gravity loading only), and following completion of the soil nail structure.
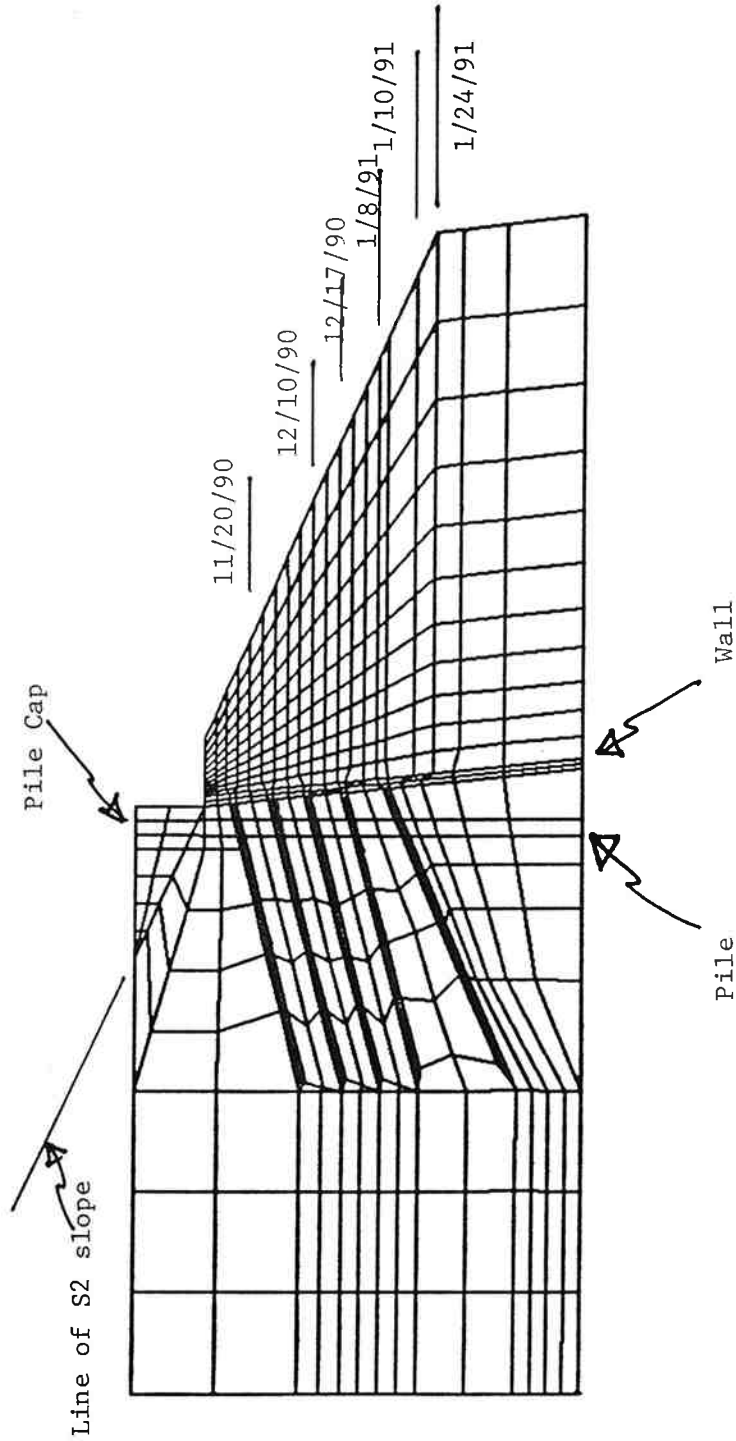
Figure 6.1 FENAIL 2D Mesh
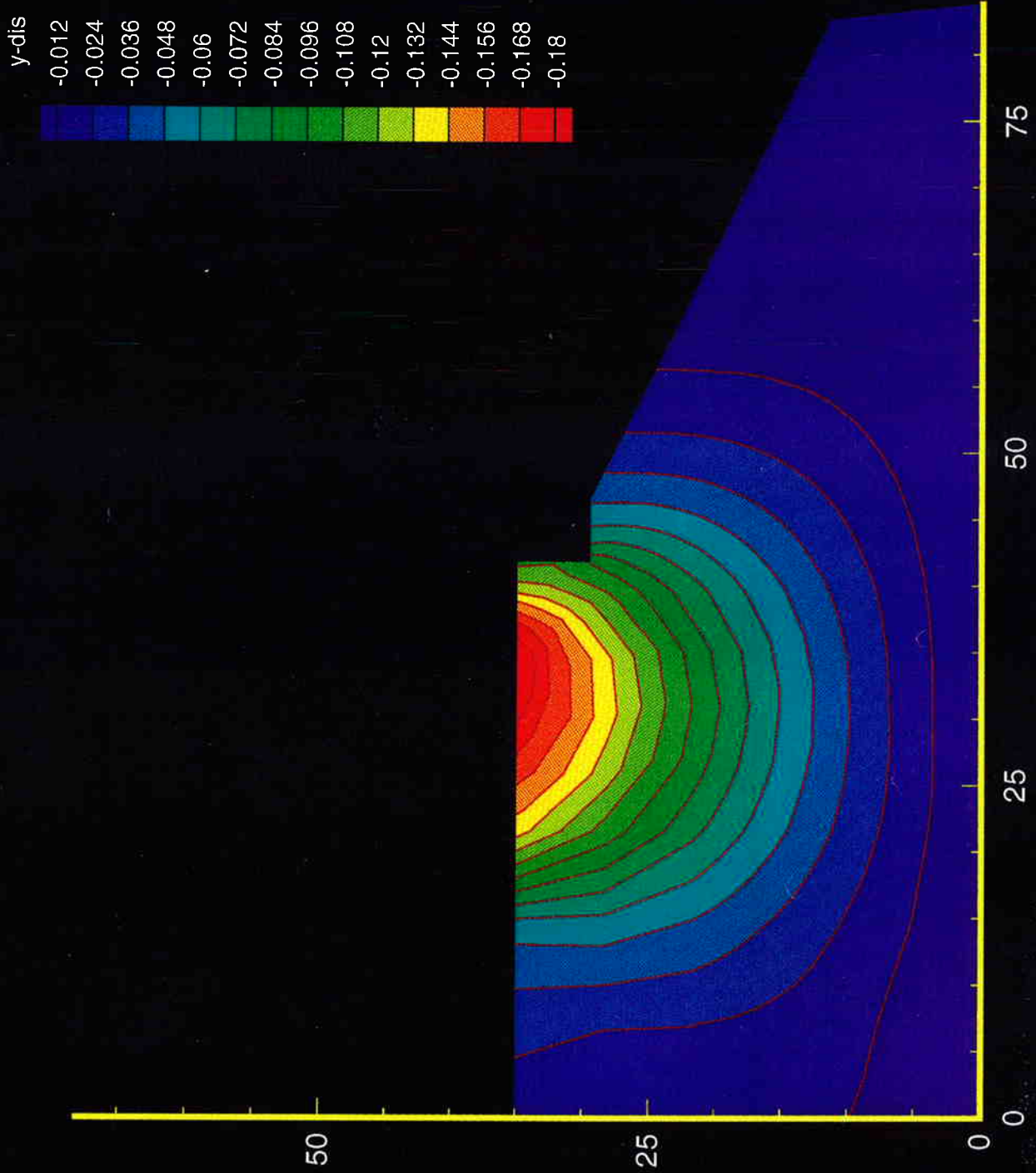
Figure 6.2 Vertical (y) Displacement for Elasticity under 1 psf

THIS PAGE INTENTIONALLY LEFT BLANK.
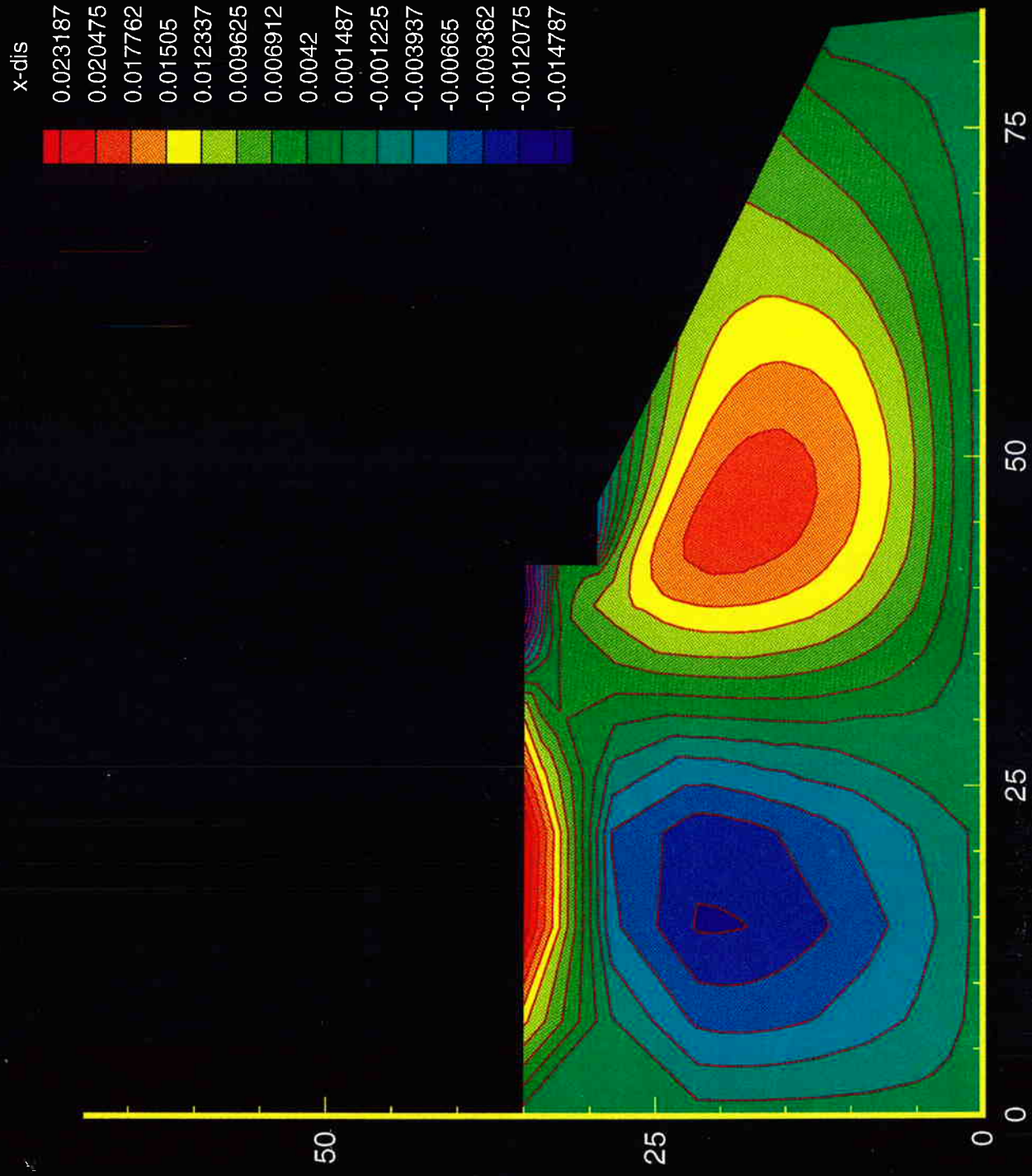
Figure 6.3 Horizontal (x) Displacement Elasticity under 1 psf

THIS PAGE INTENTIONALLY LEFT BLANK.

x-dis

0.000135
0.000103
7.156E-5
3.975E-5
7.937E-6
-2.387E-5
-5.568E-5
-8.75E-5
-0.000119
-0.000151
-0.000182
-0.000214
-0.000246
-0.000278
-0.000310
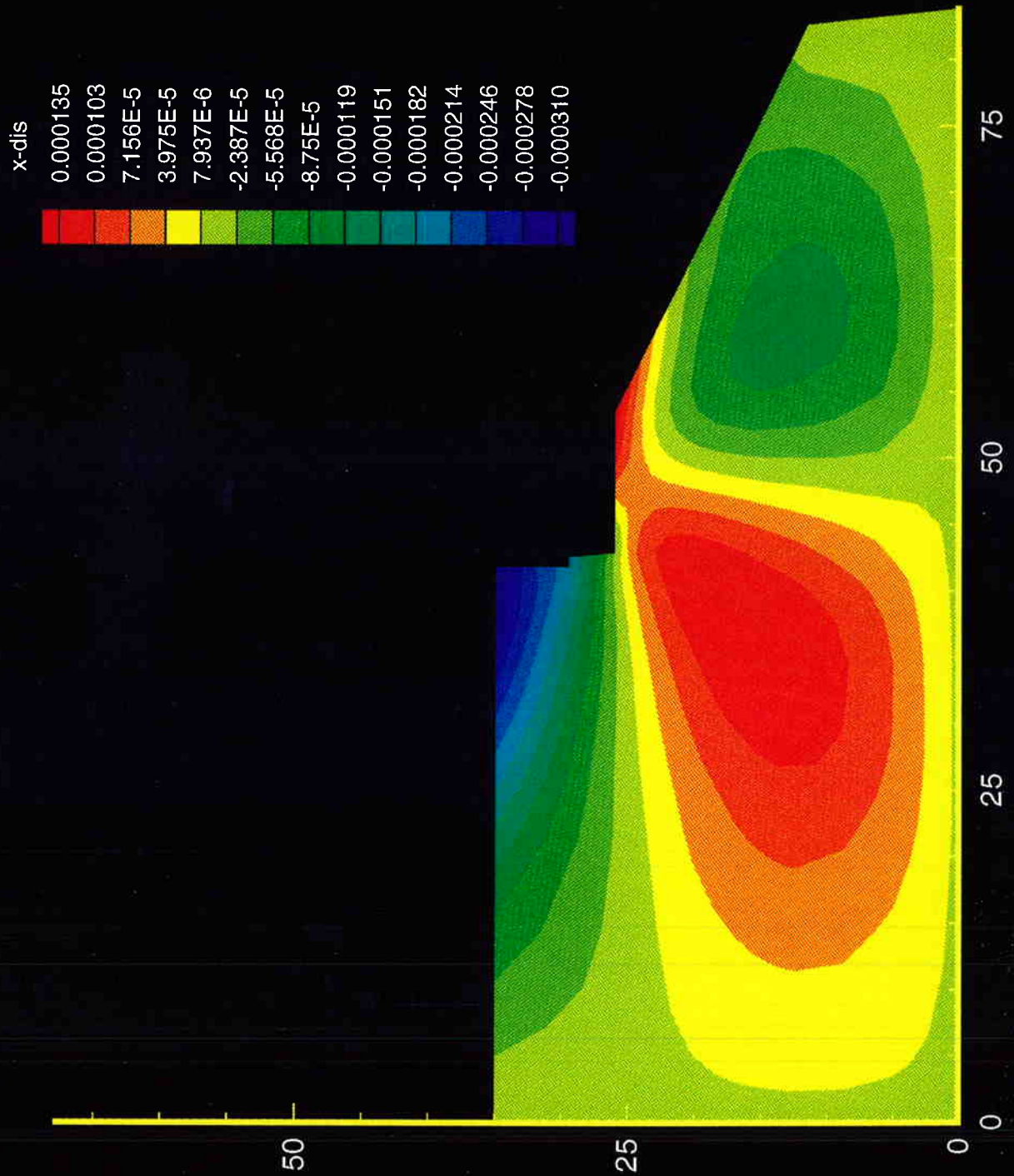
Figure 6.4 Horizontal (x) Displacement for Elasticity 2nd Excavation Sequence

THIS PAGE INTENTIONALLY LEFT BLANK.
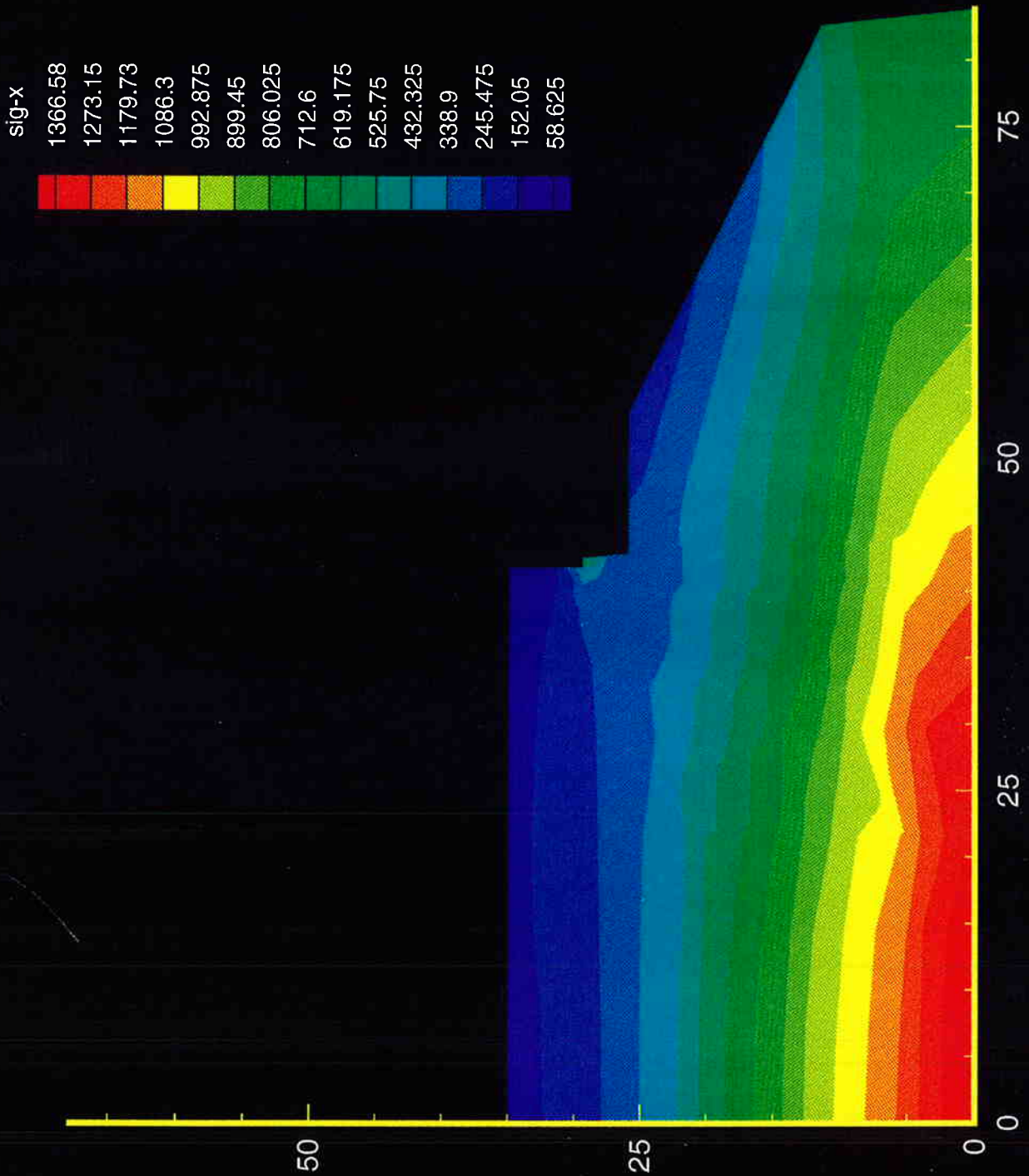
Figure 6.5 Sigma x Displacement for Elasticity 2nd Excavation Sequence

77

THIS PAGE INTENTIONALLY LEFT BLANK.
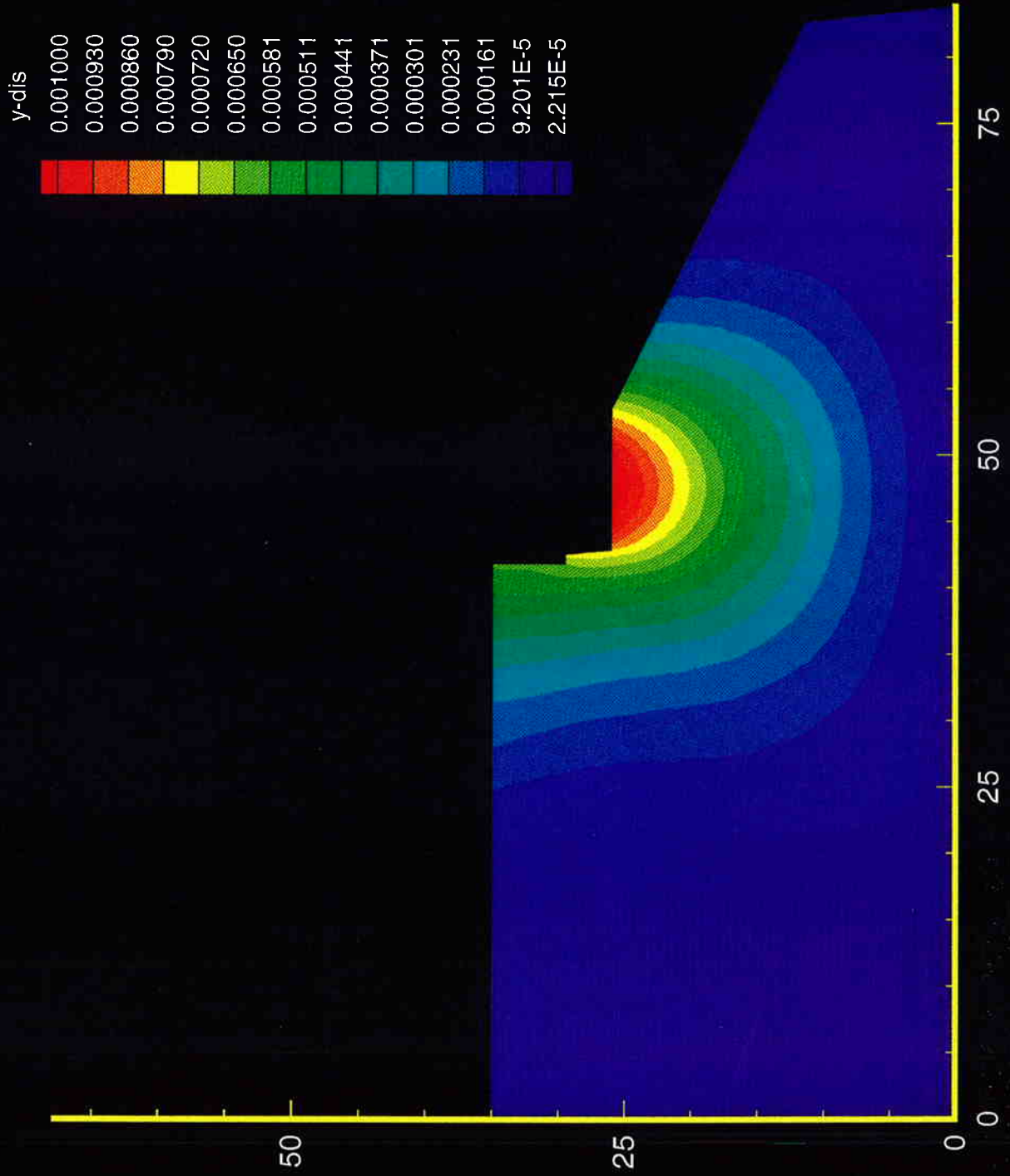
Figure 6.6 y Displacement for Elasticity 2nd Excavation Sequence

THIS PAGE INTENTIONALLY LEFT BLANK.
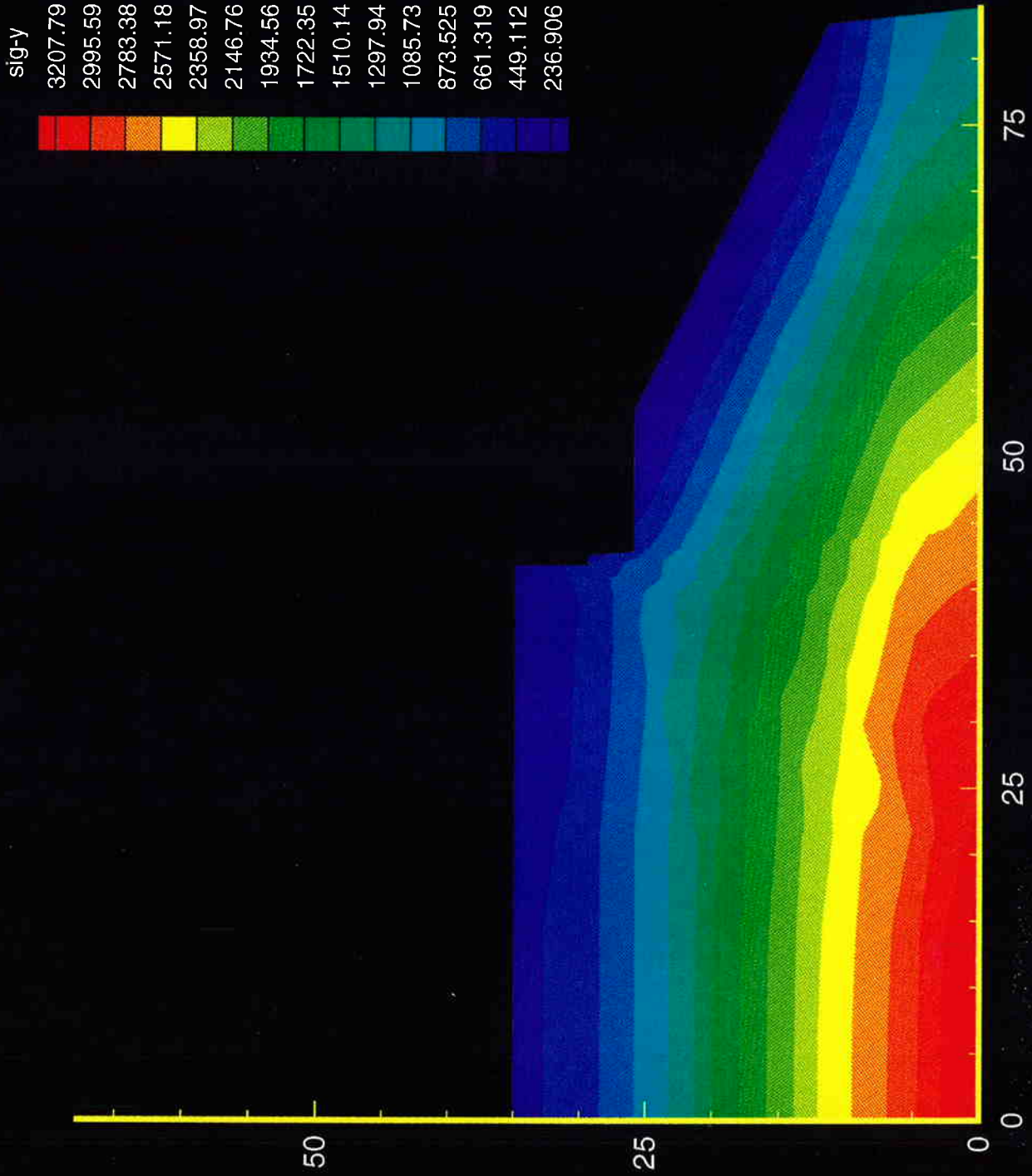
Figure 6.7 Sigma y Displacement for Elasticity 2nd Excavation
Sequence

THIS PAGE INTENTIONALLY LEFT BLANK.

x-dis

0.000860
0.000681
0.000501
0.000322
0.000143
-3.624E-5
-0.000215
-0.000395
-0.000574
-0.000753
-0.000933
-0.001112
-0.001291
-0.001471
-0.001650
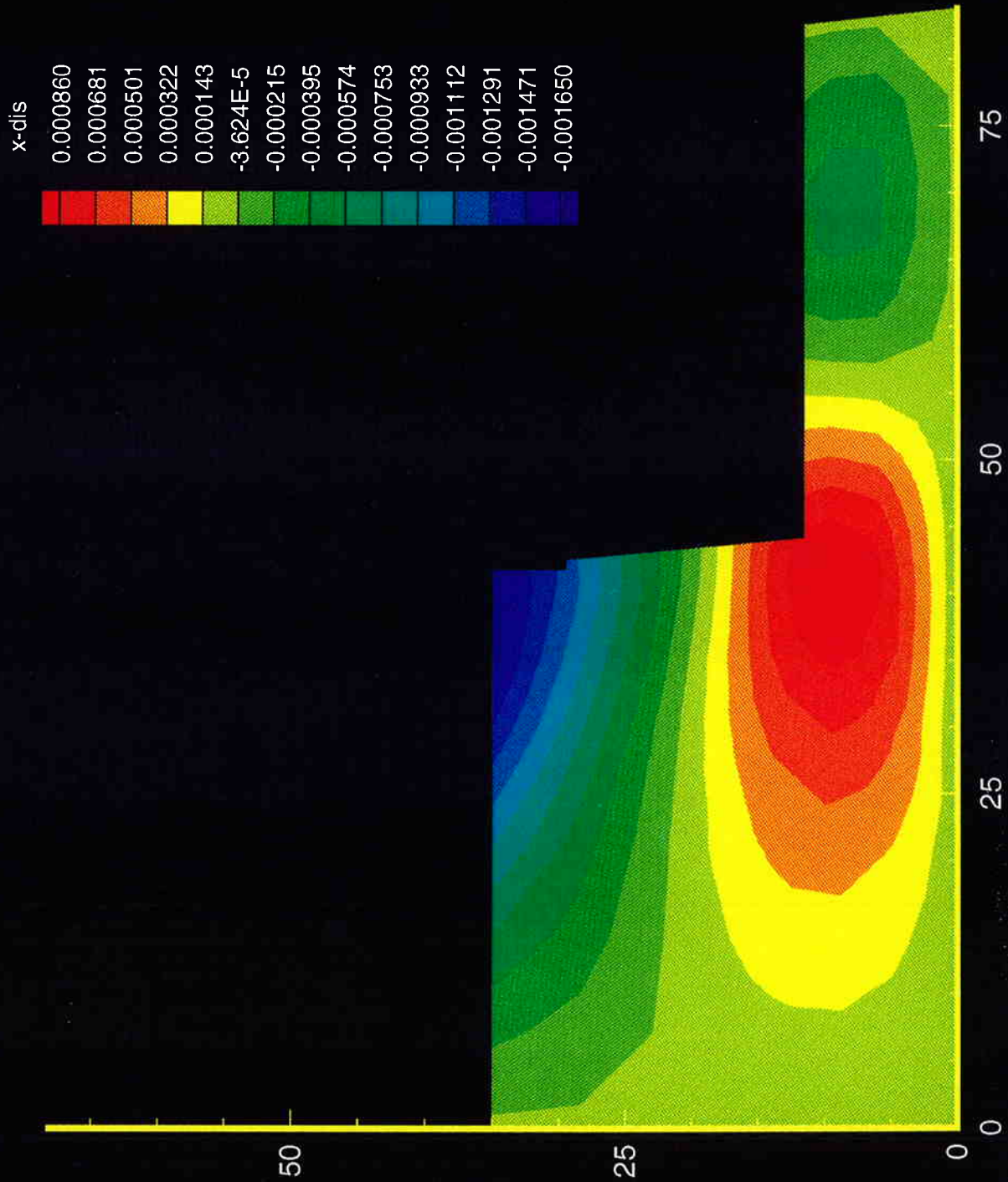
Figure 6.8 x Displacement for Elasticity Final Excavation Sequence

THIS PAGE INTENTIONALLY LEFT BLANK.
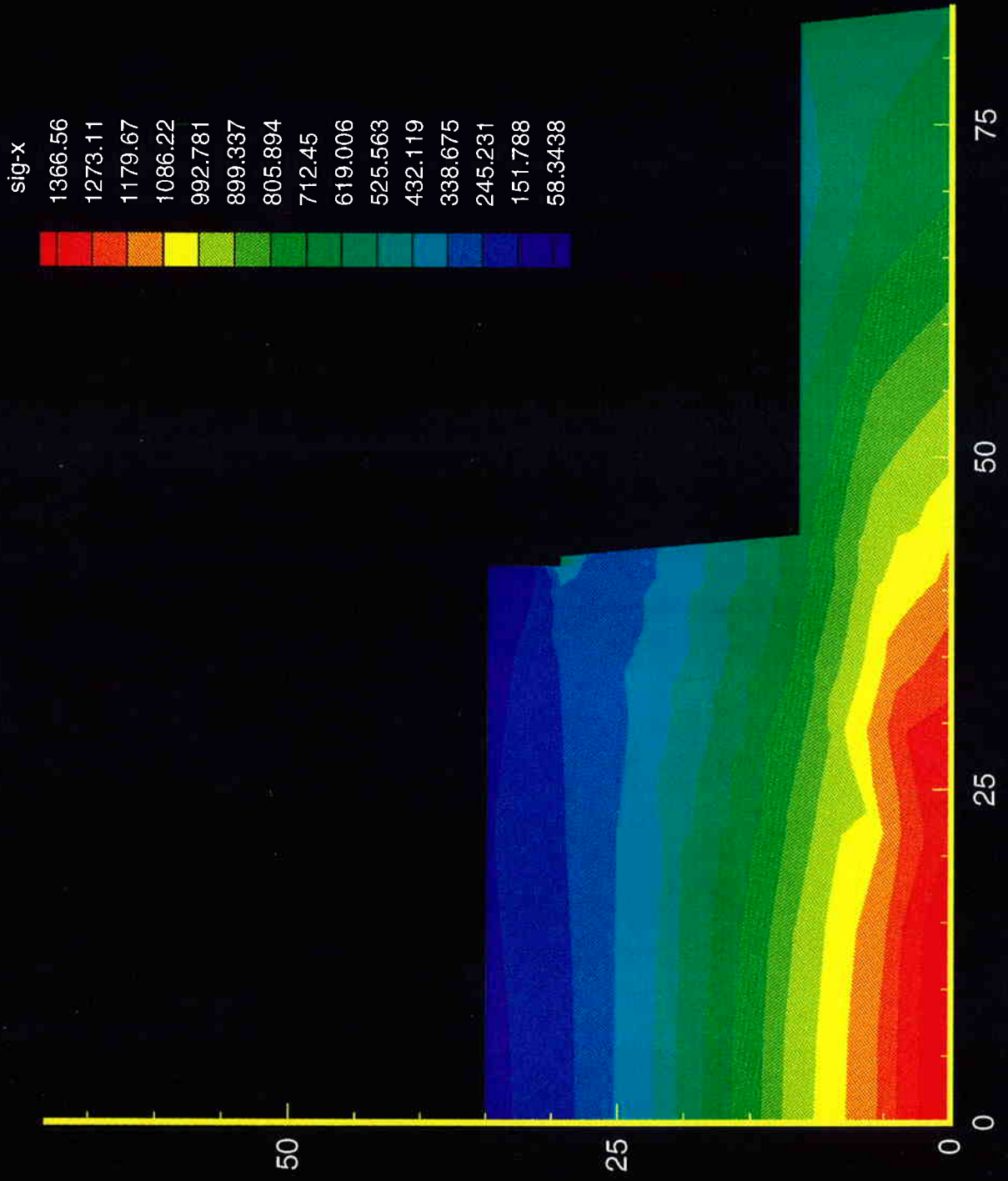
Figure 6.9 Sigma x for Elasticity Final Excavation Sequence

THIS PAGE INTENTIONALLY LEFT BLANK.
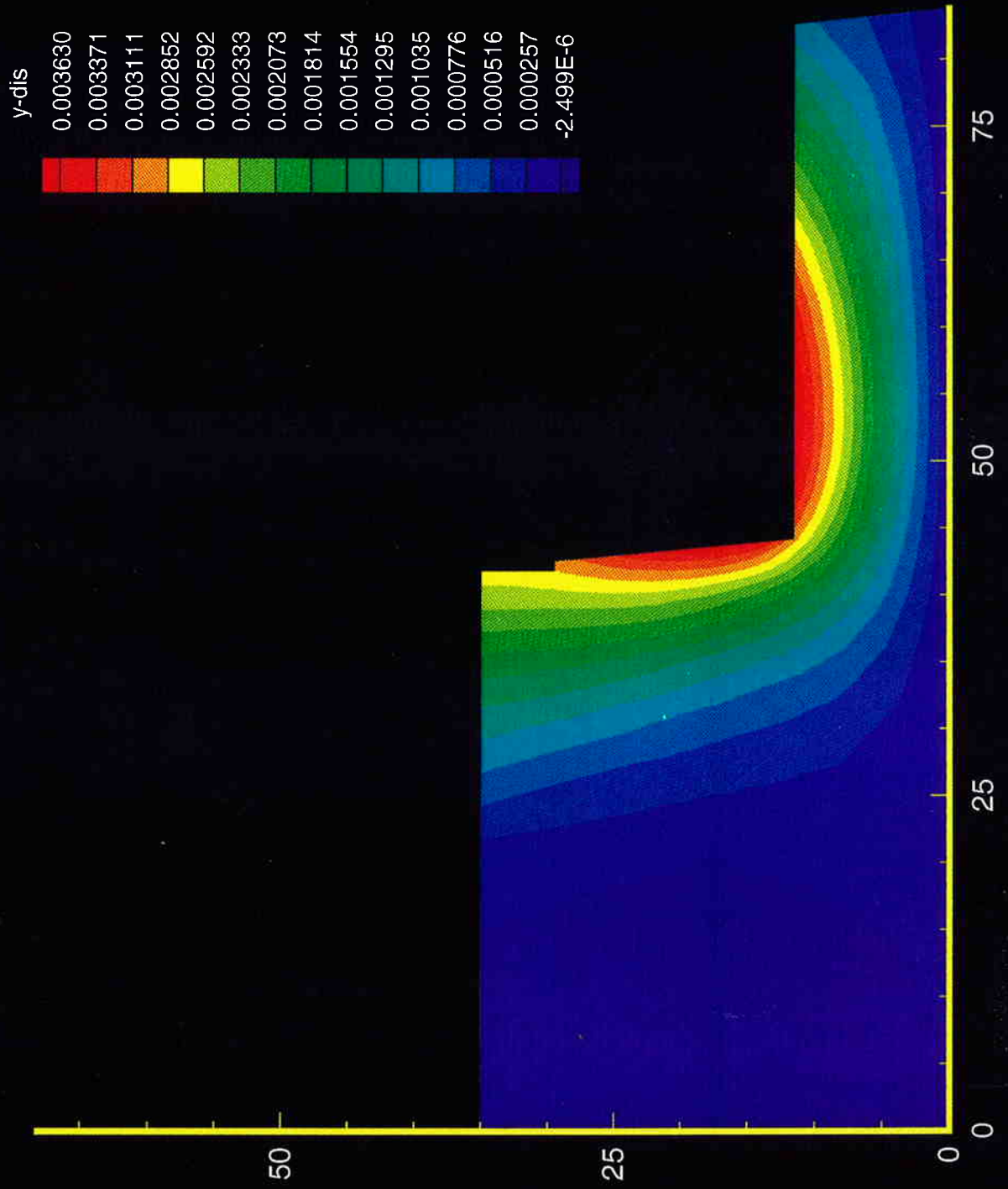
Figure 6.10 y Displacement for Elasticity Final Excavation Sequence

THIS PAGE INTENTIONALLY LEFT BLANK.
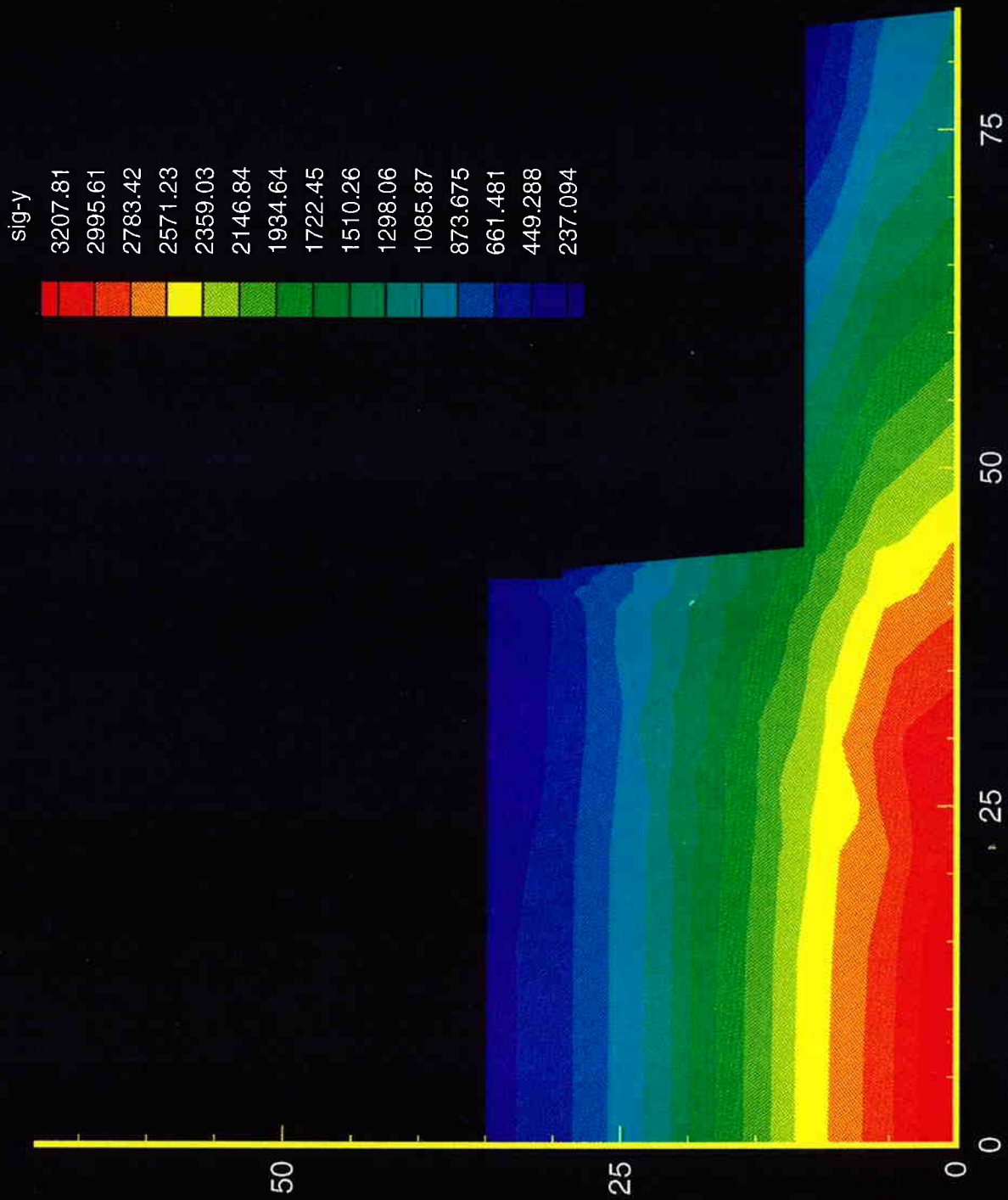
Figure 6.11 Sigma y for Elasticity Final Excavation Sequence

THIS PAGE INTENTIONALLY LEFT BLANK.

x-dis
0.034156
0.031012
0.027868
0.024725
0.021581
0.018437
0.015293
0.01215
0.009006
0.005862
0.002718
-0.000425
-0.003568
-0.006712
-0.009856
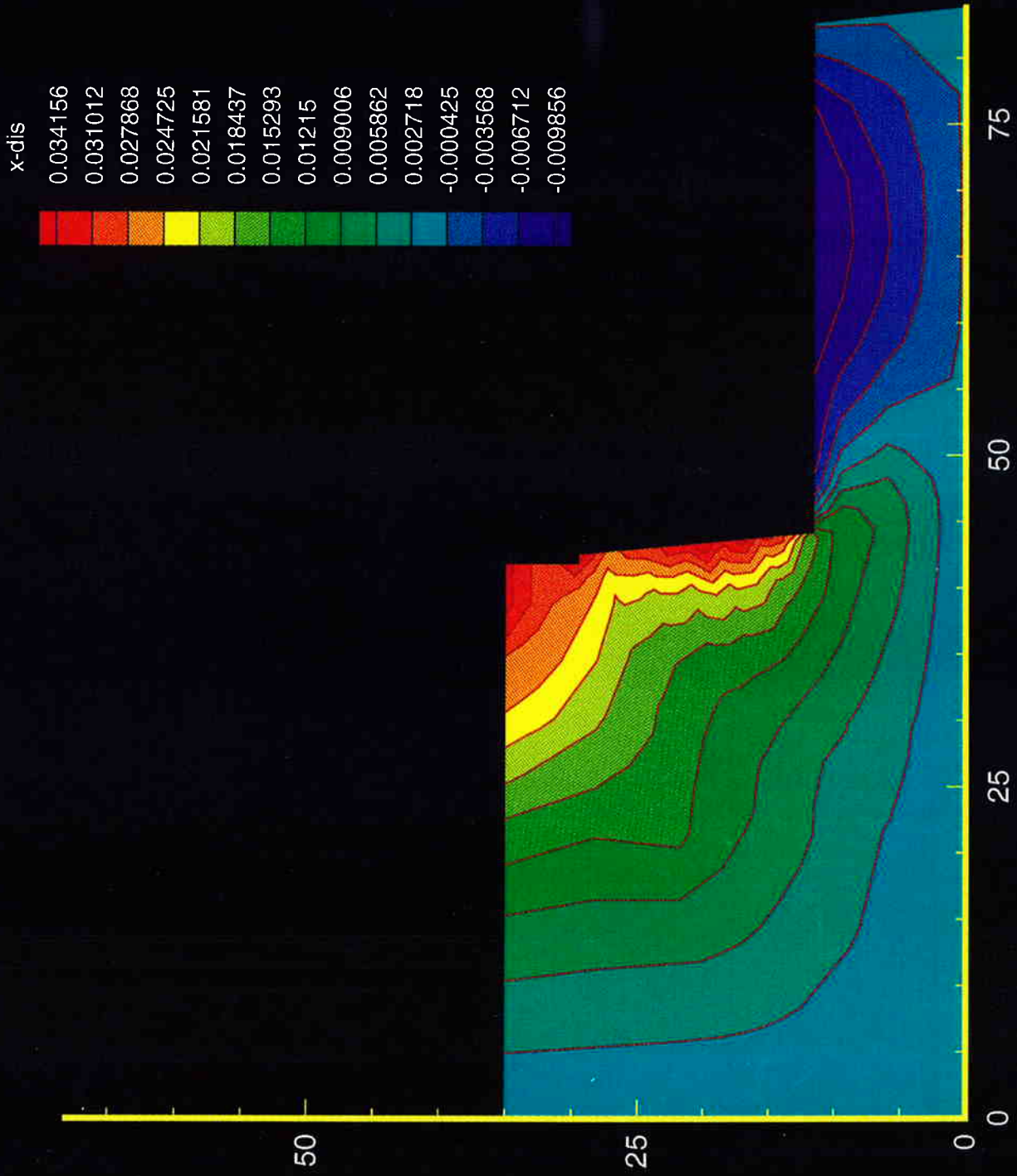
Figure 6.12 Section S1, Nonlinear soil, x Displacement

THIS PAGE INTENTIONALLY LEFT BLANK.
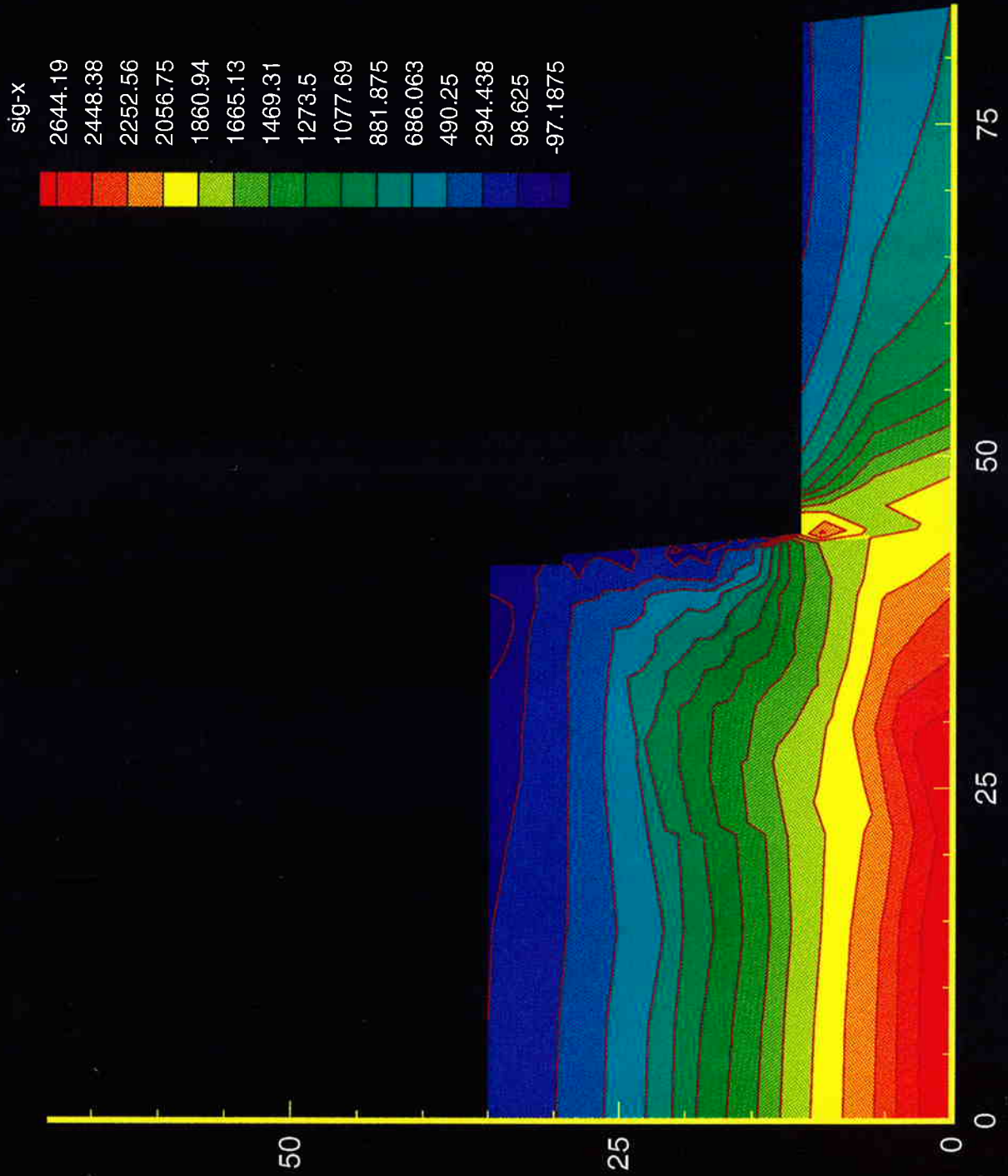
Figure 6.13 Section S1, Nonlinear soil, Sigma x

THIS PAGE INTENTIONALLY LEFT BLANK.
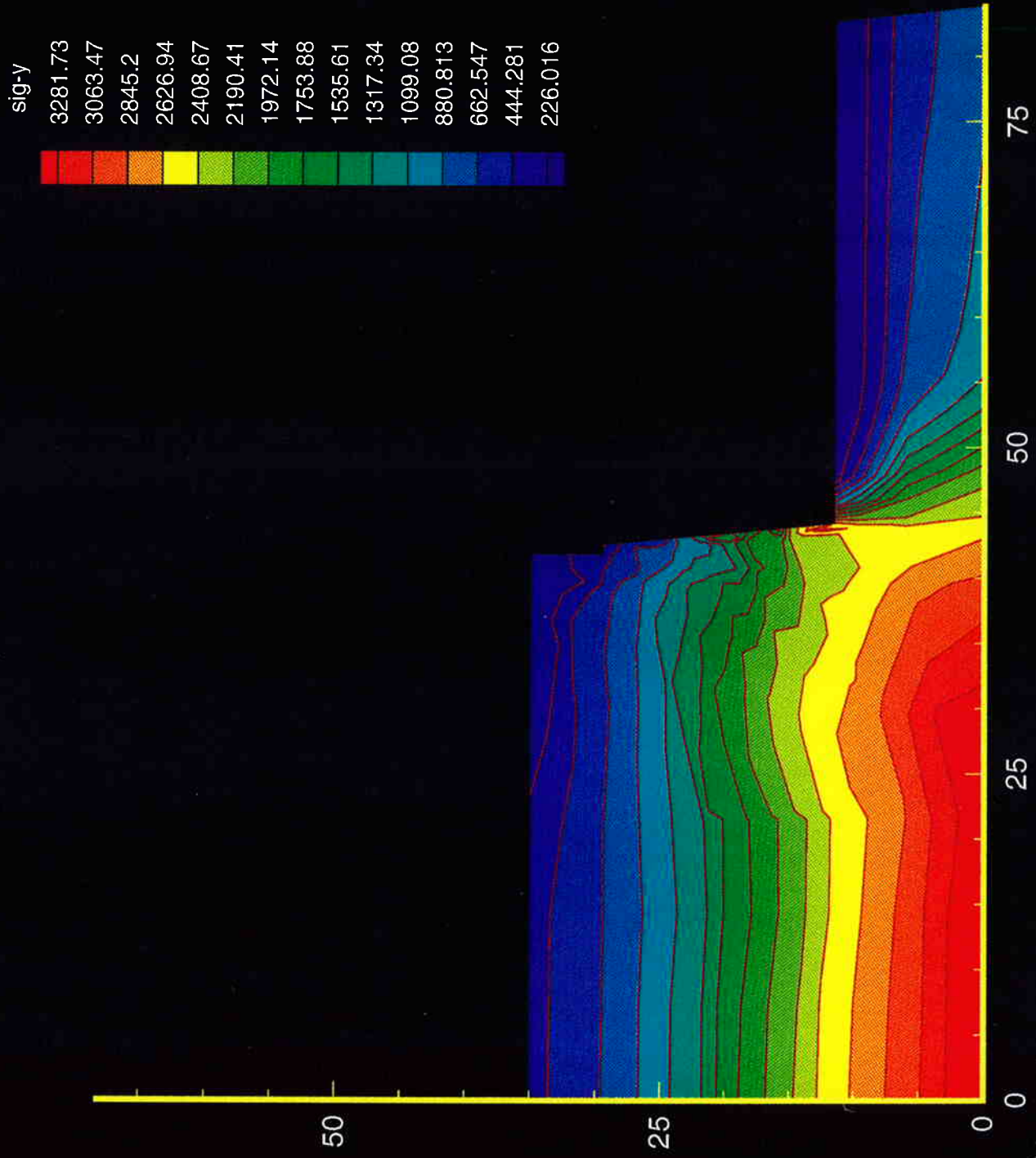
Figure 6.14 Section S1, Nonlinear soil, Sigma y

THIS PAGE INTENTIONALLY LEFT BLANK.

sig-y

	3440.82
	3211.65
	2982.47
	2753.29
	2524.12
	2294.94
	2065.76
	1836.59
	1607.41
	1378.23
	1149.05
	919.878
	690.701
	461.524
	232.347
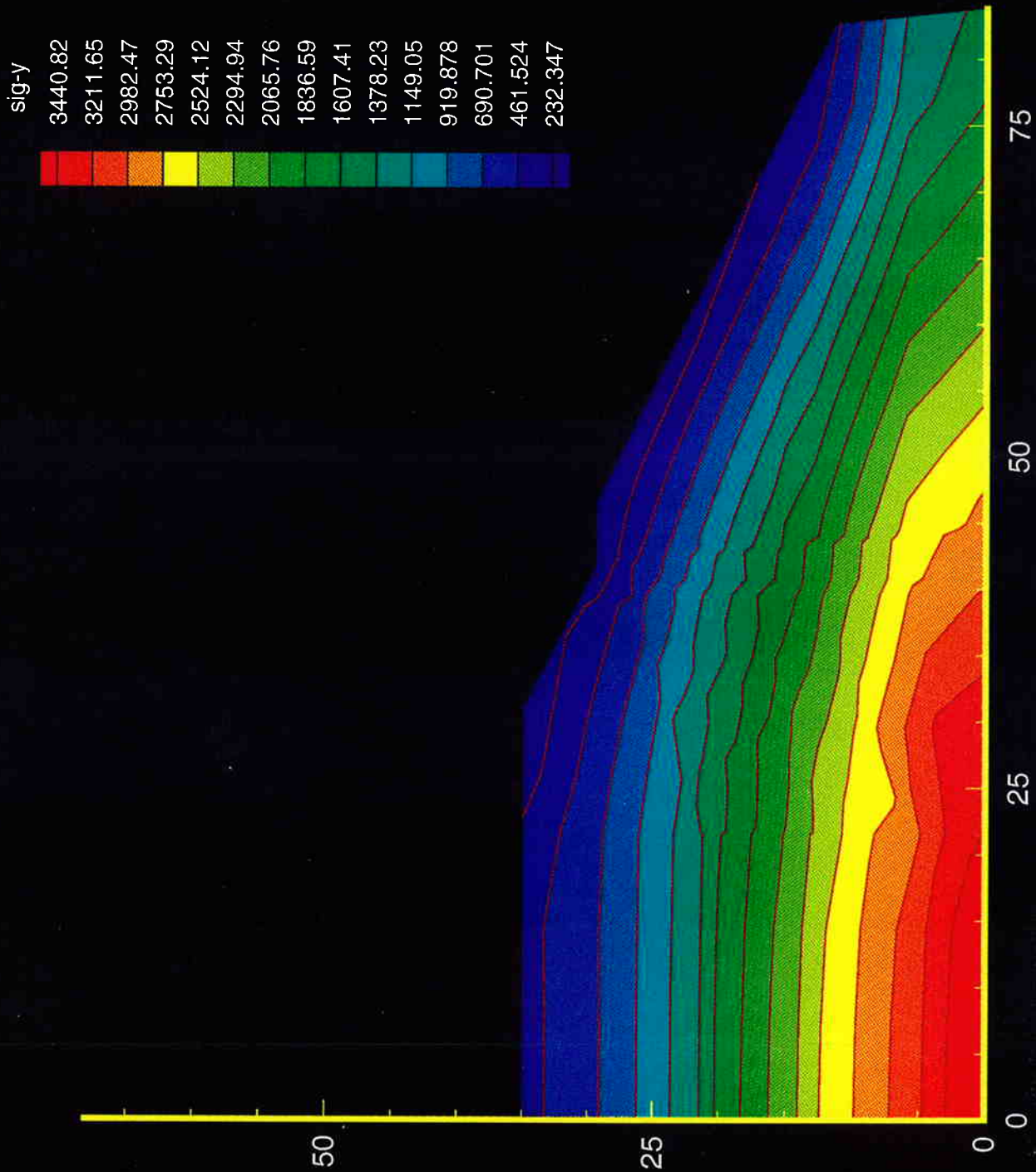
Figure 6.15 Section S2, Nonlinear soil, Sigma y under Gravity

THIS PAGE INTENTIONALLY LEFT BLANK.

tau-m
356.969
333.938
310.906
287.875
264.844
241.813
218.781
195.75
172.719
149.688
126.656
103.625
80.5938
57.5625
34.5313
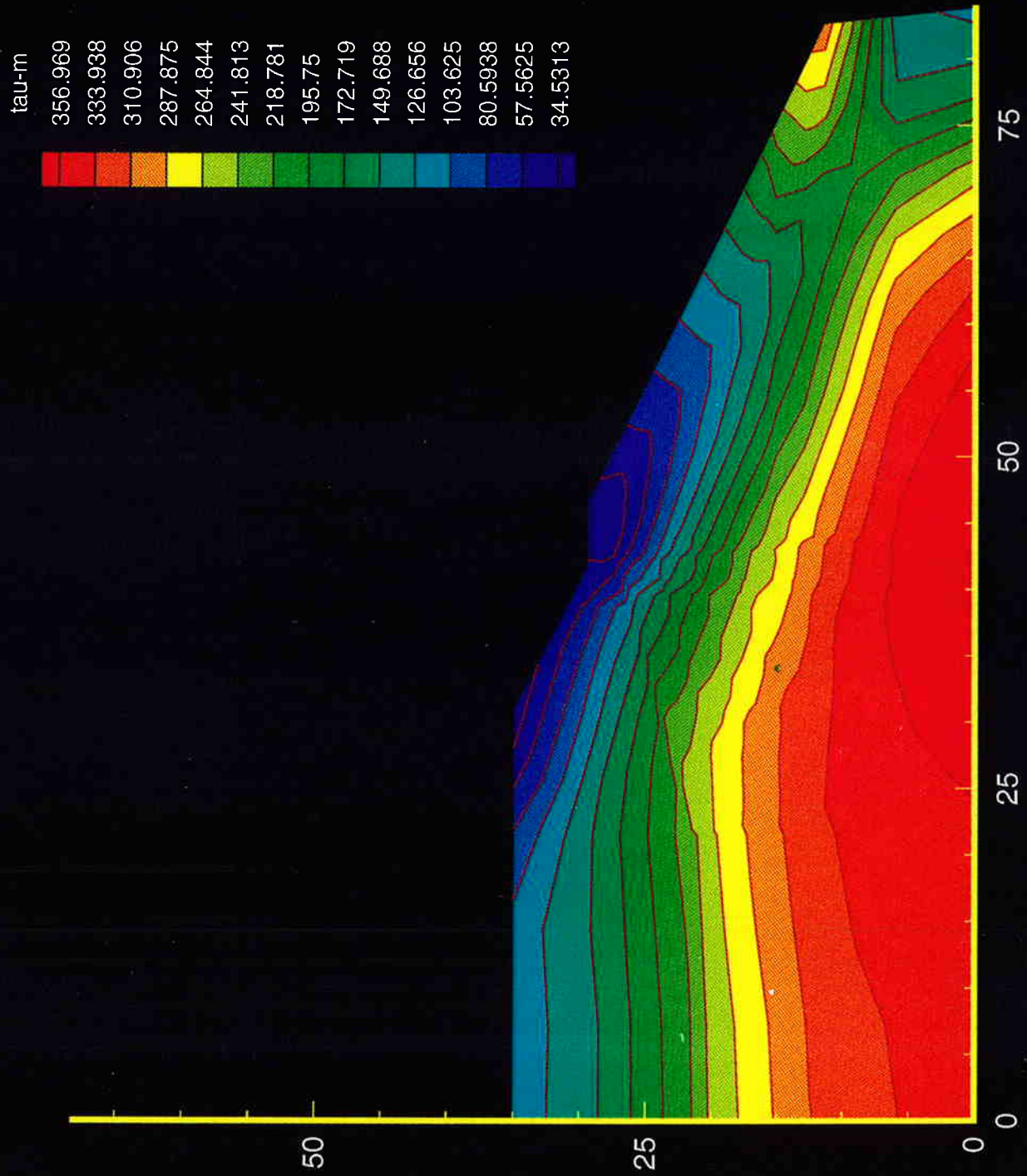
Figure 6.16 Section S2, Nonlinear soil, Maximum Shear Stress

THIS PAGE INTENTIONALLY LEFT BLANK.
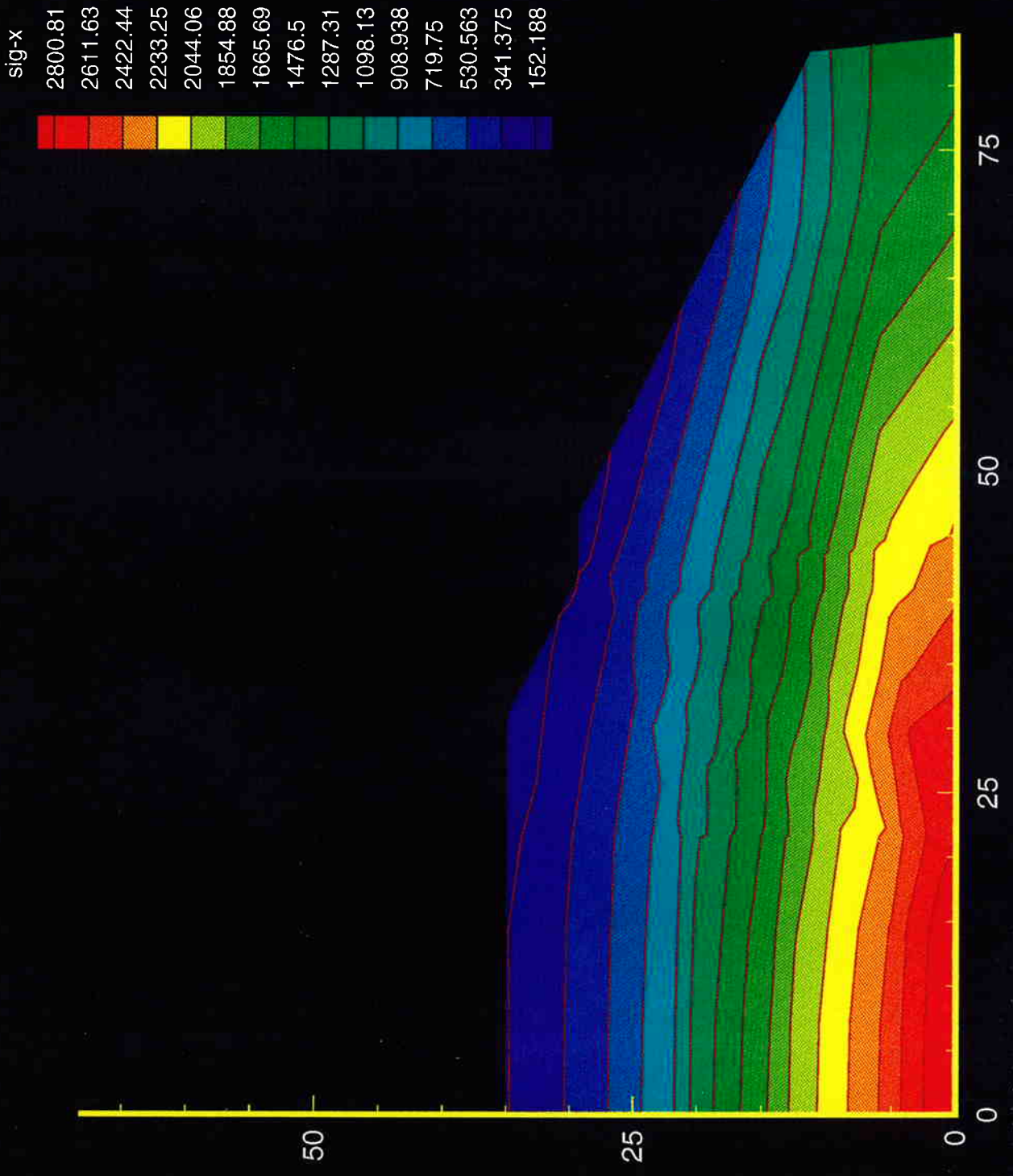
Figure 6.17 Section S2, Nonlinear soil, Sigma x under Gravity

THIS PAGE INTENTIONALLY LEFT BLANK.

x-dis

0.010583	
0.009267	
0.007951	
0.006635	
0.005318	
0.004002	
0.002686	
0.00137	
5.375E-5	
-0.001262	
-0.002578	
-0.003895	
-0.005211	
-0.006527	
-0.007843	
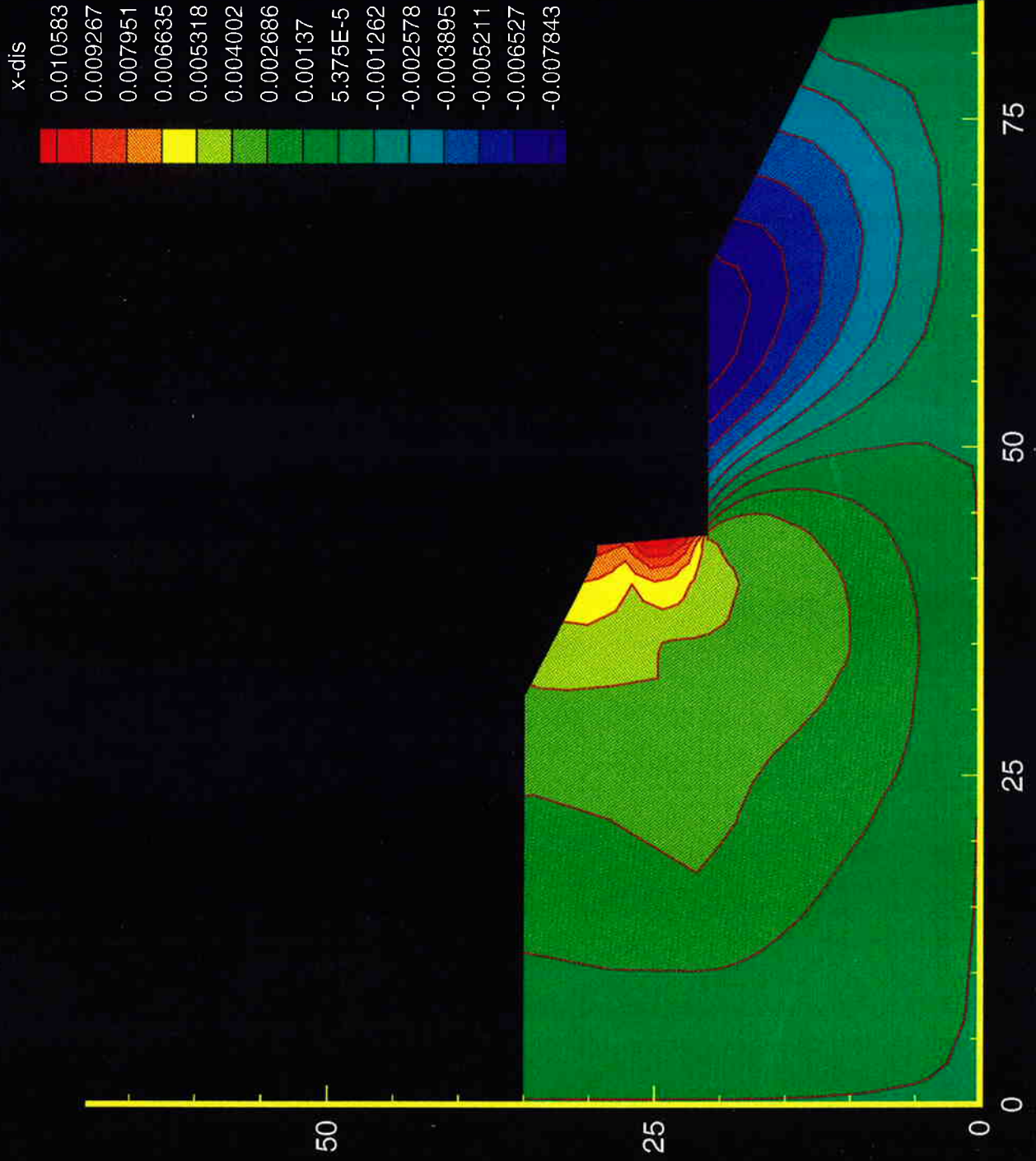
Figure 6.18 Section S2, x Displacement, 2nd Lift

THIS PAGE INTENTIONALLY LEFT BLANK.
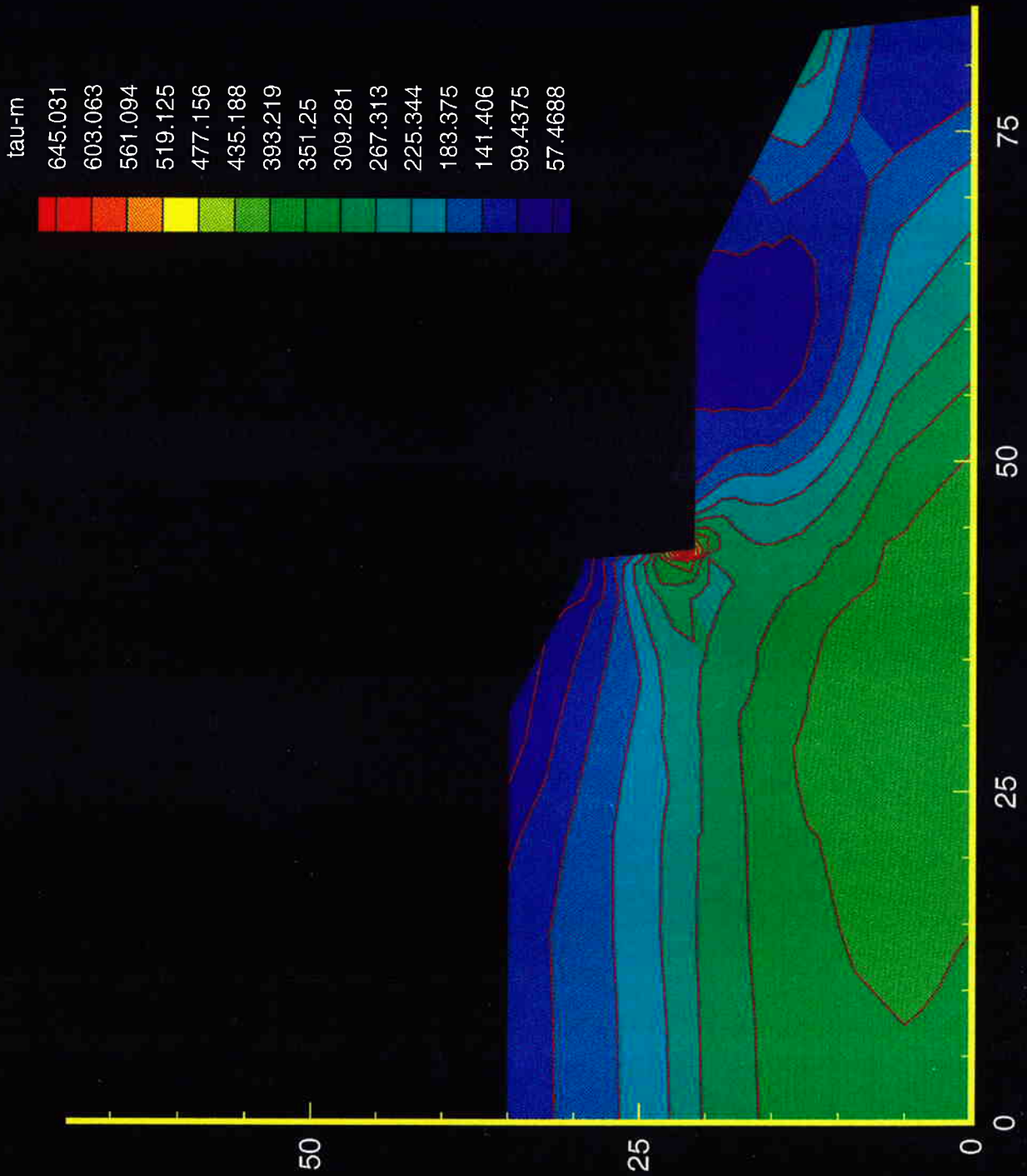
Figure 6.19 Section S2, Maximum Shear Stress, 2nd Lift

THIS PAGE INTENTIONALLY LEFT BLANK.
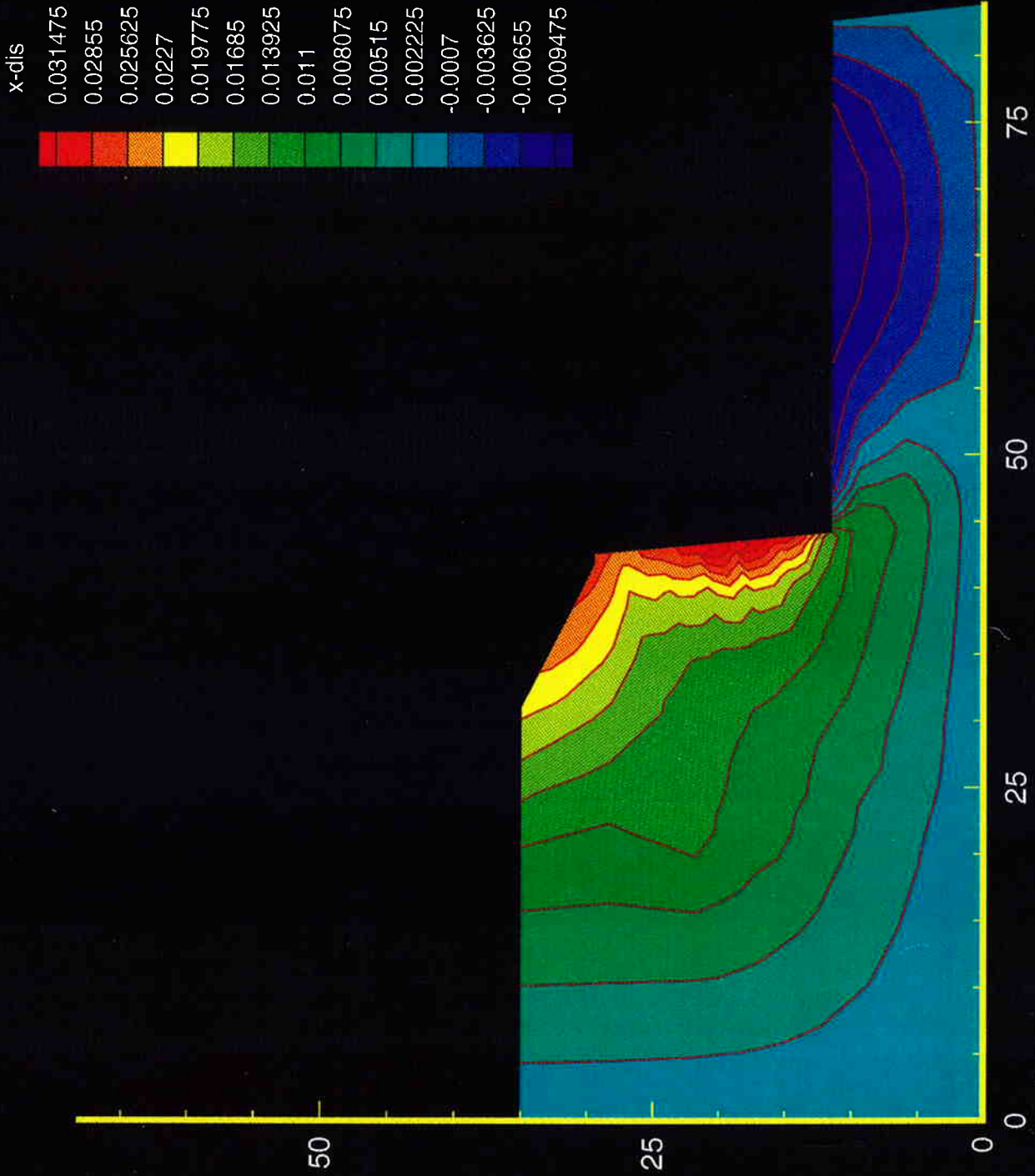
Figure 6.20 Section S2, x Displacement under Full Excavation

THIS PAGE INTENTIONALLY LEFT BLANK.

DEFLECTION
Section 2 - away from bridge

Lateral Deflection (inches)
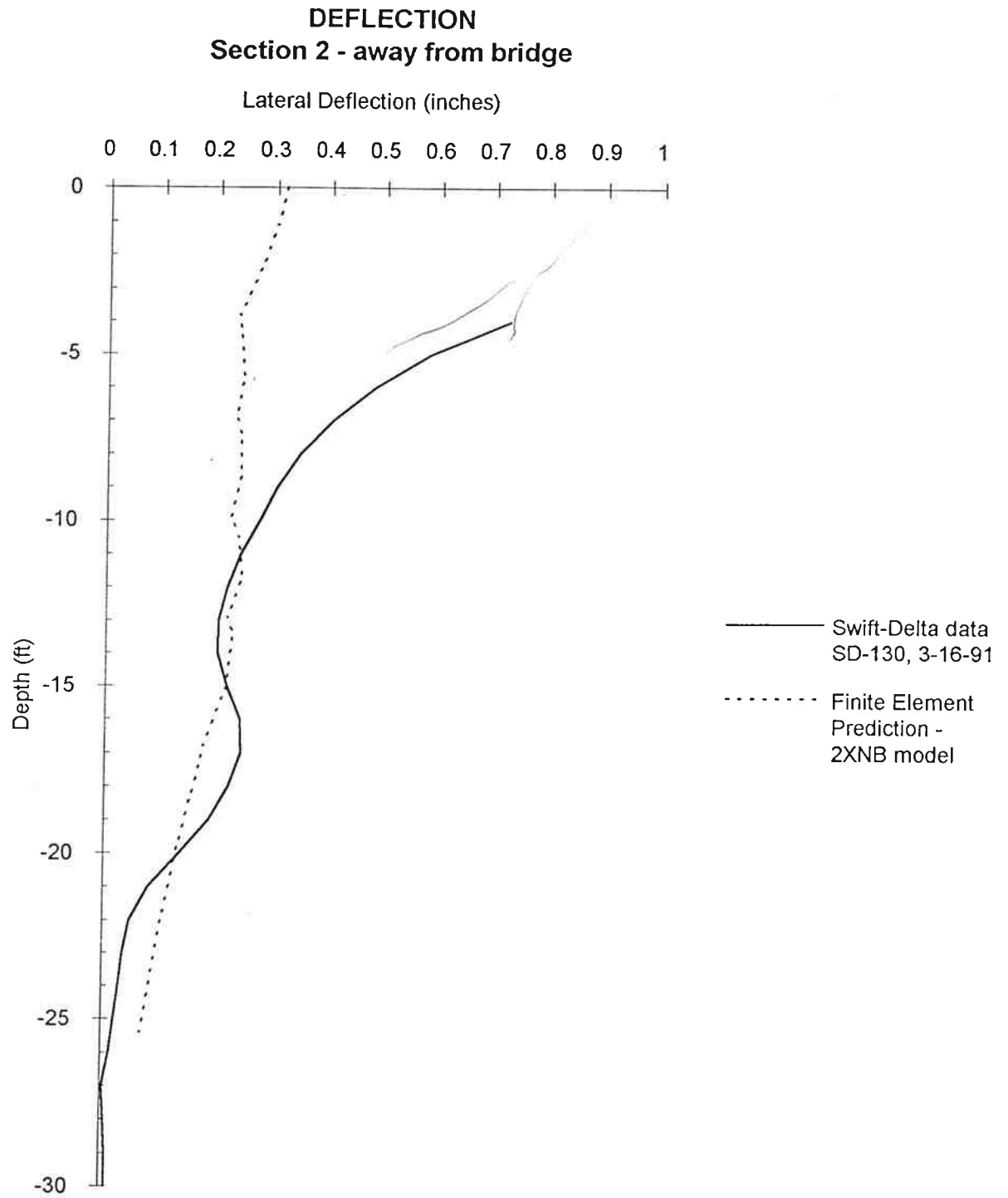
Figure 6.21 Comparison of Inclinometer SD 130 and FENAIL
Soil Predicted x Displacements at S2

THIS PAGE INTENTIONALLY LEFT BLANK.
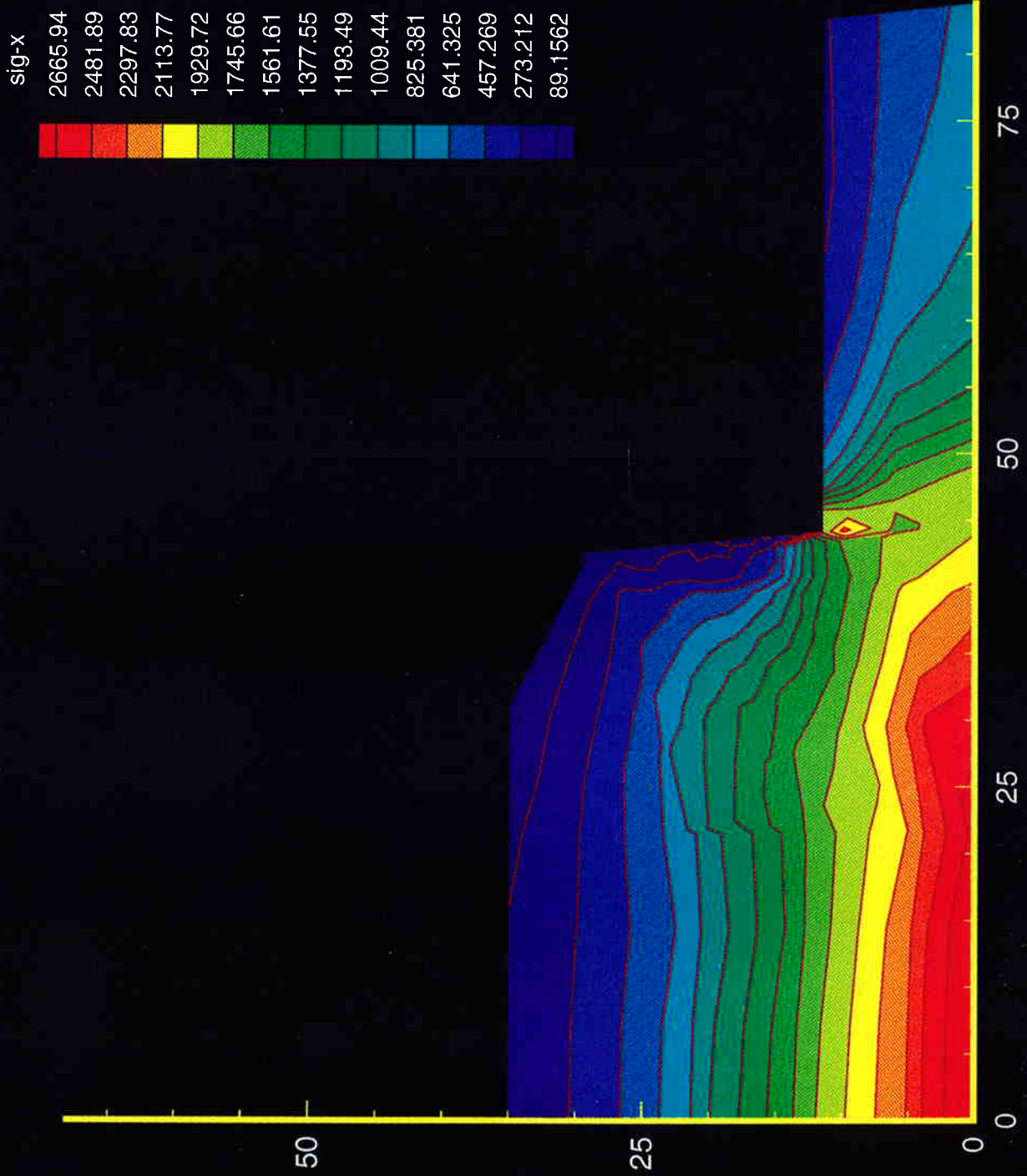
Figure 6.22 Section S2, Sigma x under Full Excavation

THIS PAGE INTENTIONALLY LEFT BLANK.
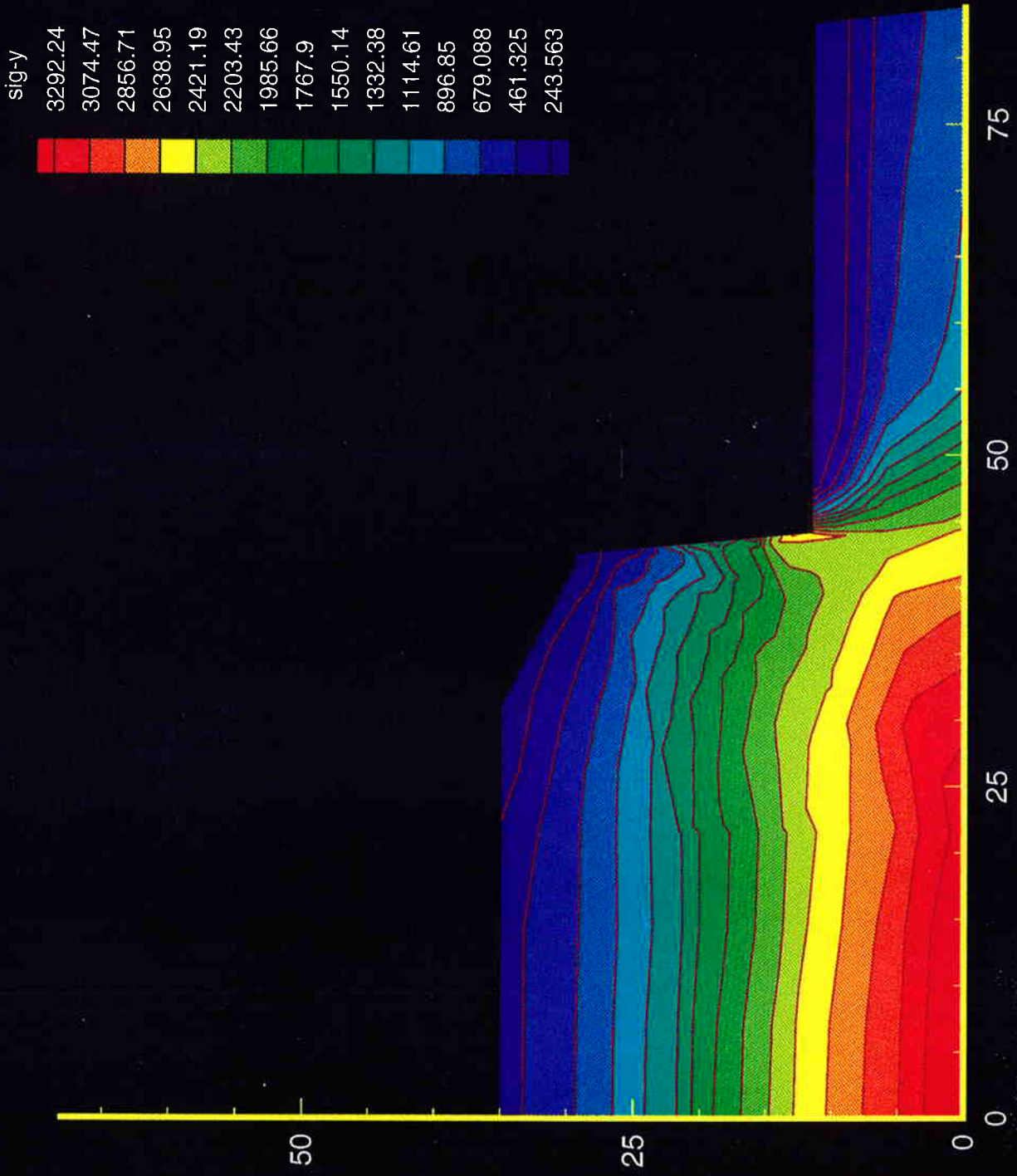
Figure 6.23 Section S2, Sigma y under Full Excavation

THIS PAGE INTENTIONALLY LEFT BLANK.
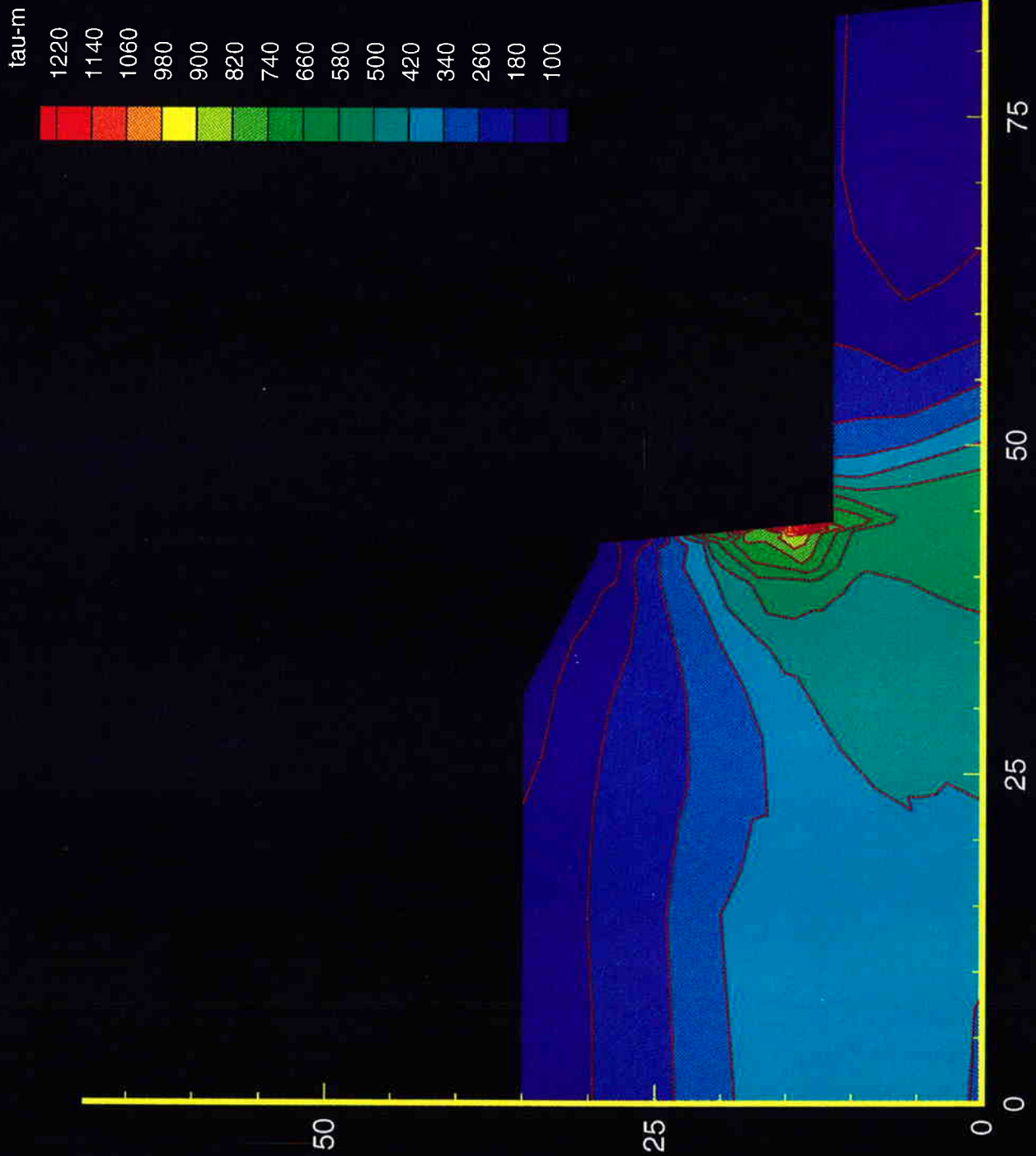
Figure 6.24 Section S2, Maximum Shear Stress under Full Excavation

THIS PAGE INTENTIONALLY LEFT BLANK.
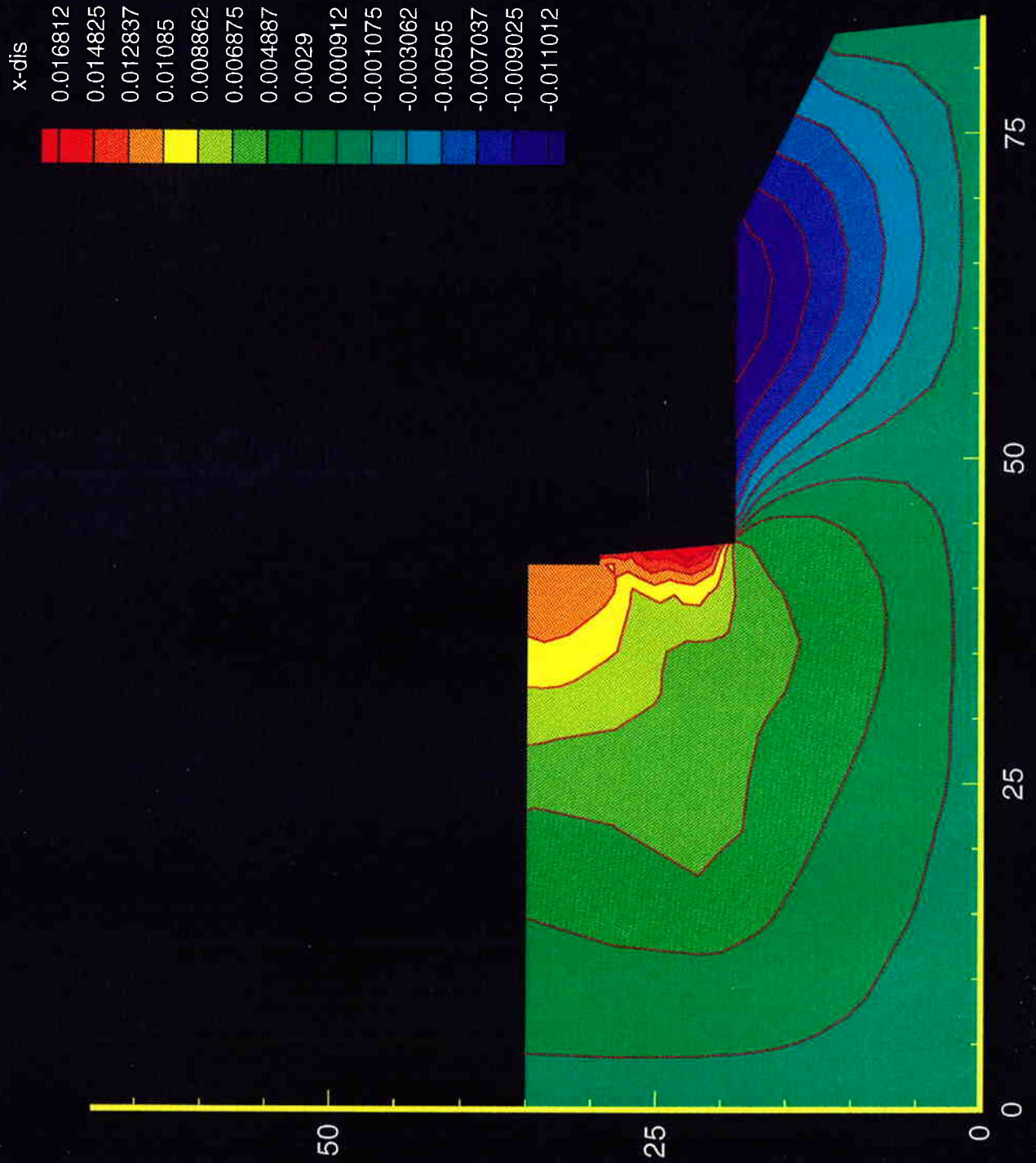
Figure 6.25 Section S1, Full Model, 3rd Excavation x Displacements

THIS PAGE INTENTIONALLY LEFT BLANK.
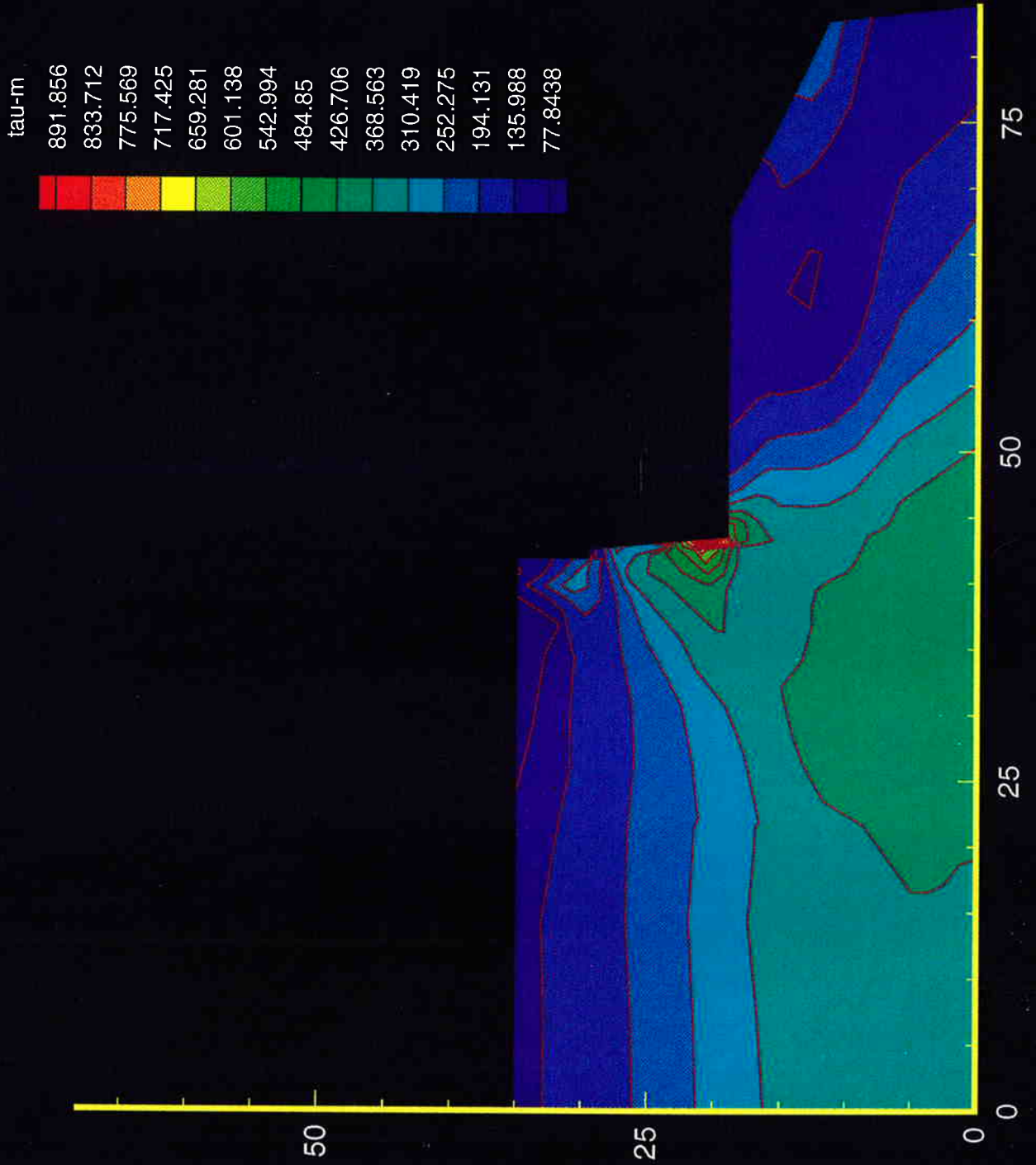
Figure 6.26 Section S1, Full Model, 3rd Excavation Maximum Shear Stress

THIS PAGE INTENTIONALLY LEFT BLANK.
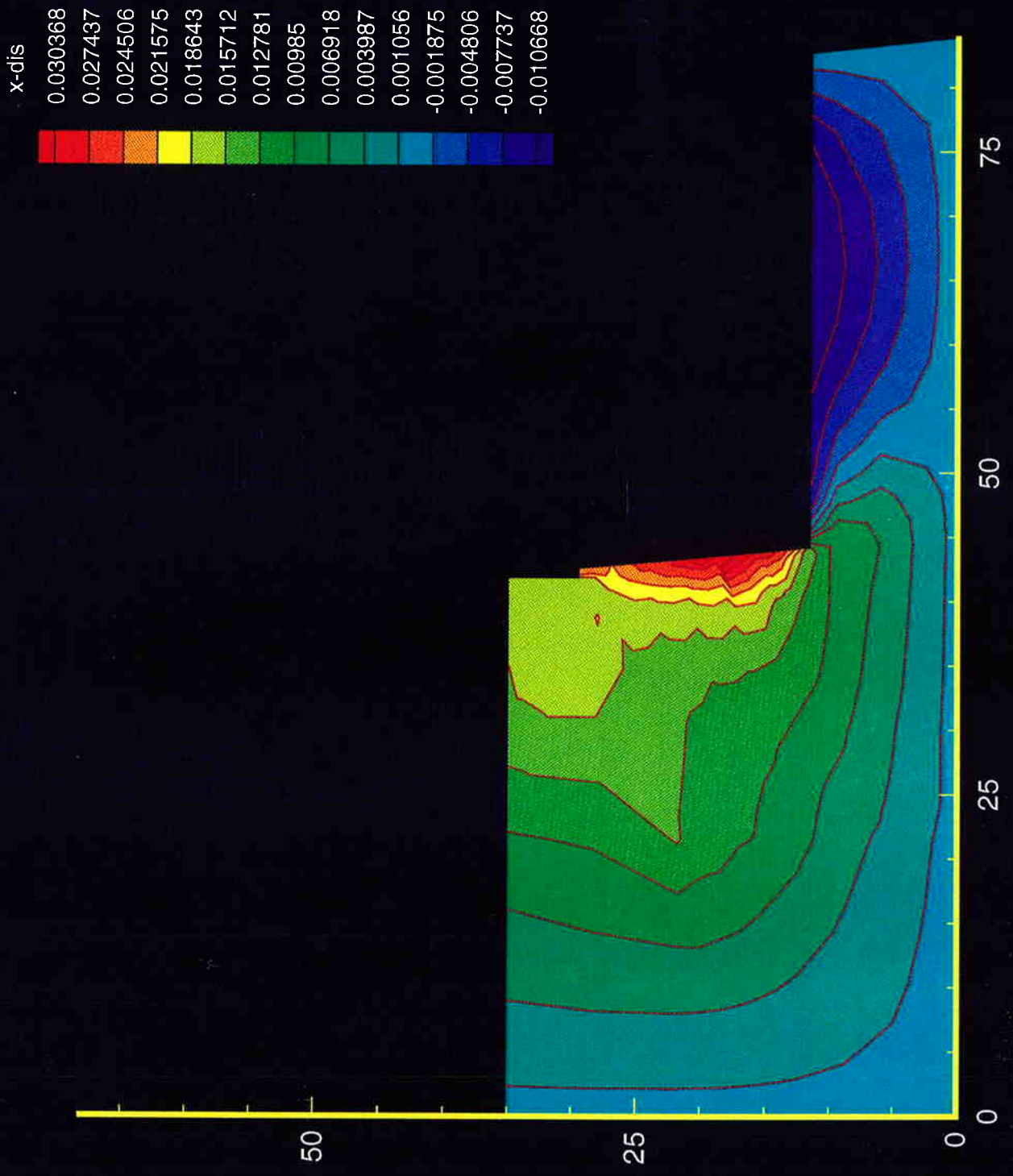
Figure 6.27 Section S1, Full Model, Final Excavation x Displacement

THIS PAGE INTENTIONALLY LEFT BLANK.
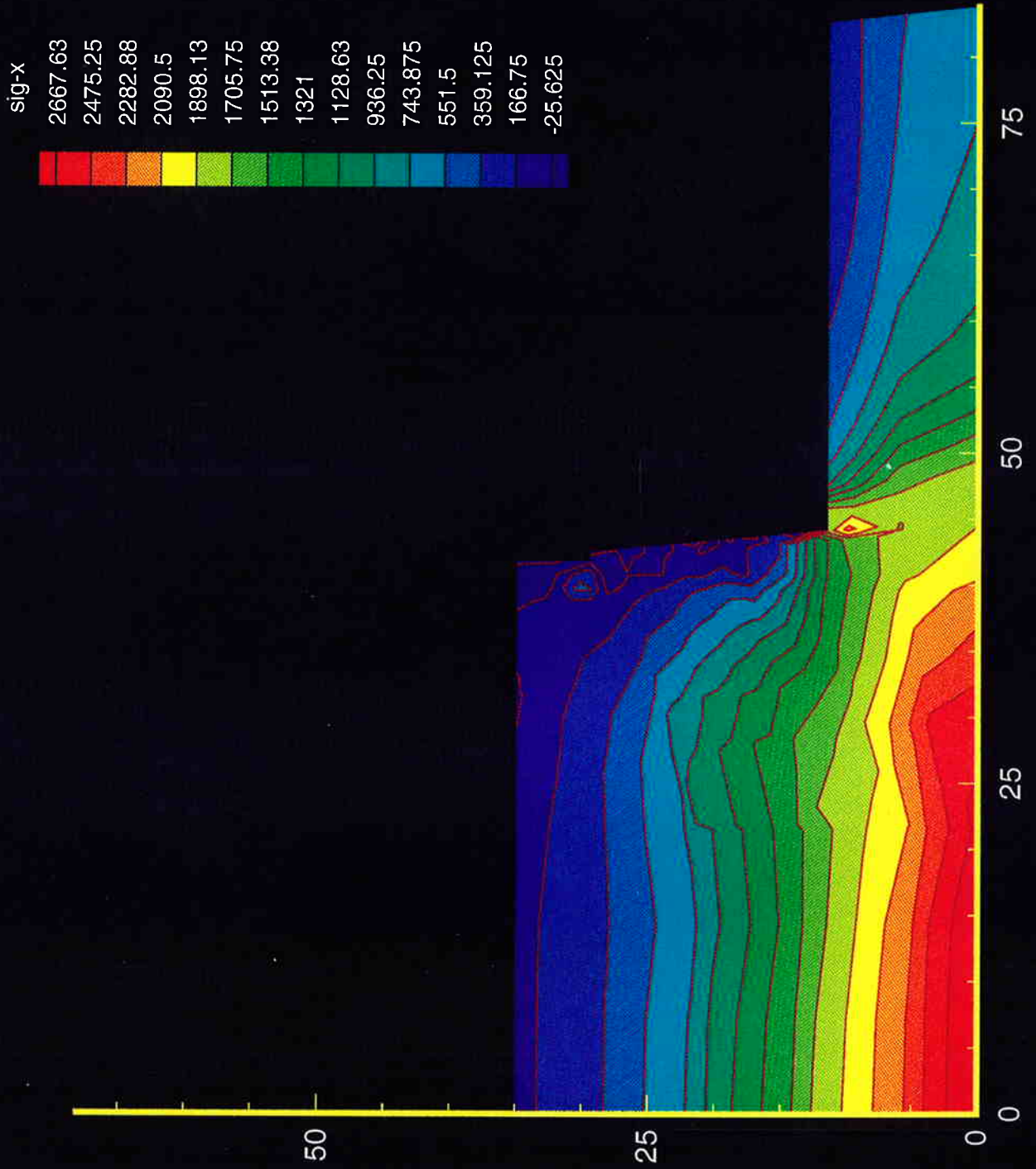
Figure 6.28 Section S1, Full Model, Final Excavation Sigma x

THIS PAGE INTENTIONALLY LEFT BLANK.
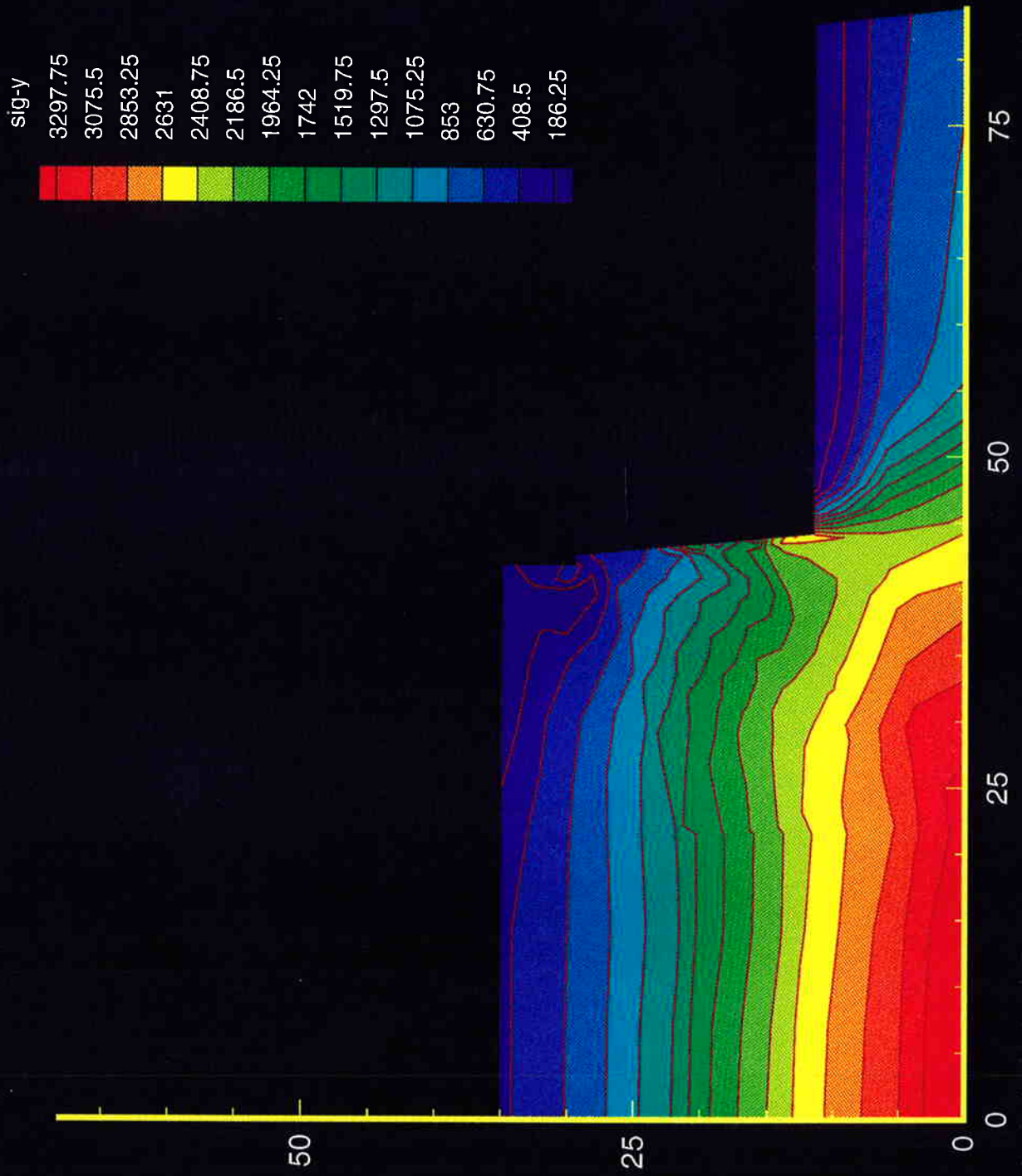
Figure 6.29 Section S1, Full Model, Final Excavation Sigma y

THIS PAGE INTENTIONALLY LEFT BLANK.
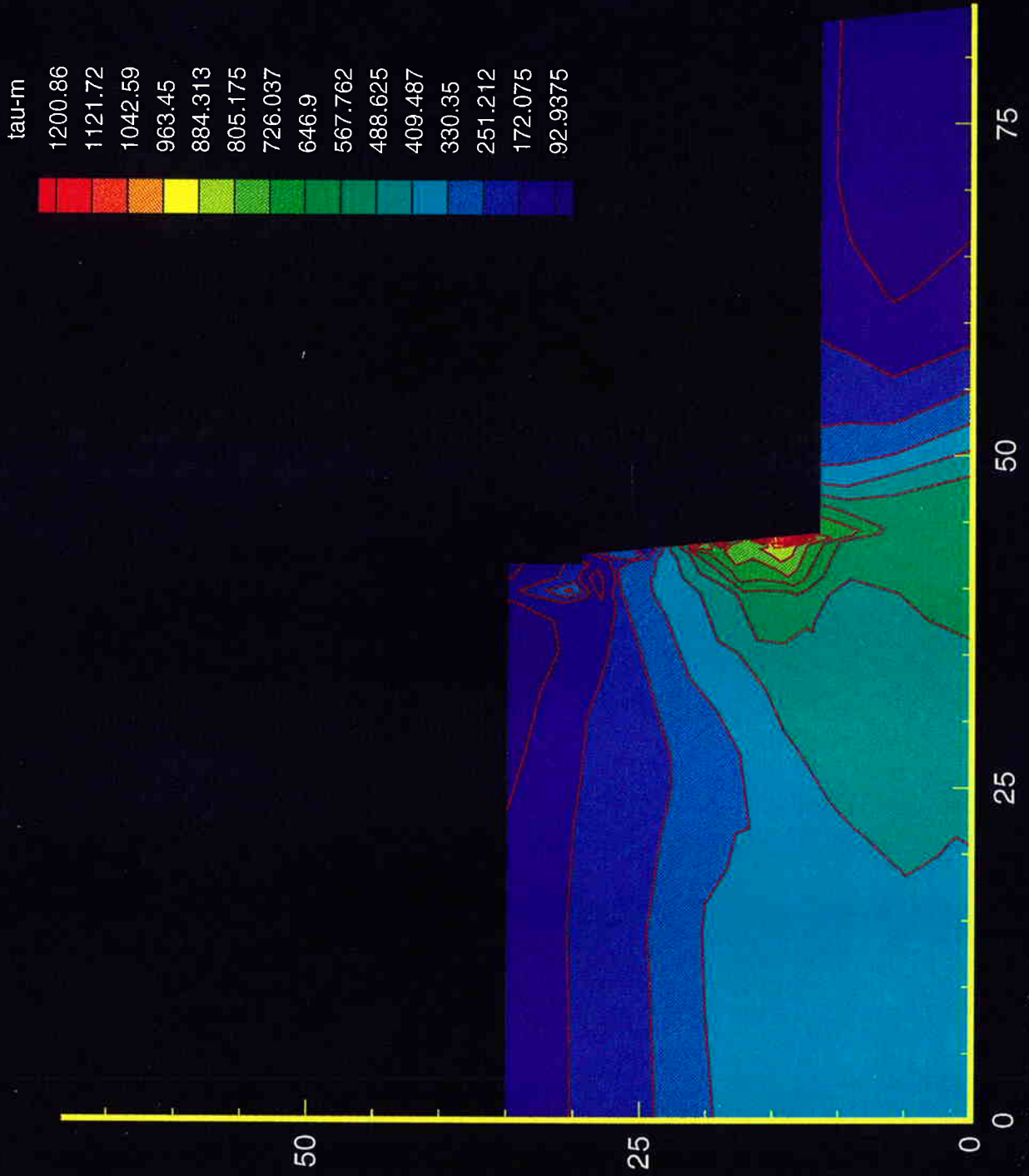
Figure 6.30 Section S1, Full Model, Final Excavation Maximum Shear Stress

THIS PAGE INTENTIONALLY LEFT BLANK.

7.0 ABAQUS THREE DIMENSIONAL STUDIES

It is increasingly recognized that Soil Nailing is closer to a soil improvement technique than a classic retaining wall. The block of soil is stiffened by the addition of the soil nails and is finally given a 'flexible' face from the shotcrete application. The nail stiffening effect to the soil is only present in the direction of the nail axis, while vertically and along the wall horizontal axis no global stiffening results. It would be expected at Swift Delta that the presence of the 36 cm (14 in.) diameter piles, would add stiffening in all three axes. It is suggested that the wall outward movement, followed by the soil behind the wall, may place additional load and bending stress in the pile. Further, the ability of the nail to carry tensile load may be enhanced by stress arching in the horizontal plane between nail to pile (a type of 'pinching' effect). No studies of this 3-dimensional nature which assess the effects from the pile to the soil nail wall, or the nail's effect to the vertical piles, are available in the literature. The three dimensional work reported in this Section were therefore designed to address these factors at the Swift Delta site, and uncover the extent to which the pile presence added further stiffening into the reinforced soil nailed mass.

Cardoso and Carreto (1989) reported the use of a technique based on anisotropic linear elasticity assumptions to predict ground deformations around a soil nail supported excavation. The length of the excavation was considered short enough to give, so called, end effects to the predicted displacements of a cemetery immediately behind the reported soil nail wall. This anisotropic analytical approach accounts for the nails presence by modifying the elastic constants, E and ν, in all three principal stiffness directions. The possibility exists to make use of the anisotropic equivalency and superimpose the free field predicted deflections onto a pile, such as that present at Swift Delta. The pile might then be analyzed under COM624P techniques to obtain peak induced bending movements from the input deflection. The monitored soil and wall deflection at Swift Delta provides a means to compare the Cardoso and Carreto (1989) anisotropic equivalency method from ABAQUS to the measured deflections in the field.

Construction and validation of 3D FEM models is not a trivial task. In view of the limited time and resources available, the ABAQUS model was restricted to the exact proportions of Swift Delta wall, and the top nail only was considered. A proposal was made to the National Science Foundation (NSF) Supercomputer Center in San Diego for a CRAY MXP account which was granted in late May 1993 with 20 units of time. The study was restricted to only directly address:

- Pile to Nail interaction effects from a study of deflection patterns and magnitudes.

- The nail tension mobilization, which may lead to possible simplifications for the pseudo 3D FENAIL model.

129

- Relative global (overall) individual stiffness contributions from both the nails and the piles.

- The validation of anisotropic elastic constants for a soil mass that replace the nails stiffening effect.

7.1 THE MODEL

The model geometry, element conductivity and selection of element types was accomplished by the PATRAN pre-processor. PATRAN errors present in the construction of curved "hyperpatches" (spacial reserved 3D volumes for mesh construction) permitted boundary violations with a semi-circular pile and semi-circular nail inside a rectangular soil model. The resulting FEM mesh under simple nail pullout loads, shown in Figure 7.1 as a wireframe, therefore could not be satisfactorily validated. To retain all the salient 3D features a comparable rectangular model superseded the semi-circular geometry and is shown in Figure 7.2. In all respects the numerical performance of this model was satisfactory. A total of 2880 hexagonal 8 node 'bricks' were employed containing 3675 nodes, each with three (3) degrees of freedom for the 6.1 m (20 ft.) high, 15.2 m (50 ft.) deep and 0.68 m (2.25 ft.) wide mesh. No modeling boundary conditions were attempted to incorporate bridge superstructure effects. All pertinent geometry, dimensions and features are shown in Figure 7.2.

Equivalent composite elastic stiffness parameters were used to translate between the Swift Delta soil nail's 14 cm (5½ in.) circular grout bulb and the model's 23 cm (9 in.) by 21 cm (8.25 in.) grout column. Nail length was set at 6.8 m (22.4 ft.). Similarly the modelled pile's solid 45 cm (18 in.) square section has an equivalent flexural stiffness (EI) to the 36 cm (14 in.) diameter pipe pile at Swift Delta. This modelling compromise is most likely to change near field stress states around the nail and pile but is not expected to significantly impact global movements, or stresses. Symmetry is made use of by employing the vertical plane through a nail centerline as one boundary and the vertical plane passing through the pile centerline as a second boundary. No lateral (y) movements are permitted on these planes which are 0.68 m (2.25 ft.) apart.

Three modeling patterns were attempted: linear elastic, anisotropic elastic and elastic plastic, the results of which are all discussed below. ABAQUS has no "gravity turn on", (discussed in Section 5) and therefore the only rational technique for creating nail tensile loads is from a pressure placed behind the back face of the wall. Equilibrium modifications of a gravity stress state in ABAQUS would demand the vertical wall face to be fixed horizontally, a clear violation of the true free boundary state. Models were executed with direct 45 kN (10 kips) nail face tension loads, 45kN (10 kips) pile top lateral loads and wall pressure conditions. Peak nail loads calculated from measured average field strains were reported in Section 2 to be of the order 45kN (10 kips). An arbitrary 9.57 kPa (200 psf) wall pressure was assigned to create 'reasonable' soil and nail outward deflections. Each model had deletion of some model features to ascertain their individual contribution to stiffness. For the horizontal nail a gradual transition from grout to sand was assumed, and no specific interface was defined.

130

In general these models require ± 20s of CRAY input processing time (including selection of wavefront solution minimization time) and a further 30s of CPU time for a solution. Communication by 'telnet' from the PSU site to San Diego CRAY MPX is the largest time dependent activity in model execution. Transmission back of the 'visual' file output by ABAQUS (.fil file) for graphical post processing by PATRAN is around 1200 s to 2000 s for a block file size of 2300. Job turnaround time for input *vi* editing, full execution and transmission of all output files to the PSU site by file transfer protocol 'ftp', then runs in excess of 1 hour. Local PSU site post processing and file translation to PATRAN is also time intensive. These procedures were fully used on the early validation models, and an example of the output generated follows in Figures 7.3, 7.4 and 7.5. For the later models 'ftp' transmission was limited to a shorter, *vi* edited, version of the numeric output file with no graphical file transmission for PATRAN post processing.

7.2 LINEAR ELASTIC APPROACH

A total of seven models were studied under this scenario, with the anagrammatical name *elasqu?* for the series. The first *elasqu 1* provided only a validation model for a short 1m (3 ft.) nail without refinement of any properties. For the remaining models the properties chosen are given below in English customary units for clarity:

<table>
<tr><td>Soil:</td><td>Taken from the highest likely initial modulus range of Young's Modulus, based on PMT data. Young's Modulus = 23.94 MPa (500 ksf), Poisson's ratio = .25</td></tr>
<tr><td>Pile:</td><td>A match of flexural stiffnesses (EI) gave equivalent Young's Modulus for the square section of 118,740 MPa (248,000 ksf), Poisson's ratio = 0.32</td></tr>
<tr><td>Shotcrete:</td><td>Concrete wall modulus 287,274 MPa (600,000 ksf), Poisson's ratio: 0.2</td></tr>
<tr><td>Soil Nail:</td><td>A transformed section was adopted with no change in axial stiffness from creep or stress-strain nonlinearity. Composite equivalent axial stiffness of 957,580 MPa (2,000,000 ksf) used, Poisson's ratio = 0.32</td></tr>
</table>

A summary of the remaining six models appear in Table 7.1 on the following page. When a model feature is listed as 'Active' then that component is assigned the properties given above. The 'Inactive' definition describes the component elements having only elastic soil properties.

Table 7.1 Catalog of Linear Elastic ABAQUS Models

Model	Model Features			Boundary Loading State
	WALL	**PILE**	**NAIL**	
elasqu 2	As Soil	Active	Active	10k Nail Load
elasqu 3	As Soil	Inactive	Active	10k Nail Load
elasqu 4	As Soil	Active	Active	10k Pile Top Load
elasqu 5	As Soil	Active	Inactive	10k Pile Top Load
elasqu 6	Active	Active	active	200psf Wall Pressure
elasqu 7	Active	Inactive	Active	200psf Wall Pressure

The deflection pattern for the *elasqu 2* model appears on the left of Figure 7.3 with the σ_x stress, in the nail axis, on the right. The units on the right hand side are for the σ_x stress only (in psf) and positive sign is tension. The rigid intrusion of the nail shows up clearly. The peak of both variables are at the nail head position, as the nail is pulled in tension. However, the mobilization of nail tension and soil shear is more realistically modelled by the pressure behind the wall, as in *elasqu 6* and *elasqu 7*. Model *elasqu 6* is shown in full detail on Figures 7.4 and 7.5 and is considered the best generic top nail elasticity representation of the Swift Delta features. A complete stress state image is shown in Figure 7.5 of all six stress components of *elasqu 6*. Comparison of horizontal x deflections between the nail pullout and wall pressure models *elasqu 3* and *elasqu 6* show clearly on the left of Figures 7.3 and 7.4. Peak wall movement, in elasticity, occurs at the wall top, not the nail, and the nail carries the principal σ_x tensile stress, as shown on the right of Figure 7.4. Perfect adhesion is present in these elastic models between the wall and the soil which results in the small tensile stress in the soil mass on the right hand side of Figure 7.4. Stress ranges are dominated in the plot by the high (expected) tensile stress carried by the nail. Some evidence of the 'pinching' effect between the nail tension and the pile can be seen in the σ_y plot, lower middle, of Figure 7.5.

A more concise output of only the nail and pile behavior is a better aid for direct comparison to the FENAIL FEM model, and also the measured Swift Delta data set. Given the linear elastic restriction of all '*elasqu*' models the absolute magnitude of displacements and stresses is of limited relevance. However, the trends, patterns and differences, in a *qualitative* sense are very instructive from Figure 7.6. These can be summarized as:

- Nail strain for *elasqu 2* and *elasqu 3* are around 70% PL/AE for the nail under the 20 kip load. All models, with the exception of *elasqu 5* where the nail is deleted, show close to uniform strain changes along the length.

132

- Comparison of nail head deflections for the wall pressure condition, in *elasqu 6* (with pile) and *elasqu 7* (no pile), illustrate only 3% gain in additional deflection. This leads to the conclusion that the nail behavior seems to care little for the piles presence.

- Under pile top lateral load *elasqu 4* and *elasqu 5* models show a 16% gain in deflections on the node at the nail head's geometric position when the nail is deleted. But they have essentially the same pile deflection profile, illustrated in Figure 7.7.

- The Wall pressure model deflections at the pile top geometric position also change very little by deleting the pile elements, from a comparison of *elasqu 6* and *elasqu 7*.

- The pile's presence can only be seen to be of some influence toward the back 60% of the nail length when under generic nail pullout conditions (*elasqu 2* and *elasqu 3*).

7.3 LINEAR ANISOTROPIC APPROACH

Following the recommendations and the example provided by Cardoso and Carreto (1989) the nail effect to global stiffness can be replicated by anisotropic stiffness properties within an ABAQUS model. For a more representative description of the Swift Delta fill sand, 2 layers were considered to introduce an increasing stiffness with depth. For this anisotropic model the nail and wall elements revert to soil properties and the pile remains active. (The nail stiffening effect is accommodated by the higher global E_x soil stiffness.) With the known nail horizontal and vertical spacing distance these properties become:

UPPER SOIL LAYER   0-10 ft.

$E_x = 1520$ ksf $v = 0.3$

$E_y = E_z = 260$ ksf $v = 0.32$

LOWER SOIL LAYER   10 ft-20 ft

$E_x = 1870$ ksf $v = 0.3$

$E_y = E_z = 630$ ksf $v = 0.38$

and the model anagrammatical name *elan?* is used.

No provision is made in the anisotropic equivalent models for wall properties to be included, thus only a direct match to the earlier *elasqu* models 2 & 4 are made. Table 7.2 and figures 7.8 and 7.9 show the comparisons between the anisotropic models *elan 2* and *elan 4* with their elastic counterpart *elasqu 2* and *elasqu 4*, for nail deflections and pile deflections.

Table 7.2 Elastic and Anisotropic Comparisons

Model Name	Model Features[1,2]	Nail Head Deflection mm (in.)	Pile Head[3] Deflection mm (in.)
elasqu 2 *elan 2*	Elastic Soil - Nail Head Load Two Layer Anisotropic - Nail Head Load	1.65 (.065) 8.2 (.32)	1.6 (.063) 0.75 (.03)
elasqu 4 *elan 4*	Elastic Soil - Pile Top Load Two Layer Anisotropic - Pile Top Load	0.84 (.033) 3.9 (.153)	4.5 (.177) 3.2 (.126)

Notes 1) No wall features appear in any model
2) The pile is active in all models
3) Measured Pile Cap deflections are of the order 7.6 mm (0.3 in.)

In general the poor results from comparison to the elastic model indicates the anisotropic simplification is inappropriate for both soil face deflections, and any study of pile deflections. Too high a wall face deflection results from the omission of the rigid nail intrusion. Pile deflections in both cases are underestimated when compared to the elastic *elasqu* series.

7.4 NONLINEAR APPROACH

To assess the possible degree of yield and soil nonlinearity effects in the pile-soil-nail system a Drucker-Prager plasticity model was used for the sand. Given the grout flow penetrating the uniform sand conditions at Swift Delta no easily defined interface bond position could be described. In reality a more gradual transition between 100% grout across to 100% sand is postulated. Thus, no interface elements are contained in the model. For a close to plane strain match to the Mohr Coulomb yield criteria, the properties discussed in Section 5 are used. For zero volume change conditions, these are:

$$\beta = 42.5^0$$
$$\Psi = 0$$
$$d = 35.2 \text{ kPa (735 psf)}$$
$$\kappa = 1.0$$
$$E = 9.58 \text{ kPa (200 ksf)}.$$

Section 2 reported the suggested peak nail loads mobilized in the field are of the order 45 kN to 50 kN (10 kips to 11 kips). ABAQUS output of the conditions described in *elasqu 2* show a linear response from the nail at these load levels with the Drucker-Prager model. For a nonlinear nail response under tension higher levels of nail load should be used. Nonlinear soil response in ABAQUS is only invoked at nails loads which approach 450 kN (100 kips). Therefore modeling of nail behavior at Swift Delta remains well within the elastic range and suggests any soil nonlinearity (for mobilization of nail loads) can be discounted in the FENAIL approach. This may not be true for the soil response during unloading at each excavation state,

134

and for the degree of movement projected at the wall top. However, due to the limitations of the gravity 'turn-on' discussed in Section 5 ABAQUS is unable to model these aspects.

THIS PAGE INTENTIONALLY LEFT BLANK.
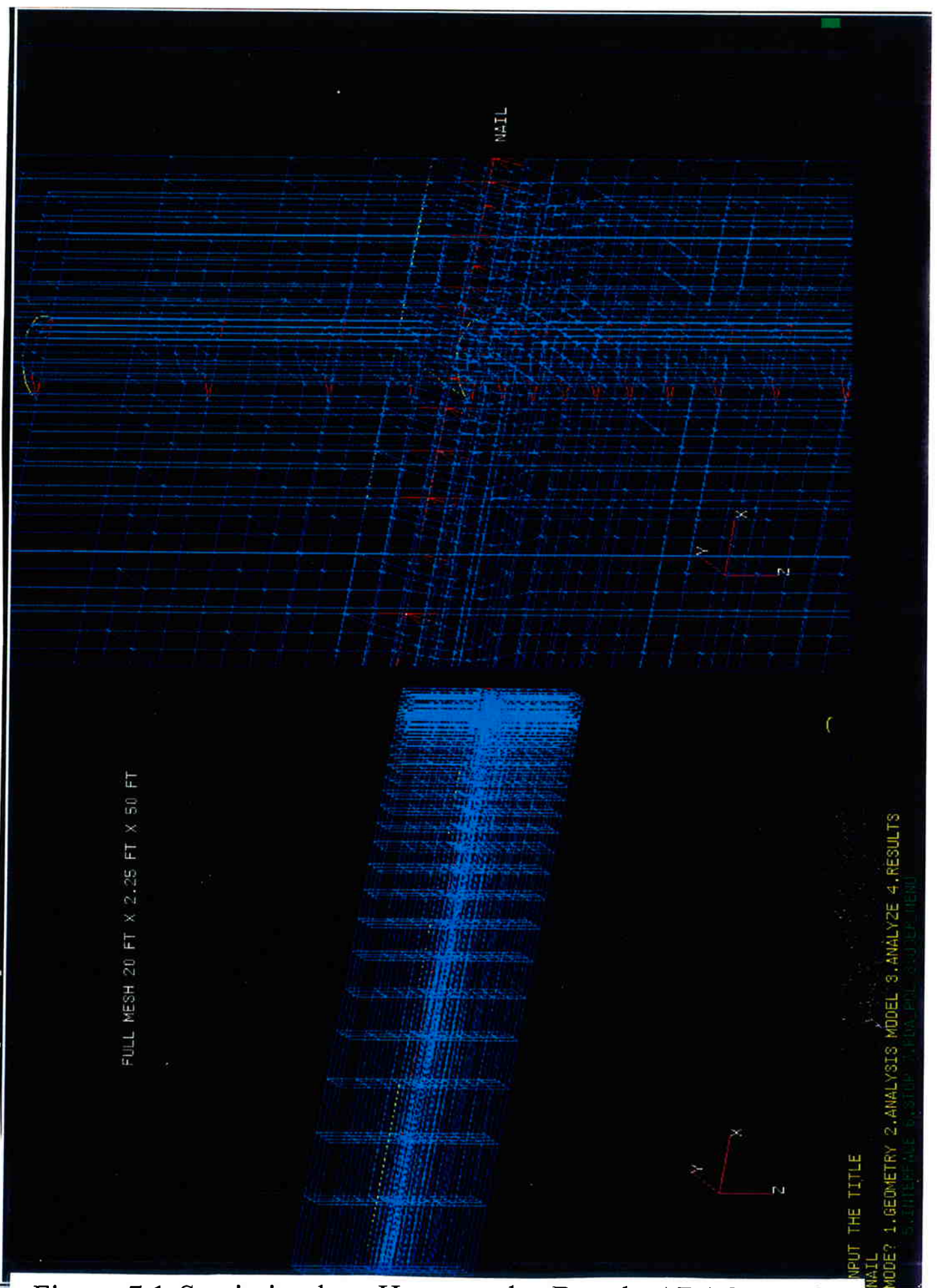
Figure 7.1 Semi-circular Hyperpatch Based ABAQUS 3D Mesh

THIS PAGE INTENTIONALLY LEFT BLANK.
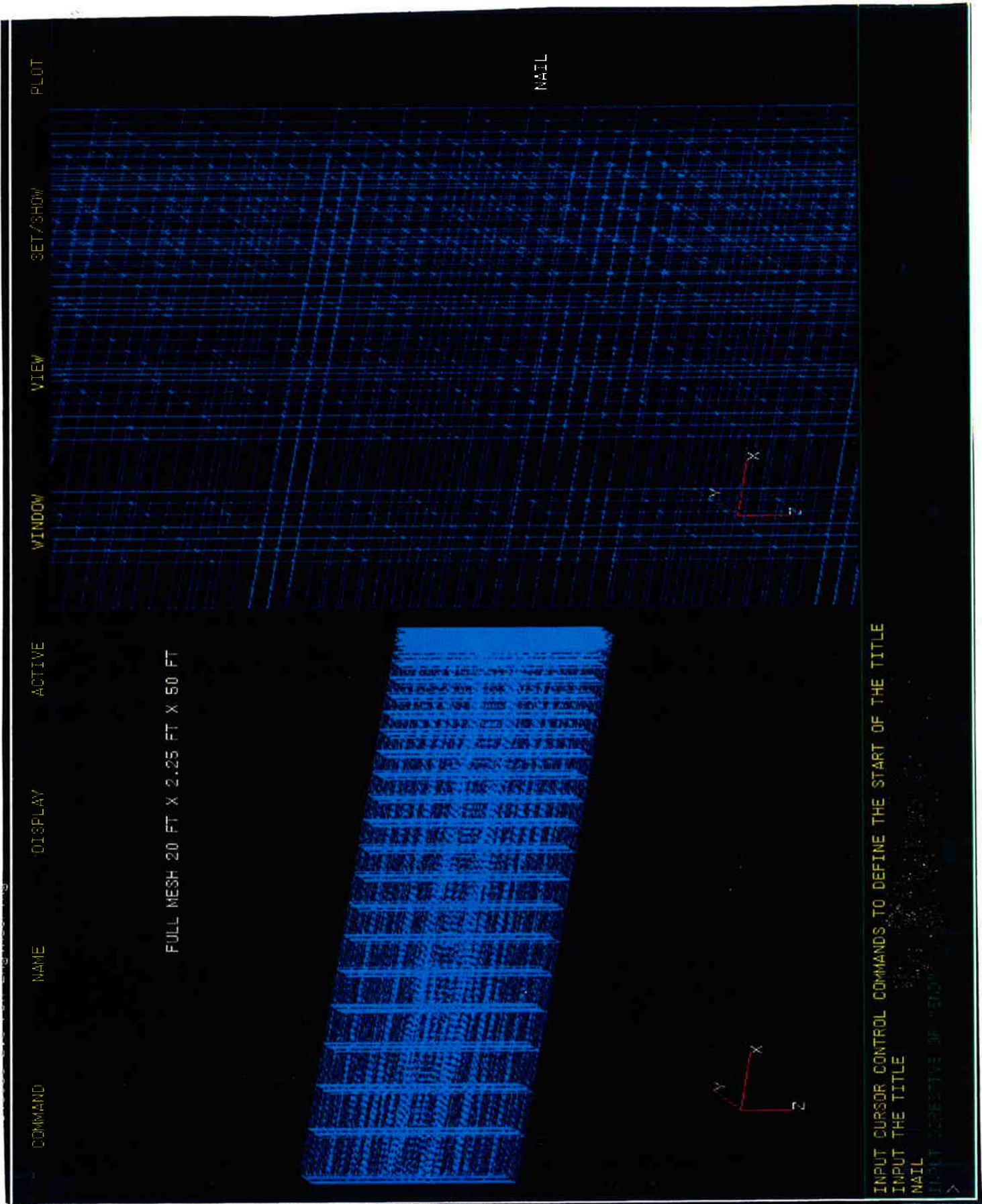
Figure 7.2 Cartesian Hyperpatch Based ABAQUS 3D Mesh 139

THIS PAGE INTENTIONALLY LEFT BLANK.
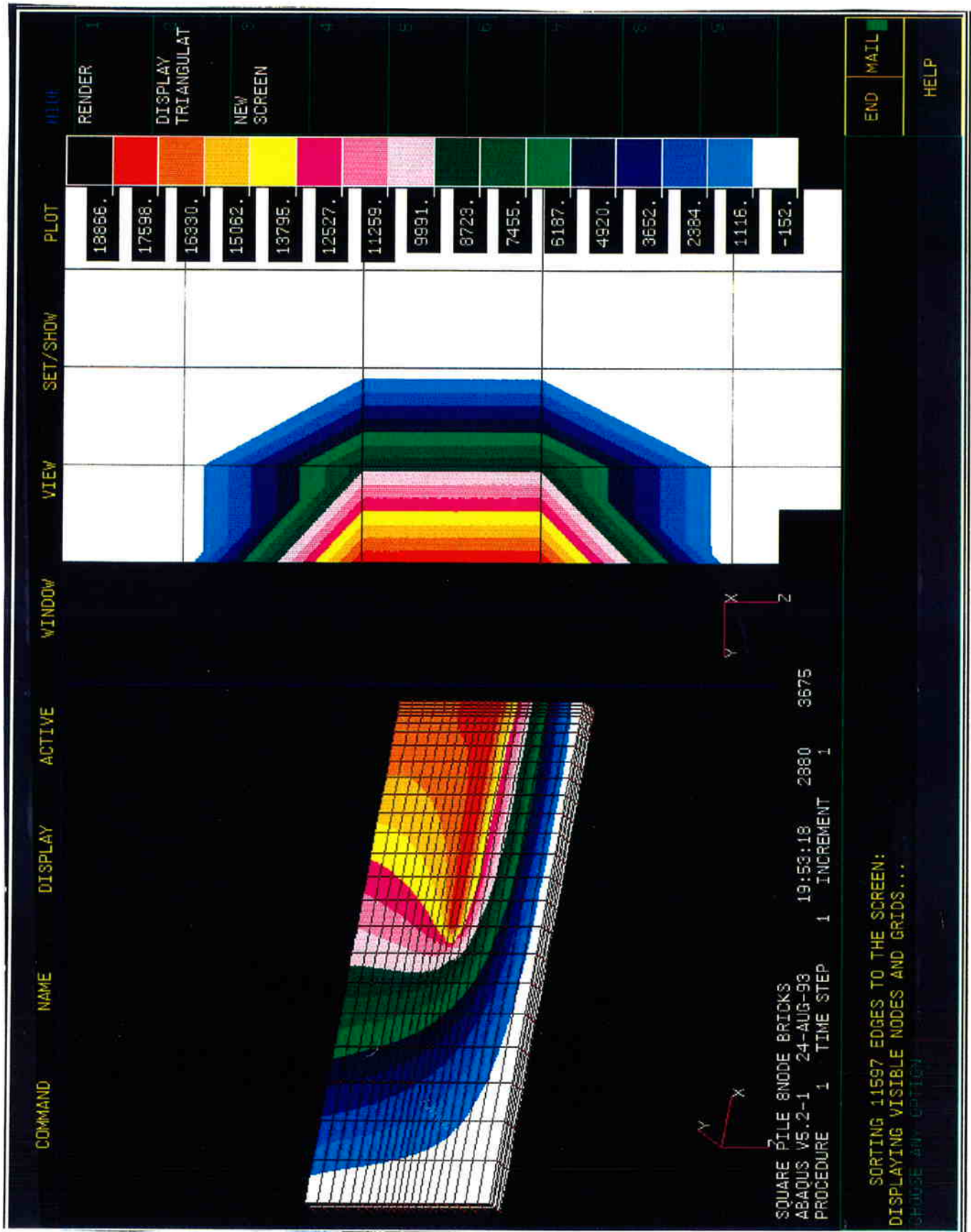
Figure 7.3 Horizontal Displacement under Nail Load in Elasticity

THIS PAGE INTENTIONALLY LEFT BLANK.
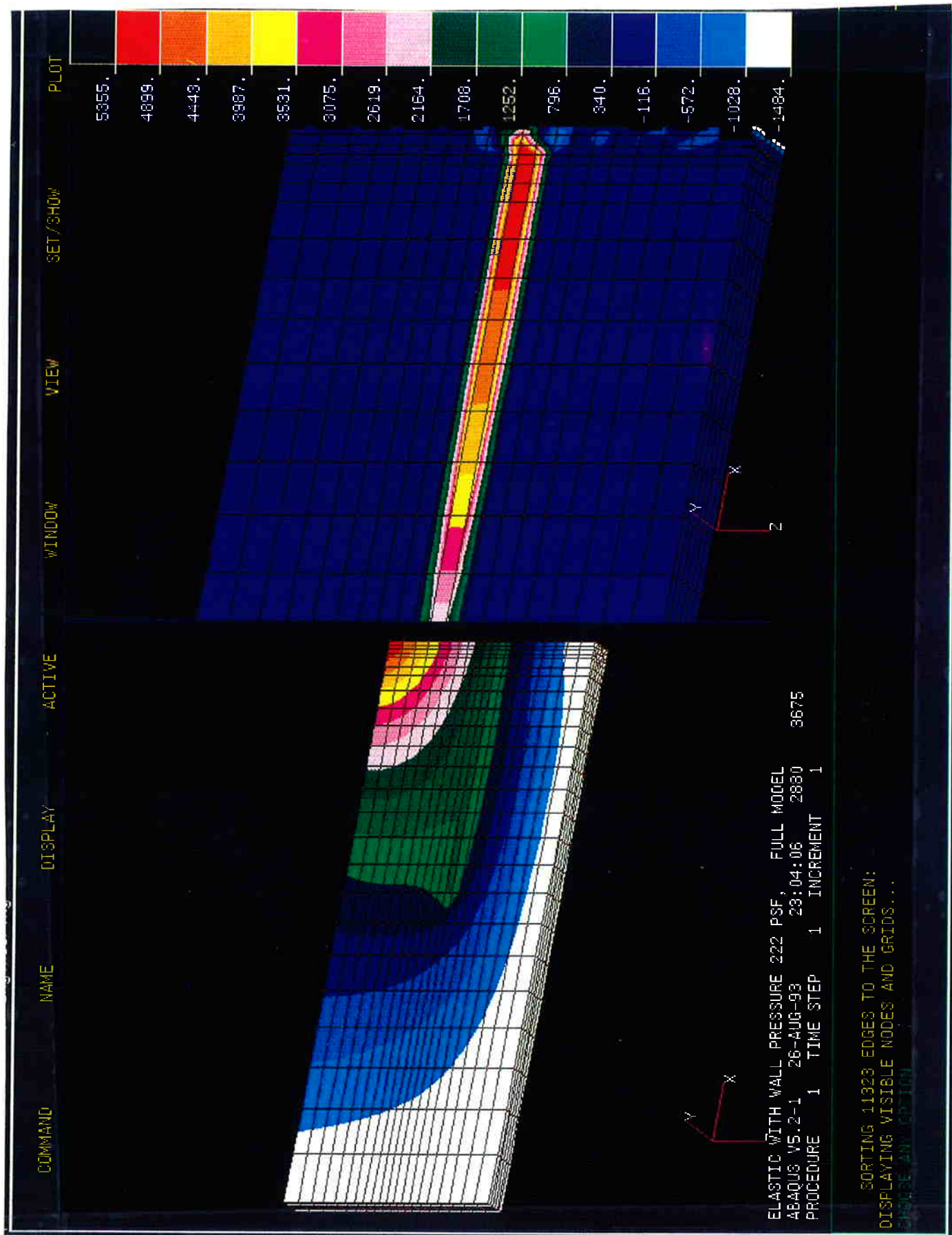
Figure 7.4 Horizontal Displacement, (Left), and Horizontal Stress, (Right), for Nail Load in Elasticity

143

THIS PAGE INTENTIONALLY LEFT BLANK.
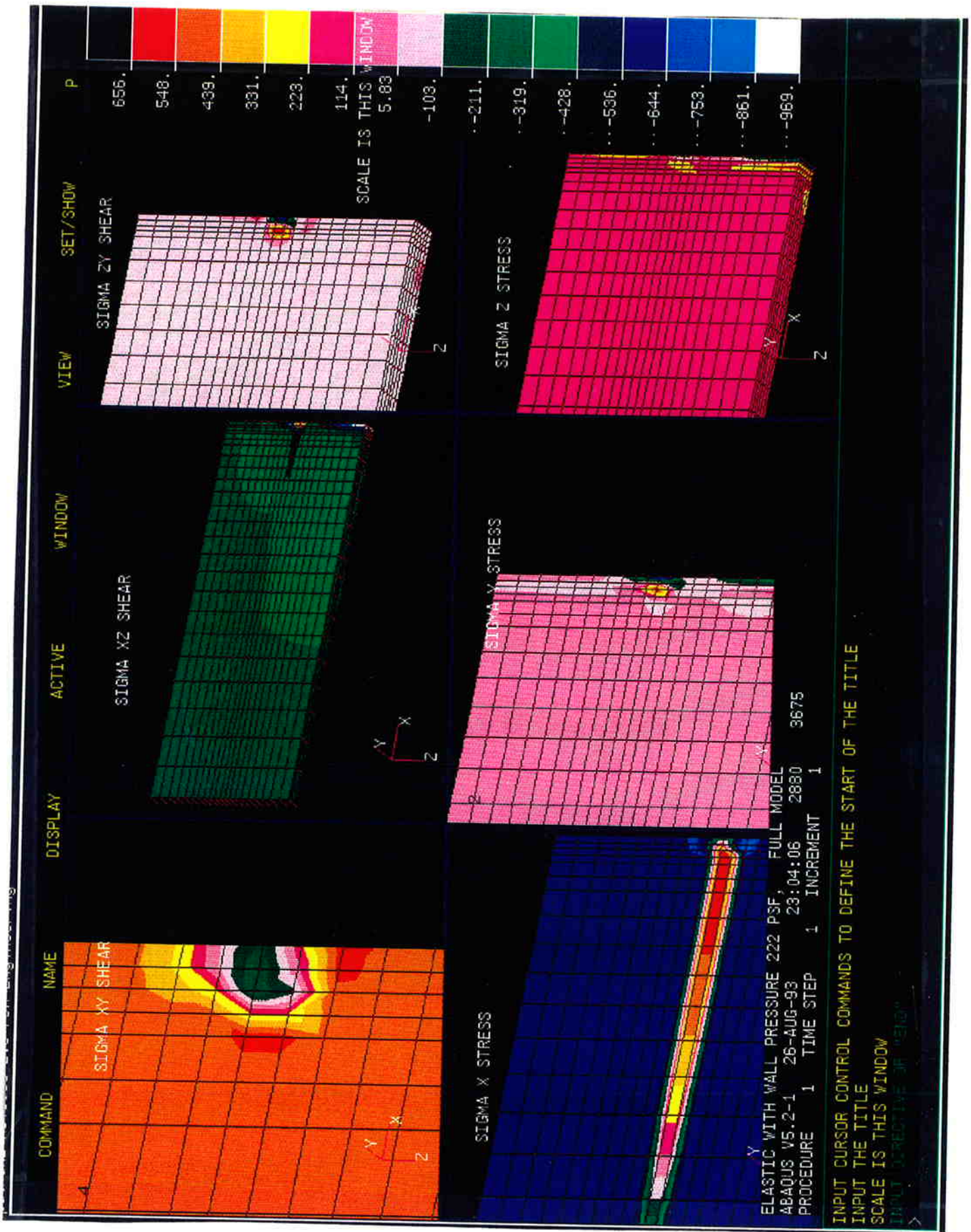
Figure 7.5 All Stress States for Nail Load in Elasticity

THIS PAGE INTENTIONALLY LEFT BLANK.
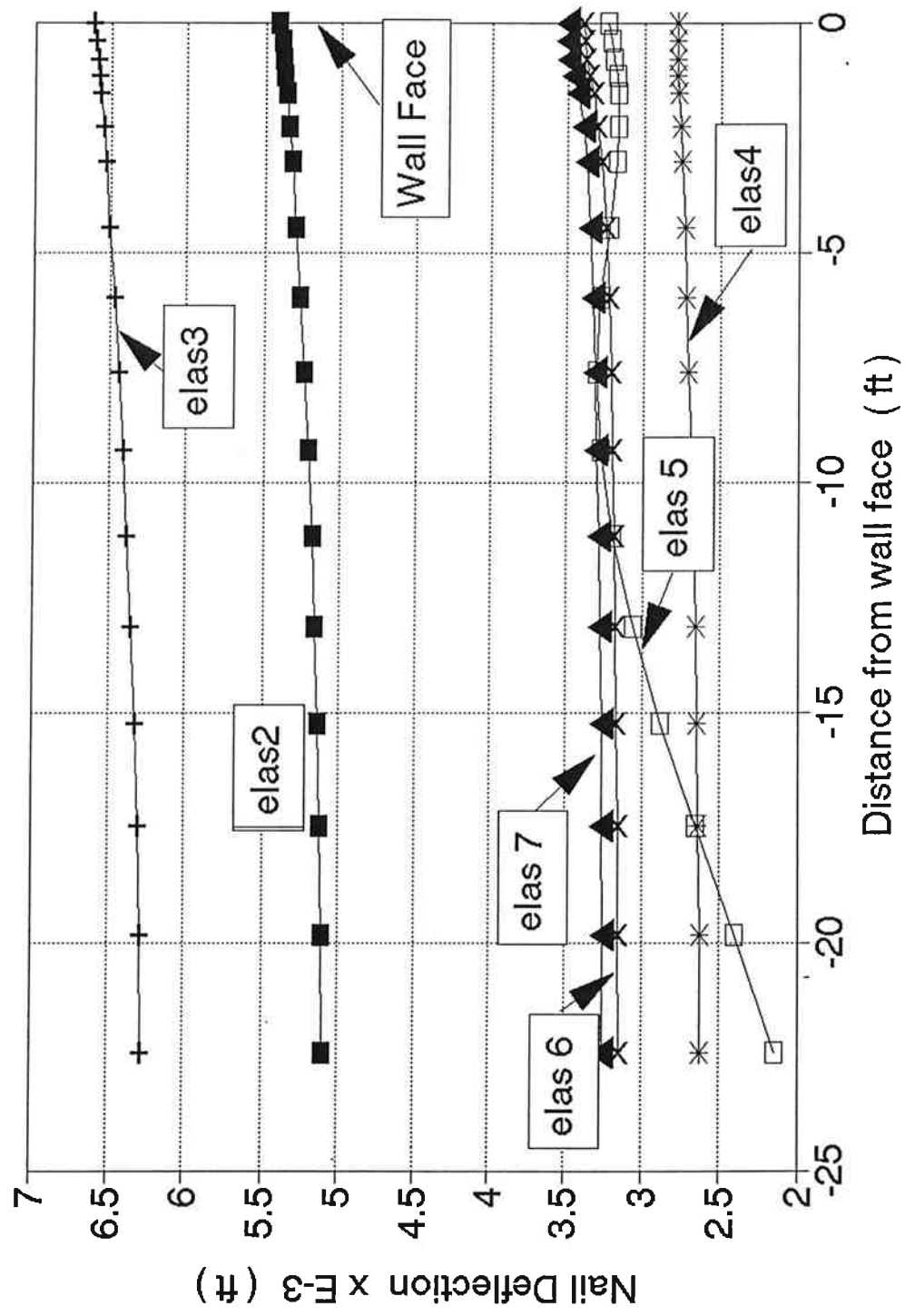
Figure 7.6 Nail Deflection for all Elasticity Models
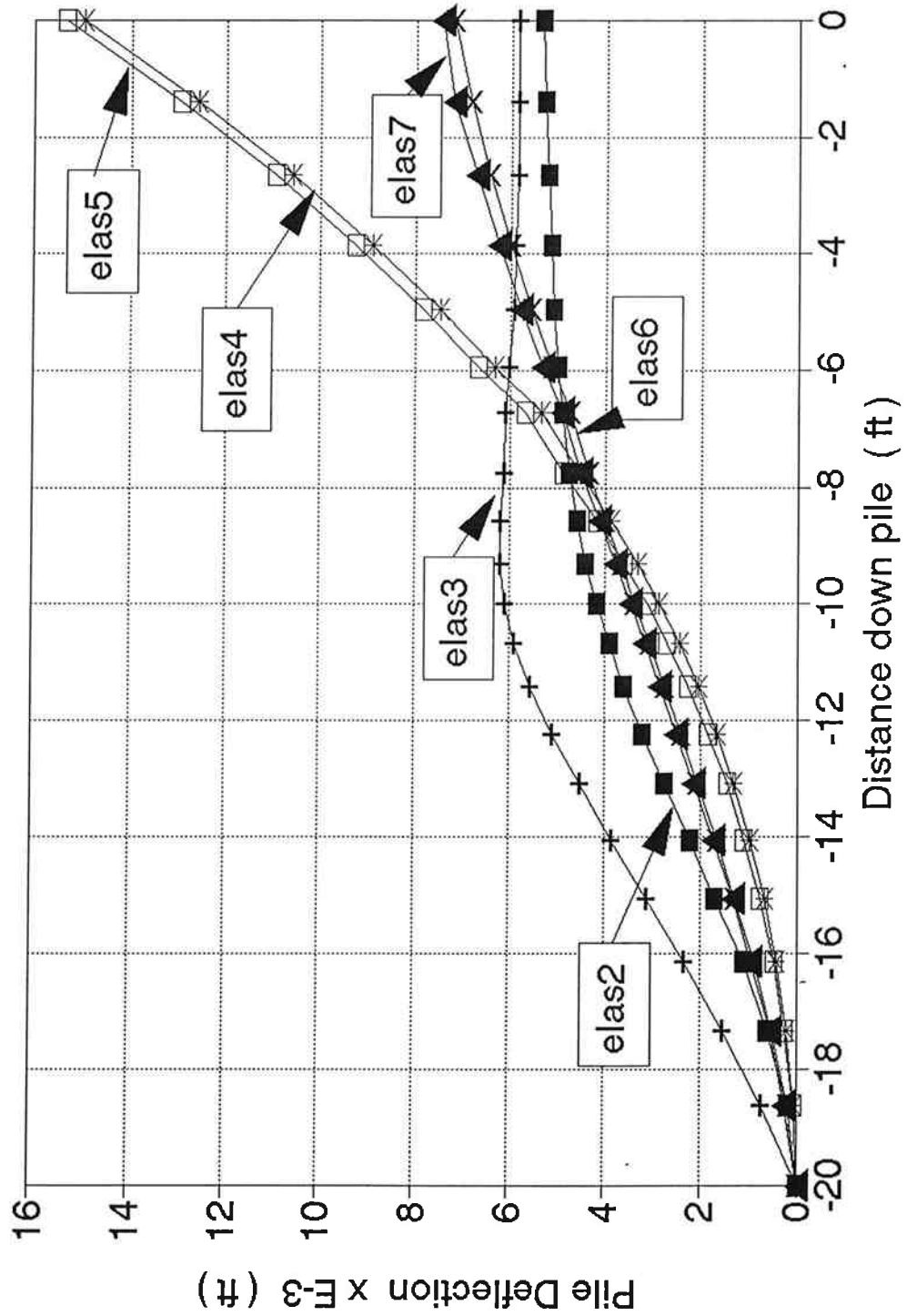
Figure 7.7 Pile Deflection for Elasticity Model

3D MODEL NAIL DEFLECTIONS
Elastic and Anisotropic Soil
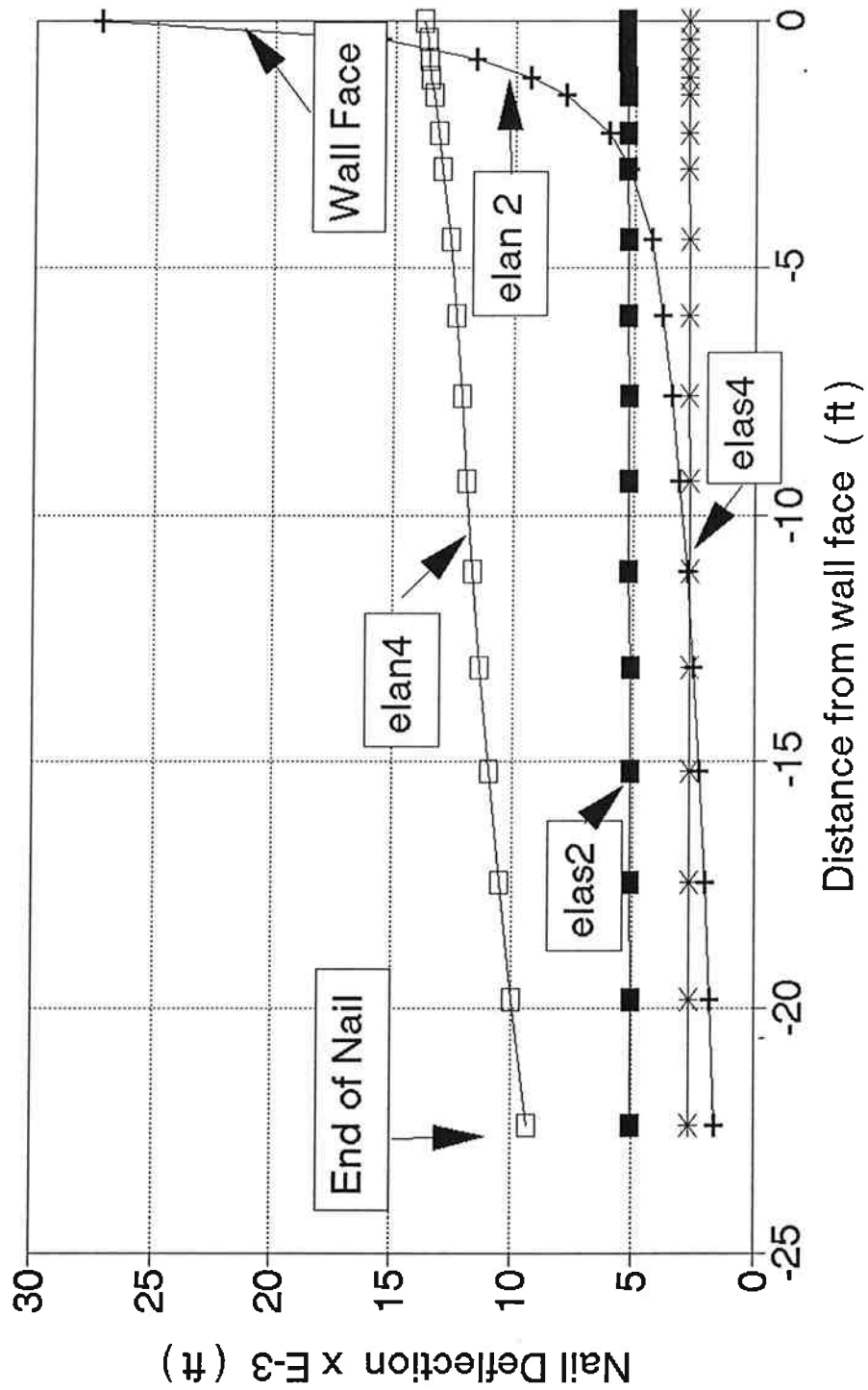
Figure 7.8 Nail Deflections for Elastic and Ansotropic Conditions

3D MODEL PILE DEFLECTIONS
Elastic and Anisotropic Soil
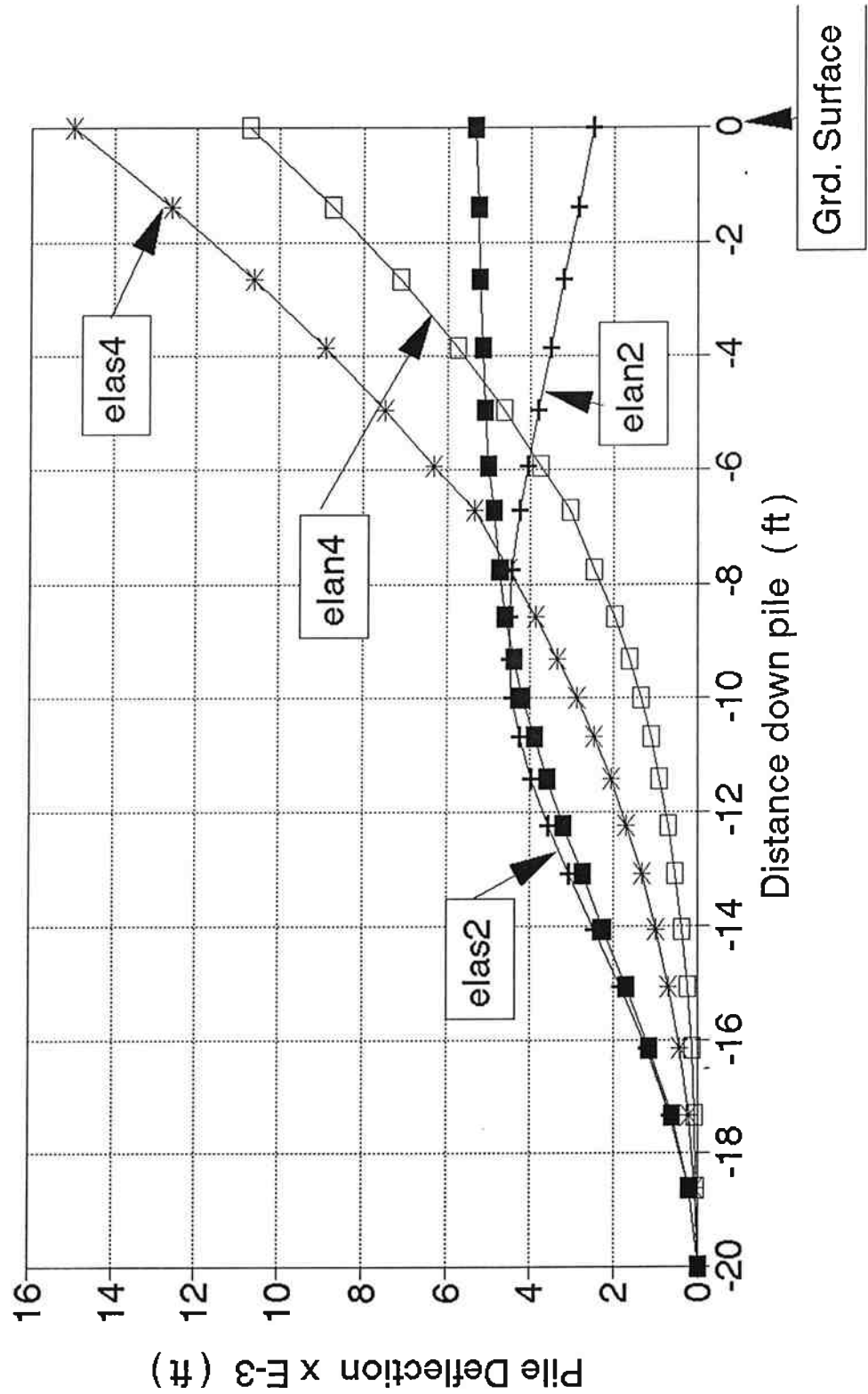
Figure 7.9 Pile Deflections for Elastic and Ansotropic Conditions

8.0 PILE PERFORMANCE SUMMARY

8.1 PREFACE

Throughout this research priority has been placed on numerical modeling for evaluation of the role played by the 356 mm (14 in) diameter foundation piles at Swift Delta. This requirement led to the necessity for creation of a new DOS based finite element code, FENAIL, that contains the numerical sophistication and element types to permit the out of plane pile presence to be modeled and their influence on nail and soil behavior studied. Section 6 introduced the FENAIL techniques used for studying both pile response and for a replication of the Swift Delta instrumentation data. This section attempts to offer a concise summary based on interpretation of all measured data, FDM and FEM work, with the focus on the pile contribution. Finally, some recommendations are made to continue development work on FENAIL, and gain further understanding of pile intrusions into a soil nailed 'field'. It should be recalled that any large data base, together with extensive model predictions, are always open to interpretation. In the case of Swift Delta, assumptions have been made to reach the results presented in this report, (made particularly difficult by the absence of high quality soils data prior to the research commencing). However, some consensus does begin to emerge and this is introduced here.

8.2 SUMMARY CONCLUSIONS

It may be useful to recall the issues raised in Section 1 which the research (at the outset) was designed to address;

1) What role do foundation piles play in the structural interaction (stiffening) of the wall-nail-fill system?

2) From a practical standpoint is it conservative to design the soil nail wall assuming no pile influence?

3) What additional lateral loads, if any, were the existing piles subjected to from the end slope removal?

4) Does a critical distance, or wall height/distance ratio, exist from the piles to the wall that prevents significant interaction?

5) What recommendations could be made, based on this Swift Delta Study, that can help future design of lane widening projects, soil nail wall design and construction and/or instrumentation projects?

The summary comments are presented in this section in two groups. The first group of comments answer directly the questions posed above. The second group are those comments which are seen as significant and result from the diverse range of modelling techniques employed throughout this research. The reader is encouraged to study this report's individual sections more fully, covering those conclusions and recommendations which are of significance to them.

Q1)   *What role do foundation piles play in the structural interaction (stiffening) of the wall-nail-fill system?*

Pile contributions show up in the FENAIL modeling in 3 areas when comparison is made of the most accurate S1 model (SNPS) with the most accurate S2 model (2XNB). These are:

a.   A drop in σ_x behind the wall face. The S1 model even moving into tension at various locations behind the wall face as some horizontal stress is shed to the pile. A close to linear distribution of σ_x is predicted on S2, but the distribution is less clear at S1.

b.   A nominal increase in horizontal (x) deflection maximum from 9.1 mm (0.36 inches) in model 5NPS to 9.6 mm (0.38 inches) in model 2XNB. However a more pronounced wall bulging pattern is seen *without* the piles at S2.

c.   If the piles presence had significantly stiffened the soil mass in the horizontal direction nail loads, and load distributions, would be different between S1 and S2. However similar loads are predicted by FENAIL in models 5NPS and 2XNB. It does emerge from 3D FEM work that the pile response is strongly tied to the nail presence, when under pile top lateral load. The fortunate corollary is the nail cares much less about the pile's presence when asked to restrain wall pressures by nail tension. The reason being is the nail's stiffened axis is in the predominate pile deflection direction. However, when the nail is required to hold significant tension the flexible pile is unable to contribute very much. Given the peak horizontal wall movements following the $\Delta x \simeq 0.002H$ relationship, pile movements (which are along for the ride!) fail to come close to yield fibre strains in bending. It appears appropriate to conclude that the piles interaction and additional load from it being in the nail 'field' is not of concern at Swift Delta. However for taller walls the possibility of pile distress from excess lateral deflection does remain.

Q2)   *From a practical standpoint is it conservative to design the soil nail wall assuming no pile influence?*

Since the pile is shown to reduce the horizontal stress against the wall face the nail loads and face bending stresses both would be overpredicted. This should lead to conservative

152

wall designs. However, peak nail loads occur well *behind* the wall face and at Swift Delta the FEM models show little difference with and without piles. Any predicted reduction in this peak nail load (to optimize design nail spacings for example) will depend upon the pile centerline to wall face distance.

Q3) *What additional lateral loads, if any, were the existing piles subjected to from the end slope removal?*

It was noted above that FENAIL predicted wall pressures are less with the pile in the model. The modeling sequence follows the chronologic activity which add the nail and wall facing immediately after each slope excavation . The models response output data does not therefore separate the effects of end slope removal as an independent activity, from nail and wall construction. FENAIL pressures for S1 are in the range 0 - 9.5 kPa (0-200 psf) and at S2 in the range 4.3 - 9.5 kPa (90-200 psf). This does imply some soil arching is mobilized by removal of restraining soil ahead of the pile.

The single issue of the loss of restraint from slope excavation can be investigated, to a limited extent, by the finite difference method. However the direct use of the beam on elastic foundation methods, i.e. COM624P, do have great difficulty being applied satisfactorily to the Swift Delta problem. Their lack of true time scaling in boundary condition changes (such as excavations), absence of any interaction phenomenon with nails and the discrete soil (winkler) spring models, are severe handicaps. COM624P suggests the loss of soil restraint ahead of the pile from excavation *is* the single most significant feature. But interpretation of back calculated soil pressures (from BMCOL studies) does not indicate any soil pressure arching to the pile. Further, COM624P requires in excess of 5 inches of piletop movement be detected under Model 4b conditions before the 1250 kip-in yield moment is reached. All indications from the numerical work and interpretations of measured data are that the piles behind the wall at Swift Delta are not close to yield, or suffering distress, by construction of the wall.

Q4) *Does a critical distance, or wall height/distance ratio, exist from the pile to the wall that prevents significant interaction?*

In this study no parametric variations of the pile, nail and wall dimensions were attempted. The code FENAIL does permit this exercise to be attempted. It does seem possible that the significance of the results from Swift Delta would be different if the pile were located at or behind the peak nail load zone. At Swift Delta the pile is present between the peak nail load position and the wall face. With the piles position at the predicted peak nail load position increased soil arching to the pile (and pile bending) is possible.

Q5) *What recommendations could be made, based on this Swift Delta Study, that can help future design of lane widening projects, soil nail wall design and construction and/or instrumentation projects?*

153

Before definative recommendations can be made on future projects be the study suggested in the response to question 4) should be completed.

As a general observation from the Swift Delta Study it would seem pile design without considering the system stiffening from nails is conservative. The soil nail wall design without considering the piles presence is also conservative. The temporary condition reached after slope excavation and before the nail has attained acceptable tension performance may be the worst case. A staged excavation along the wall length might be an option. Providing the largest possible horizontal distance between pile face and wall face is also desirable if significant loads to more rigid piles are to be avoided.

In addition to these responses the following, more general, conclusions are offered.

- Overall the FEM FENAIL replication of Swift Delta measured data is good. Of particular note is the global confirmation of the present understanding of how soil nail walls function, i.e. as gravity structures. All deformation patterns are 'reasonable' given the modeling technique. Soil nail loading distributions and the wall pressures are well within acceptable ranges, and compare well to the interpreted Swift Delta data.

- With flexible shotcrete facing the pattern of wall deflections are modified, somewhat, by the close proximity of a pile.

- Initial wall face soil pressures may be dominated by the small "lock off" torque of the nail. The amount of subsequent creep load readjustment throughout the first six months following construction might be controlled, somewhat, by this torque. The continual post construction wall deflection and nail load adjustment on soil nail walls are well documented. There does not appear much consensus on the mechanism responsible for the adjustment, but generally is attributed to creep, even in sand. This same phenomena is exhibited in the Swift Delta instrumented data. The modeling of creep movements by FEM approaches is a specialty subset group of codes, and is not modelled by any of the codes used throughout this research study. Further, no satisfactory modification to either the FDM or FEM codes is yet available. This does place a further restriction on the prediction of the nail load readjustment and wall deflection increase, which have been measured at Swift Delta but cannot be used to validate FENAIL. Creep movements at Swift Delta are of the order 15% to 35% increase at the wall and no attempt has been made to FENAIL model this phenomena.

- The pile's presence may have dampened the post construction creep movements as much by vertical shear adhesion, between the pile and the sand (as the shotcrete weight induces vertical downward movement), as well as by horizontal soil arching across the piles.

- The free face cut accumulated 'slip', by the wall shotcrete to soil shear bond holding the shotcrete face weight, is less likely at Swift Delta due to the piles close proximity. But some nail bending still shows in the instrumentation data. Some portion of the shotcrete

weight may be taken axially in the piles. This leads to less nail bending, and is likely to be desirable for taller walls. Piles therefore play a role in holding the temporary wall in vertical stability during each excavation cut. However, this mechanism cannot prevent local face sloughing.

8.3 RECOMMENDATIONS

- FENAIL development should continue to include: replication of other walls, optimizing of mesh generation schemes for users, wider range of constitutive models which focus on unloading-reloading hysteresis and composition of a FENAILIN pre-processor.

- Better characterization of the 'interference' elements by 3 dimensional studies of the local arching conditions between horizontal nails and vertical piles, in a range of soil types, is required.

- Improved understanding is required of the grout/soil interface from instrumented load tests that provide bond breakers in the grout column to isolate the unbonded nail length during tests.

- Composite nail/grout/soil studies by FEM should be undertaken to replicate pullout tests at Swift Delta. This may aid refinement of the constitutive input.

- For well instrumented piles with reliable bending strains, and both total and incremental maintained deflections, its final condition may be evaluated by the following. The simple relationship $\Delta x = 0.002H$, or FENAIL predictions, can be imposed via COM624P to the pile. However, the valid restraint P-y curves are not yet established. The output may then be compared to the measured data for validation. (5)

And finally:

- *FENAIL use should be strictly controlled and restricted to experienced FEM users only.* **Substantial engineering judgement is necessary to interpret, validate and apply the results.**

Note: No responsibility should be assigned to the Department of Civil Engineering at PSU, or Geotechnical Engineering Modelling (GEM), for the accuracy of FENAIL results.

THIS PAGE INTENTIONALLY LEFT BLANK.

9.0 REFERENCES

1.   ABAQUS (1992), Five Volumes of User Manuals, Hibbet, Karlsen, & Sorrenson, Providence, Rhode Island.

2.   BMCOL 7 (1987), "User Manual", Department of Civil Engineering, Portland State University, August 1987.

3.   Cardoso, A.S., and Carreto, A.P. "Performance and Analysis of a Nailed Excavation", Proceedings of the 12th International Conference of S.M.F.E., Rio de Janeiro, August 1989.

4.   Carter, J.P. (1978) "CAMFE, A computer program for the analysis of a Cylindrical Cavity Expansion in soil", Cambridge University Report, CUED/C-SOILS-TRS, 1978.

5.   Denby, C., Argo, D., and Campbell, D. (1992), "Soil Nail Design and Construction Swedish Hospital Parking Garage, Seattle", Proc. ASCH Geotechnical Seminar, March 1992, University of Washington.

6.   Desai, C.S. and Mugtadir (1986), "Interaction Analysis of Anchor-Soil Systems", ASCE, JGED, May 1986.

7.   Elias, V. and Juran, I. (1991), "Soil Nailing for Stabilization of Highway Slopes and Excavations", FHWA-RD-89-193.

8.   FENAIL (1993), "A User Manual", Research Report GE-ODOT-02-93, Portland State University, Department of Civil Engineering.

9.   Finno, R.J. et.al. (1991), "Analysis of Performance of Pile Groups Adjacent to Deep Excavation", ASCE, JGED, Vol. 117, No. 7, June 1991.

10.   GEOTECK-PRO (1991), "User Manual Version 2.0", National Laboratories Inc., Evansville, Indiana.

11.   GOLDNAIL (1990), Golder Associates, Seattle, Washington.

12.   Herrman, L. and Mish (1983), "User Manual SAC", University of California, Davis, September.

13.   Juran, I., Baudrand, G., Farrag, K., and Elias, V. (1990), "Kinematical Limit Analysis for Design of Soil-Nailed Structures", ASCE, JGED, Vol. 116, Nov., Jan., 1990.

14.   Konder, R.L. (1963), "Hyperbolic Stress-Strain Response: Cohesive Soils", ASCE, JSMFD, Vol. 89, No. SM 1.

15.   Kimmerling, R. and Chassie R. (1993) "Performance Monitoring of A Soil Nailed Wall Used in a Bridge Abutment Application", Int. Symp. on Soil Reinforcement, Paris, France, November 1993.

16.   Marin, H.E., Kiefer, F., Anderson, L. (1993), "Finite Element Modeling of Soil-Structure Interaction Systems; Selection of Hyperbolic Parameters", Sym. Eng. Geology & Geotec, Eng., Reno, NV, March 1993.

17.   Neumann, D. (1987), "Hyperbolic Parameters From the Pressuremeter", Thesis for M.Sc. degree, PSU, 1987, Department of Civil Engineering

18.   ODOT (1988) "Foundation Investigation Report, Swift Delta Interchange", ODOT, Highway Division, Milwaukie, December 1988.

19.   PATRAN (1992), Four Volumes of User Manuals "PDA Engineering", Palo Alto, California.

20.   Sakr, C. (1991) "Soil Nailing of a Bridge Fill Embankment" Construction Report, OR89-07, August 1991.

21.   Sakr, C. (1993) "Soil Nailing of a Bridge Fill Embankment", Design and Field Performance Report, ODOT, OR89-07, October 1993.

22.   Salama, M.E., "Analysis of Soil Nailed Retaining Walls", Thesis submitted to University of Illinois for Ph.D., 1992, Urbana-Campaign, Civil Engineering.

23.   Smith, T.D. and Denham, M. (1991) "Multi-Cylinder Control Units for Prebored Pressuremeters", Geotechnical Testing Journal, ASTM, June 1991, pp.212.

24.   Smith (1992), "MADAM: Metastable Analysis of Dams", 3 volumes, Portland State University, Department of Civil Engineering.

25.   SNAIL (1990), California Department of Transportation, Sacramento, California.

26.   STIFF 1 (1992), "User Manual", Ensoft, Austin, Texas 1992.

27.   TECPLOT (1993), Amtee Engineering, Bellevue, Washington.

Appendix A

A SET OF USER FEEDBACK COMMENTS FOR COM624P

As a result of the work reported in Section 4 considerable time was spent overcoming the difficulties with the ODOT supplied code COM624P. As a way of formally providing some feedback that may be of use to future users the following comments are made:

- The units used for unit weight of soil, pounds per cubic inch, are non-standard and make interpretation of the output and creation of the model difficult.

- The input dialog menu does not necessarily save all entered data to the input file. This may only be circumvented by using an ascii text editor.

- Use of the input dialog menu automatically restores the pile boundary conditions to fixed head. It should not.

- The code does not allow the mixed use of user defined P-y curves and internally generated P-y curves. The depth where input generated P-y curves are first required is always considered the surface by the program. Therefore, in order to model a cut alongside the pile, one must input P-y curves along the entire depth of the pile.

- The calculated (or manipulated) slope P-y curves should appear as input echo on the output.

Appendix B

BOREHOLE LOG TB124 AND TB125

SOILS AND GEOLOGICAL EXPLORATION LOG
HIGHWAY DIVISION

Project	SWIFT INTERCHANGE - DELTA PARK INTERCHANGE		Hole No. TB-124
Highway I-5		County Multnomah	Prefix C6261979-000-908
Purpose of Work	Retaining Wall Foundation		Bridge No. 16526A
Equipment	Mobile B-53		Tube Elev.
Geologist	C. J. Eshelman	Driller T. Lauinger	Recorder D. Marsh
Hole Location VS Line, Sta. 113 + 80 Lt.		C.L. Rt. 23'	Ground Elev. 47⁶

Tests			Drilling Method		Groundwater Level	
					Date	Depth
"N" — Standard Penetration,	No.	20		Auger Depth		
"M" — Oregon Miniature Pile,	No.	0	BW	Casing Depth 78.0'	11-16-88	33'
"C" — Core, Barrel Type	No.	0		Open Depth 1.5'		
"U" — Undisturbed Sample, Size	No.	0		Total Depth 79.5'		

Date Started 11-16-88	Date Completed 11-16-88	Sample Data Sheet No.

Depth, ft.	Test Type No.	Driving Resistance	Measured Recovery.	% Recovery	Hardness R.Q.D.	Graphic Log	% Natural Moisture	Material Description — Color / Consistency / Plasticity / Organic Content — Wet-Dry / Jointed-Broken / Angular-Rounded / Drill Remarks etc.
2	N-1	14-35-50/0.4'	0.9	64		SM / GM		N-1 - (2.0 - 3.4') - SAND, fine, with some small gravels, trace of silt brown, moist, dense, (SM - GM). Origin: Fill material
4	N-2	31-50/0.4'	0.3	33		SM / GM		N-2 - (4.0' - 4.9') - SAND, fine, with some silt, some coarse sand and small gravels, brown, moist, very dense, (SM). (Fill material).
6	N-3	50/0.3'	0.2	66		GM (NEW FILL)		N-3 - (6.0' - 6.3') - Small gravel fragments. (Fill).
8	N-4	50/0.2'	0.2	40		GM (10')		N-4 - (8.0' - 8.5') - Gravel and asphalt fragments with sand. (Fill).
10	N-5	4-4-4	1.0	67		ML	33	N-5 - (10.0 - 11.5') - SILT with some clay, trace of fine sand, brown, moist, medium stiff, (ML). LL = 36, PI = 1 Contact of old fill at 10.0'.
13	N-6	3-1-2	1.0	67		GM (OLD) FILL	38	N-6 - (13.0 - 14.5') - 13.0 - 14.0 - SILT with trace of clay, fine sand, brown, moist, soft, (ML). LL = 40, PI = 10. 14.0 - 14.5' - Gravels with some sand, gray, moist, loose, (GM).

Test Type No.	Driving Resistance	Measured Recovery.	% Recovery	Hardness R.Q.D.	Graphic Log	% Natural Moisture	Material Description — Color / Consistency / Plasticity / Organic Content — Wet-Dry / Jointed-Broken / Angular-Rounded / Drill Remarks etc.
N-7	42-50/0.3'	0.8	100		GM		N-7 - (16.0 - 16.8') - Small gravels and concrete fragments, very dense, (GM) (Fill).
N-8	50/0.4'	0.2	50		GM		N-8 - (18.0 - 18.4') - Same as N-7. (Fill).
N-9	10-10-9	0.2	13		GM		N-9 - (20.0 - 21.5') - Same as N-7, mediun dense. (Fill).
N-10	10-12-13	0.6	40		SP		N-10 - (22.0 - 23.5') - SAND, fine to medium, clean, with some small gravels gray - brown, moist, medium dense. (SP). Origin: Subex. Fill
N-11	17-19-16	0.6	40		SP		N-11 - (24.0' - 25.5') - Same as N-10.
N-12	3-3-5	0.4	27		SP		N-12 - (26.0' - 27.5') - SAND, clean, fine gray, moist, loose. Origin: Subex. Fill (SP).
N-13	7-8-7	0.1	7	.	SP GP		N-13 - (28.0 - 29.5') - SAND, coarse, with small gravels. (SP - GP).
N-14	10-11-15	0.1	7		SP GP		N-14 - (33.0 - 34.5') - Same as N-13.
					35'		
N-15	8-10-15	1.5	100		ML	32	N-15 - (38.0 - 39.5') - SILT with some fine sand, trace of clay, moist, gray, medium dense, (ML). LL = 37, PI = NP.
N-16	4-6-7	1.5	100		ML	45	N-16 - (43.0' - 44.5') - Same as N-15, medium stiff. LL = 45, PI = 12.
N-17	3-3-5	1.5	100		ML		N-17 - (48.0 - 49.5') - SILT with some fine sand, trace of clay, gray, moist, medium stiff, (ML).

Depth	Test Type No.	Driving Resistance	Measured Recovery.	% Recovery	Hardness R.Q.D.	Graphic Log	% Natural Moisture	Material Description — Color, Consistency, Plasticity, Organic Content / Wet-Dry, Jointed-Broken, Angular-Rounded, Drill Remarks etc.
58	N-18	2-5-7 ·	1.5	100		ML		N-18 - (58.0 - 59.5') - Same as N-17.
68	N-19	10-11-12	1.0	66		SM		N-19 - (68.0 - 69.5') - SAND, fine, with some silt, gray, moist, medium dense, (SM).
78	N-20	15-23-29	1.3	87		SM		N-20 - (78.0 - 79.5') - SAND, fine with trace of silt, gray, moist, medium dense, (SM).
						79.5'		
								BOTTOM OF HOLE - 79.5'

SOILS AND GEOLOGICAL EXPLORATION LOG
HIGHWAY DIVISION

Project	SWIFT INTERCHANGE - DELTA PARK INTERCHANGE		Hole No. TB-125
Highway	I-5	County Multnomah	Prefix C6261979-000-908
Purpose of Work	Retaining Wall Foundation		Bridge No. 16526A
Equipment	Mobile B-53		Tube Elev.
Geologist	C. J. Eshelman	Driller J. Lee	Recorder T. Lauinger
Hole Location	VS Line, Sta. 113 + 85 Lt.	C.L. Rt. 21'	Ground Elev. 47³

Tests

	No.
"N" — Standard Penetration,	0
"M" — Oregon Miniature Pile,	0
"C" — Core, Barrel Type	0
"U" — Undisturbed Sample, Size 2½"	2

Drilling Method

HQ	Auger Depth	
	Casing Depth	40.0'
	Open Depth	2.0'
	Total Depth	42.0'

Groundwater Level

Date	Depth
11-17-88	21'

Date Started	Date Completed	Sample Data Sheet No.
11-17-88	11-17-88	A-35339

Depth, ft.	Test Type No.	Driving Resistance	Measured Recovery.	% Recovery	Hardness R.Q.D.	Graphic Log	% Natural Moisture	Material Description (Color, Consistency, Plasticity, Organic Content / Wet-Dry, Jointed-Broken, Angular-Rounded, Drill Remarks etc.)
10	U-1		1.5					U-1 - (10' - 12') - Shelby sample
40	U-2		2					U-2 - (40' - 42') - Shelby sample
								BOTTOM OF HOLE - 42'